University of Colorado
Department of Aerospace Engineering Sciences
ASEN 4028

Project Final Report (PFR)

High Altitude Lifting Orbiter
(HALO)

Monday 4th May, 2020

Project Customer

Name: Dale Lawrence Email: Dale.Lawrence@colorado.edu Phone: 303-492-3025

Team Members

Name: Braden Barkemeyer Email: brba2456@colorado.edu Phone: (970) 729-0545 Position: Orbit and Aerodynamics Lead	Name: Nolan Ferguson Email: nofe9992@colorado.edu Phone: (720) 289-5349 Position: Systems Engineer
Name: David Cease Email: david.cease@colorado.edu Phone: (203) 980-0832 Position: Project Manager	Name: Ryan Lansdon Email: ryan.lansdon@colorado.edu Phone: (303) 802-7260 Position: Electronics Lead
Name: Kelly Crombie Email: kecr9321@colorado.edu Phone: (630) 577-7412 Position: Software Lead	Name: Jacob Marvin Email: jacob.marvin@colorado.edu Phone: (303) 995-7565 Position: Safety Lead
Name: Jared Dempewolf Email: jade6560@colorado.edu Phone: (303) 718-7913 Position: Testing and Verification	Name: Kyle McGue Email: kymc8415@colorado.edu Phone: (843) 697-8747 Position: Environmental Lead
Name: Tyler Faragallah Email: tyfa7215@colorado.edu Phone: (720) 315-6513 Position: Manufacturing Lead	Name: Paolo Wilczak Email: paolo.wilczak@colorado.edu Phone: (303) 960-2756 Position: Chief Financial Officer

Team Advisor: Matthew Rhode

Premable

Contents

List of Figures

List of Tables

List of Acronyms:

AFOSR: Air Force Office of Scientific Research
ANSYS: Analysis System
AVL: Athena Vortex Lattice
BEM/BET: Blade Element Momentum Theory
CAD: Computer Aided Design
CDAS: Controlled Descent and Arrest System
CDD: Conceptual Design Document
CDR: Conceptual Design Review
CFD: Computational Fluid Dynamics
CONOPS: Concept of Operations
CP: Cost Plan
CPE: Critical Project Element
DR: Design Requirement
EBP: Electronic Box/Payload
ESC: Electronic Speed Controller
FAA: Federal Aviation Administration
FBD: Functional Block Diagram OR Free Body Diagram
FFR: Fall Final Report
FR: Functional Requirement
GPS: Global Positioning System
HAB: High Altitude Balloon
HALO: High Altitude Lifting Orbiter
HYFLITS: Hypersonic Flight in the Turbulent Stratosphere
IMU: Inertial Measurement Unit
NASA: National Aeronautics and Space Administration
OC: Organizational Chart
RPM: Revolutions per minute
TP: Test Plan
WBS: Work Breakdown Structure
WP: Work Plan

1. Project Purpose

Author(s): David Cease, Ryan Lansdon

1.1. Mission Statement

The High Altitude Lifting Orbiter (HALO) mission seeks to innovate the process of collecting turbulence data in the stratosphere. This will be accomplished by designing a tethered payload system which will autonomously execute controlled orbits around the wake of a high altitude balloon. Additionally, this orbiter system will actuate controlled altitude oscillations between 25 km and 35 km while recording and transmitting temperature, IMU, and GPS sensory data.

1.2. Motivation

Currently, there is limited knowledge of turbulence patterns present in the stratosphere. This is largely due to the fact that current turbulence measurement methods are inefficient and expensive. Recently, the Air Force Office of Scientific Research (AFOSR) funded the Hypersonic Flight in the Turbulent Stratosphere (HYFLITS)[12] project to collect turbulence data in this region of the atmosphere. Collection of this data would allow for more informed development of aircraft that operate in this high altitude region. HYFLITS utilized a single-use balloon system to capture turbulence data between altitudes of 20 *km* and 35 *km* for roughly 1.5 hours. This data collection method was limited by the balloon's wake; turbulence data could not be collected during ascent because the turbulence sensor was located directly within the wake of the balloon.

The High Altitude Lifting Orbiter (HALO) project seeks to improve this endeavor by moving the scientific payload out of the balloon wake and implementing multiple controlled ascents and descents between 25 *km* and 35 *km*. These improvements will allow for increases in data collection per balloon launch. Increasing the quantity of turbulence data collected per balloon launch is significant because the HYFLITS balloon and sensor package are designed for single time use only. This increase in turbulence data collection will be desirable so long as the useful-data per dollar ratio is increased.

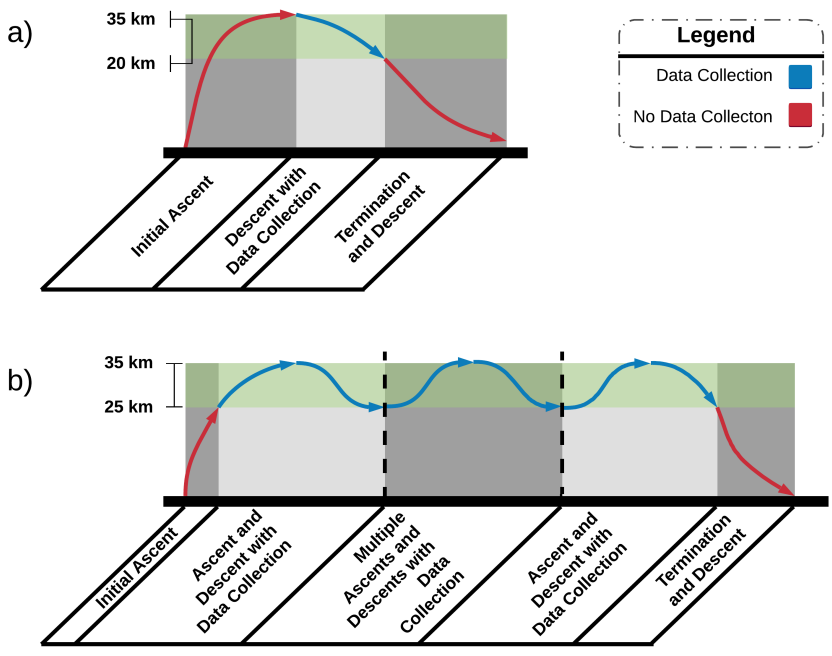

Figure 1. Flight profiles of the HYFLITS and HALO mission

Figure 1a displays the flight profile of the HYFLITS mission, while Figure 1b displays the proposed flight profile of the HALO mission. Figure 1b shows three ascent and descent data collection phases, which would produce six times the amount of data produced by HYFLITS. This is a tentative number of data collection phases that may be

reevaluated throughout the testing process; the current expectations for the HALO system involve three to four data collection ascents and descents.

2. Project Objectives and Functional Requirements

Author(s): Nolan Ferguson, Jacob Marvin, David Cease, Jared Dempewolf

2.1. Project Objectives

In the initial phases of the HALO project, three primary project objectives were identified, set forth by discussions with the customer pertaining directly to the HALO path apart from the heritage HYFLITS mission.

1. We aim to improve upon the longevity and data collecting capabilities of the current HYFLITS payload.
2. We aim to provide a product that provides ease of use and safety to both those involved and not involved with launch and mission duration.
3. The HALO system will be cost effective relative to the improved data collection capabilities of the system.

All design choices, requirements, and considerations for trade studies flowed from these baseline requirements.

2.2. Functional Requirements

Functional requirements below stem from the final design and have been modified and adjusted over the course of the semester.

FR 1.0: There will be a method of controlling the altitude of the balloon and payload.

Purpose: Altitude control is necessary to accommodate data collection periods throughout the flight, whether by a single ascent/descent, or by multiple ascents/descents. Turbulence measurements and prediction will improve with the increased characterization of a large range of the stratosphere.

FR 2.0: The payload must be capable of orbiting beneath the balloon.

Purpose: As a proof of concept, it is necessary that orbiting beneath the balloon must be undertaken for the ability to collect data outside the wake of the balloon. This will allow extended data collection periods throughout a large majority of the stratosphere.

FR 3.0: The payload must be able to survive the conditions presented throughout the entirety of the mission.

Purpose: In order to collect the data, the payload must be able to sustain the harsh weather with little insulation, as well as unpredictable wind

FR 4.0: The payload will be able to transmit collected data to the ground receiver.

Purpose: While the primary goal is to institute an orbiting payload for data collection outside the balloon wake, this data will need to be transmitted and characterized for turbulence modeling.

FR 5.0: Balloon and its payload must meet all FAA guidelines, including those subjecting the balloon and its payload to designation as an unregulated balloon. In addition, Balloon and payload shall meet specifications set forth by customer.

Purpose: As requested by the customer, in order to keep the balloon and its payload launchable by small teams and without significant regulation from the FAA, unmanned free balloon regulations (FAA Part 101) must be considered as the ultimate design specifications.These restrictions are accounted for in the design requirements. This requirement, while met, proved to be unnecessary, as legal restrictions prevented flight regardless. This is elaborated on further in the document.

FR 6.0: The balloon will terminate flight resulting in a controlled descent upon mission completion.

Purpose: As required by the customer, the system will self execute into descent so that the balloon is not free floating in the air space. Free floating and uncontrolled balloon's could potentially cause collisions between high altitude aircraft.

FR 7.0: As specified by the customer, the balloon must contain a controlled descent arrest system (CDAS) to prevent harm to property or person upon balloon burst.

Motivation: As specified by the customer, the balloon must contain a controlled descent arrest system (CDAS) to prevent harm to property or person upon collision with earth after balloon burst.

FR 8.0: As specified by the customer, launch setup must be able to be conducted by a maximum of two people, and launch must be able to be conducted by a single individual.

Purpose: As required by the customer, in order for the developed payload and balloon system to remain modular and transportable by small teams in varied terrains and locations, it is necessary that the system does not provide unreasonable effort to setup and launch.

FR 9.0: Project HALO will cost no more than $5,000 to develop, and no more than $2,000 per flight when components are purchased in quantities of 50.

Purpose: As required by the customer, these cost values are set to allow multiple launches without needing a massive budget. This guarantees theoretical cost benefit for the additional data collection of the HALO mission.

2.3. Levels of Success

Success for this project will be categorized into three distinct levels for each of the main functional components. These levels of success can be found in the following table.

	Tethered Orbiter	Altitude	Data Collection	Descent Arrest
Level I	The payload shall orbit below the balloon. This orbit will be stable and periodic.	The balloon and payload will achieve a target altitude of 150 ft and be neutrally buoyant via Moored test. The balloon will remain at this altitude until termination.	The orbiting payload will contain an IMU and GPS to verify a successful orbiter trajectory. This data will will be transmitted to a receiving antenna throughout the Moored test.	System will include a fail-safe descent arresting device in the event of balloon burst. The payload will then enter a controlled descent at a maximum speed of 5 m/s.
Level II	The payload will be in a stable orbit below the balloon, demonstrating the ability to remove itself from the wake. It will also generate enough lift or drag to bring the balloon and payload to a velocity of 2m/s +/- 20% in ascent and descent.	Controls will be implemented that will allow the tethered orbiter to change the balloon and payload altitude. The balloon will reach neutral buoyancy at 20 km, descend to 15 km, ascend to 25 km, and terminate. GPS measurements will be used to approximate the altitude of the balloon. These altitudes will be allowed an uncertainty of 1 km.	Temperature, GPS, and IMU data will be collected on the payload throughout its flight. This data will be transmitted to a receiving antenna during flight.	Controlled descent will be initiated autonomously as triggered by low battery notification on board.
Level III	The stable payload orbit will remain fully outside the balloon wake for the entire flight, ignoring occasional perturbations due to wind gusting. It also must be capable of generating lift or drag to bring the balloon system to a velocity of 2 m/s +/- 20% during ascent or descent. Orbiter speed will not introduce turbulence measurement bias.	The payload will reach a target altitude of 30 km and then oscillate between 25 km to 35 km until power depletion. GPS measurements will approximate the altitude of the balloon. These altitudes will be allowed an uncertainty of 1 km.	Turbulence sensors will be incorporated	

Figure 2. Levels of Success

The lowest level of success, level 1, would be achievable solely through ground testing. A Moored test will be conducted, which involves activating the system while connected to a balloon at an altitude of 150 ft. This balloon will be tethered to the ground. The tethered orbiter will be able to orbit below the balloon in a stable and periodic

fashion. The venting system will be tested to ensure that the balloon can become neutrally buoyant. IMU and GPS data will be transmitted to a receiving antenna in order to test data collection. Finally, a drop test will be conducted in order to verify the operation of the controlled descent and arrest system (CDAS).

The next level of success, level 2, would be achieved through a low-altitude flight test. Instead of the desired altitudes between 25 and 35 *km*, this low-altitude flight test will be between 15 and 25 *km*. The lifting orbiter will be able to generate enough lift to bring the balloon system to an ascent and descent speed of approximately 2 m/s while demonstrating the ability to remove itself from the balloon wake. Temperature, GPS, and IMU data will be transmitted to the ground throughout flight. A controlled descent phase will be triggered by a low-battery notification from the electronics package.

The highest level of success, level 3, is denoted by the concept of operations in Figure 3. In this scenario, the balloon system would oscillate between altitudes of 25 *km* and 35 *km* until mission termination. These oscillations will be induced by the lifting orbiter which will be outside of the balloon wake throughout the vast majority of the flight. Finally, turbulence sensors will be incorporated in order to actually measure turbulence at these altitudes.

2.4. Concept of Operation

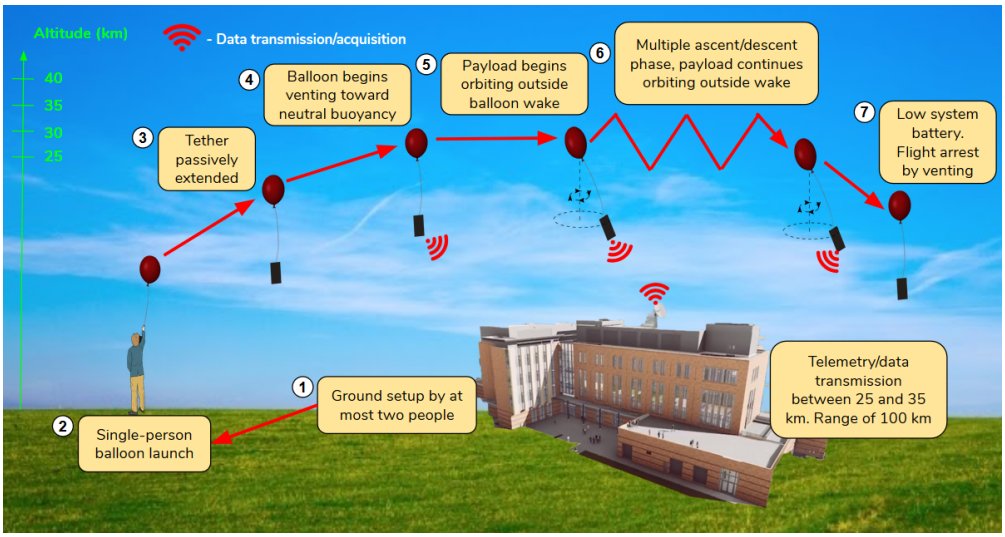

Figure 3. HALO Concept of Operations

Shown above is the Concept of Operations for the HALO mission. This figure depicts the expected pinnacle of success upon system launch. The overall mission can be seen during this cycle. The balloon and payload starts on the ground and is launched by ideally one person. It then rises up to about 30 *km* and starts to vent over time until it reaches a neutral buoyancy at 30 *km*. From here, the orbiter will begin orbiting around the wake and collecting data as the wing generates the needed lift to move the balloon up and down through the range of 25 - 35 *km*. The oscillations in altitude allow a broad range of data points to analyze. After multiple cycles have occurred and the battery runs low, a signal will be sent to the vent which will slowly let the helium out of the balloon and create a slow, safe decent back to the ground. The entire time the orbiter is running and the sensors are taking data, this data will be transmitted down to a receiver on the ground.

Unfortunately, it was later determined that the CU administration would not allow for such a flight to take place without an FAA waiver, which has yet to be obtained. Continuation of this project would require an FAA waiver in order to actually fly.

2.5. Project Deliverables

1. Lifting orbiter package (extruded polystyrene wing + tail combination, servos, carbon fiber spars, booms, motor, propeller)
2. Electronics package (batteries, sensors, ESC, thermal control, Arduino Mega)
3. HAB-TX-1500 Balloon

4. Three helium tanks (located in manufacturing shop)
5. Braided Kevlar Tether
6. Legacy vent from HYFLITS mission, altered for direct wiring rather than radio communication
7. Slip ring
8. Critical project element models and simulations (found in digital archive)
9. Arduino code for servo actuation, data reading (found in digital archive)

2.6. Functional Block Diagram

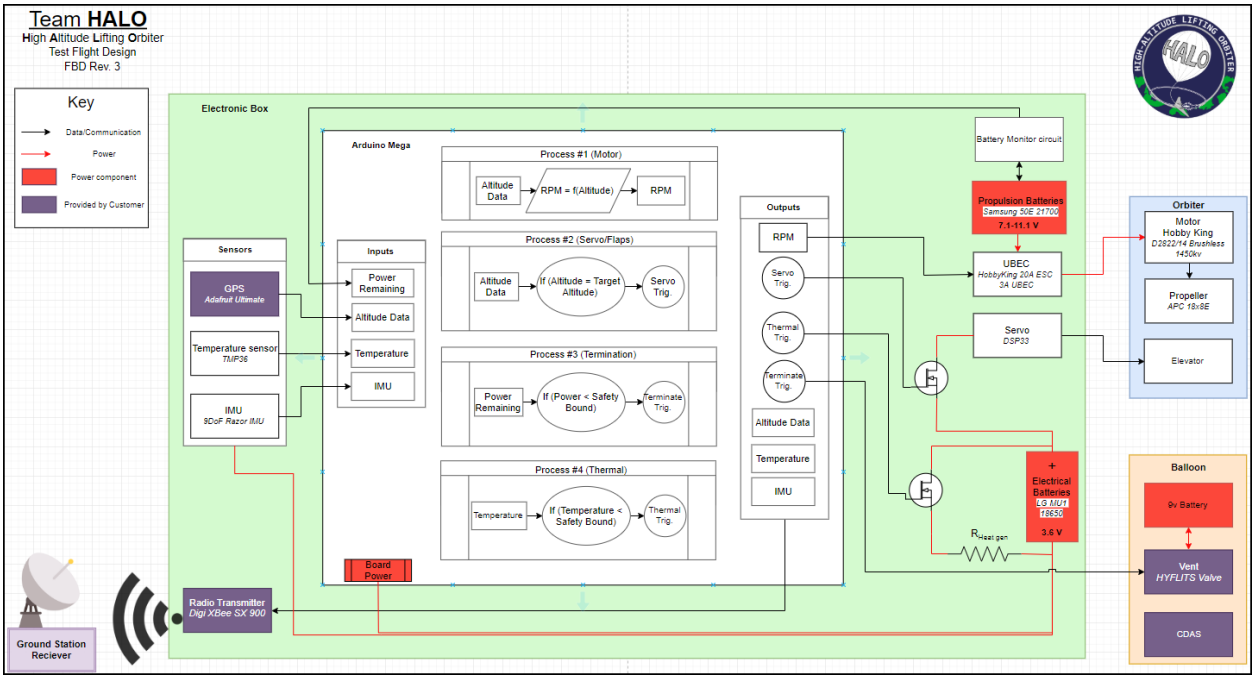

Figure 4. Functional Block diagram for flight payload for HALO mission.

Contained in the above Functional Block Diagram (Figure 4) is the test flight design of the HALO system. The system consists of three major subsystems: the Electronics Box Payload (EBP), the orbiter, and the balloon. Components and hardware at the center of the HALO mission are contained within the EBP. The EBP is contained within the lifting orbiter, placed within a hollowed section of the modeled plane, and re-sealed with foam. This includes the sensor packaging of GPS, temperature, and IMU sensors, which are connected to the main MCU (Arduino Mega). This also includes the battery monitoring system, motor ESC, elevator control servo, radio transmitter, active thermal control, and two separate battery systems for the motor and electronic components.

The orbiter system contains primarily control surfaces of the lifting orbiter external to the EBP. This system also contains the propeller driving the lifting orbiter, attached to the Motor.

The final major system containing significant amounts of components is the balloon system, located physically above the lifting orbiter. This consists of a separate battery system, the HYFLITS mission heritage valve, and the controlled descent and arrest (CDAS) system.

Connections between separate systems exist primarily through triggers. Altitude data is collected from the GPS and converted to a motor RPM through on-board processes, functionally derived from modeling conducted and explained later in this document. This RPM is sent to the motor UBEC (ESC), powered separately by propulsive batteries. The UBEC outputs the correct amount of voltage and current to the propeller driving motor. Altitude data is used in a secondary matter for the servo trigger. If the bottom or top of the sinusoidal altitude oscillation is reached (25 or 35

km), the second on board process will output a trigger to the servo. This will switch the servo position on the elevator, changing the direction of generation of lift, driving the payload/balloon in the opposite direction.

Connections between the EBP and the balloon consist of the termination/neutral burn triggers. For a neutral venting burn, altitude data will trigger the beginning of an hour of continuous venting to achieve neutral buoyancy. GPS points will be summed over the course of neutral burning, allowing a rate of ascent calculation. After the rate of ascent has fallen to an acceptable range, neutral buoyancy will be considered reached. The termination burn is power based; once five percent power remaining is recognized the propulsion batteries (or the point where severe voltage drop off for batteries occurs), a termination trigger will be sent to the HYFLITS vent valve. This will most likely consist of a MOSFET switch located on the balloon system mount.

3. Design Process and Outcome

Author(s): Braden Barkemeyer, Tyler Faragallah, Jared Dempewolf, Nolan Ferguson, David Cease, Kyle Mcgue, Jacob Marvin

3.1. Design Requirements

Throughout this conceptual design section, preliminary design ideas will be discussed for each of the critical project elements (CPEs). For each CPE, trade studies were conducted in order to select optimal designs in each respective space. Note that certain design selections were shifted after this preliminary phase in light of new information. These shifts will be discussed alongside the preliminary concepts. Design requirements below pertain to the functional requirements above, and are for the final design.

- **DR 1.1:** Balloon system altitude ascent and descent maximum speed shall be within 20% of 2 $\frac{m}{s}$.

  Motivation: As requested by the customer, speed must remain relatively low (within 20% of 2 $\frac{m}{s}$) as not to disturb data collection received by instruments.

- **DR 1.2:** Balloon system must be able to achieve neutral buoyancy to some capacity at a specified altitude.

  Motivation: In order to improve the current data collection capacity, it is necessary that neutral buoyancy is reached. Neutral buoyancy will allow the designed method of altitude control to be effective for cycles of data collection. It will allow the orbiter to increase its lift and change the altitude of the balloon.

- **DR 2.1:** Payload must have some ability to determine the position of the orbit and position of orbit relative to the center of the balloon.

  Motivation: In order to determine the stability of the orbit, as well as to aid in determination of whether the orbiting payload is collecting adequate data, it is necessary to determine the position in the orbit.

- **DR 2.2:** Orbiting system or device must not damage or deform balloon.

  Motivation: Data collection must not interfere with the balloon flight, in order for the mission to proceed safely and effectively.

- **DR 3.1:** The payload must be able to initiate control surfaces autonomously.

  Motivation: Improves efficiency and reliability, and is able to carry out mission without complication of command transmission.

- **DR 3.2:** The electronics must fit inside a specified area enclosed in the lifting payload.

  Motivation: If the electronics do not fit within the lifting payload, they will be vulnerable to environmental conditions.

- **DR 3.3:** The payload must be structurally resilient to wind gust and orbit motion.

  Motivation: If damage occurs on the lifting body, atmospheric translation could be inhibited, leading to potential failure in data collection.

- **DR 4.1:** Data transmission must be collectible within a 100 km range of the stationary ground station.

  Motivation: The range was designated to be 100 km by the customer to ensure the transmission of the data while taking into account balloon altitude gain and lateral drift from the ground station. This range would be verified through testing later in the project.

- **DR 5.1:** The payload will be weight constrained.
  Motivation: Any payload above the weight classes designated below subjects the balloon to a title of an "Unmanned free balloon", which requires the payload and balloon to be further regulated.
  - **DR 5.1.1:** The payload will be under four pounds, OR
  - **DR 5.1.2:** If the payload consists of a single package, and weighs between 4 to 6 pounds, the payload must have a weight to size ratio of less than three ounces per square inch on any surface of the package (determined by dividing the total weight in ounces of the payload package by the area in square inches of its smallest surface), OR
  - **DR 5.1.3:** If the payload consists of two or more packages, these must weigh under six pounds individually.
- **DR 5.2:** Tether or other suspension device must NOT be able to withstand an impact force of 50 lb.
  Motivation: Any payload with tether or other suspension device with a impact strength greater than 50 lb is classified as a "Unmanned free balloon", which subjects the payload to further regulation.
  Verification: Strength of tether or suspension device will be tested to ensure the ability to withstand weight of payload, and break with an impact force of 50 lbs.
- **DR 5.3:** Lifting gas of balloon will be Helium.
  Motivation: As specified by the customer, the lifting gas will be helium.
  Verification: Balloon will not be subject to testing or filling of other lifting gases.
- **DR 5.4:** Payload shall not be toxic to environment.
  Motivation: The payload, as specified by customer, will not be toxic or harmful to the environment, in the event of no payload recovery.
- **DR 6.1:** If payload is to make soft landing in water, the payload shall self-scuttle.
  Motivation: Removes the possibility of the payload becoming floating debris for waterborne vehicles.
- **DR 7.1:** The CDAS will passively deploy upon balloon failure or flight termination.
  Motivation: The CDAS must be activated to establish a safe descent speed regardless if activation is passive or intentionally triggered.
- **DR 7.2:** The CDAS must provide a descent speed of a maximum of 5 m/s [a] .
  Motivation: After termination, the payload and balloon must descend at a safe speed, as not to cause harm to body or property.
- **DR 8.1:** Weight of payload must be able to be handled by one individual.
  Motivation: For launch to be physically conducted by a single individual, the payload must be of reasonable weight. This allows the individual to handle both the balloon and the payload for a given launch.
- **DR 8.2:** Tether or suspension devices must not be longer than 10 meters at launch.
  Motivation: In order for launch to be conducted smoothly, with a reasonable and non-destructive acceleration of the payload, the length of the tether at launch must be under 10 meters, as specified by the customer.

3.2. Balloon Design Process

Balloon selection is one of the crucial elements of the HALO mission as it serves as the primary lifting source for the payload system. This design must be decided upon early because the balloon properties will directly affect the mass allowance of the payload. It is critical to consider the expansion of the balloon as it ascends to altitudes up to 35 *km*. Only balloons which are capable of withstanding the low-temperature and low-pressure conditions of these altitudes will be considered. Table 1 shows a table with various parameters on different civilian grade balloons.

[a]The value of 5 m/s was provided by the customer as a estimate.

This table contains information about the burst diameter, neck size and length, burst altitudes range, mass, and cost of specific High-Altitude Balloons (HAB).

Balloon	Neck Length	Neck Size	Burst Diameter	Burst Altitude Range	Cost
HAB 350	3 cm	12 cm	412 cm	14.6 - 21.3 km	$30.00
HAB 600	3 cm	12 cm	602 cm	22.9 - 27.4 km	$45.00
HAB 800	3 cm	12 cm	700 cm	27.4 - 30.5 km	$65.00
HAB 1000	3 cm	12 cm	786 cm	30.6 - 33.5 km	$75.00
HAB 1200	3 cm	12 cm	863 cm	29.3 - 33.5 km	$90.00
HAB 1500	3 cm	12 cm	944 cm	32.0 - 35.1 km	$105.00
HAB-TX-1500	3 cm	12 cm	944 cm	32.0 - 38.1 km	$120.00
HAB 2000	5 cm	12 cm	1054 cm	32.6 - 35.7 km	$230.00
HAB 3000	5 cm	12 cm	1300 cm	35.1 - 38.1 km	$360.00

Table 1. Balloon Options and Properties[11]

The naming convention for the above balloons denotes the balloon mass in grams; for example, the HAB 350 has a mass of 350 *g*. In order to ensure mission success, it will be necessary to choose a balloon that will not burst at target altitudes. While maintaining a safety margin for burst altitudes, a balloon with the least mass and cost will be favorable. This leads to the selection of the HAB 1000, HAB-TX-1500, and HAB 3000 to be considered for the mission; other balloons were not chosen because they did not provide sufficient benefits relative to their costs. For example, the HAB 1200 was not chosen since it has a worse burst altitude range, higher mass, and higher cost than the HAB 1000. It is important to note, however, that this table is a useful reference since any of these balloons may be used when it comes to the testing phase of the mission.

Plots relating initial balloon volume as well as helium mass versus balloon diameter at altitude can be found below. These plots will be useful in determining the initial helium fill and comparing estimated balloon diameter to burst diameter. It is important to note that these plots are assuming a calorically perfect gas; the ideal gas law equation is utilized in calculating balloon volumes at varying altitudes. Further, standard atmospheric conditions are assumed.

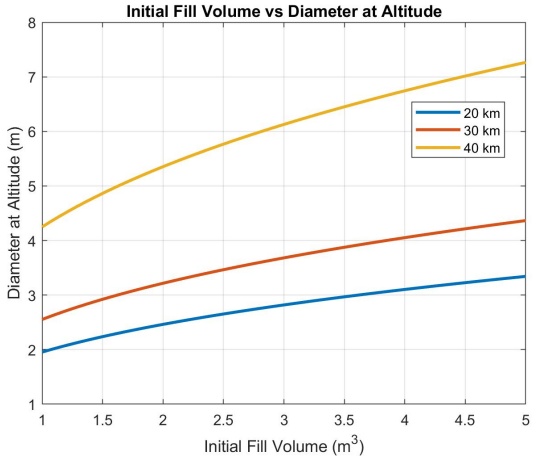

Figure 5. Initial Balloon Volume vs Diameter at Altitude

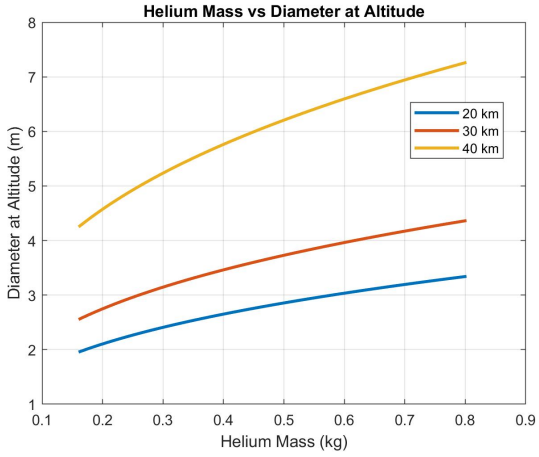

Figure 6. Helium Mass vs Diameter at Altitude

3.2.1. Balloon Design Alternatives

HAB 1000

The HAB 1000 balloon has a mass of 1,000 *g*, which is the lowest mass balloon to be considered. This is ideal in terms of weight; less lifting force will be required to control altitude if the balloon is of a lower mass. Its neck length is 3 *cm*, which will be significant when considering venting and termination options. Its burst range is from 30.6 *km* to

33.5 *km*, which would be acceptable to reach levels of success 1 and 2. Finally, its cost is $75.00, which is the lowest of the considered balloons.

Pros	Cons
Lowest mass	Lowest burst altitude
Lowest cost	

Table 2. HAB 1000 Pros and Cons

HAB-TX-1500

The HAB-TX-1500 balloon has a mass of 1,500 *g*, which is the second lowest balloon mass to be considered. Its neck length is also 3 *cm*, which will be relevant when considering venting and termination options. Its burst range is from 32.0 *km* to 38.1 *km*, which would be suitable for reaching the third level of success. Finally, its cost is $120.00, which is much less expensive than the more massive balloons.

Pros	Cons
Relatively low mass	Wide burst altitude range
High maximum burst altitude	
Relatively low cost	

Table 3. HAB-TX-1500 Pros and Cons

HAB 3000

The HAB 3000 balloon has a mass of 3,000 *g*, which is the most massive balloon to be considered. Its neck length is 5 *cm*, which will be relevant when considering venting and termination options. Its burst range is from 35.1 *km* to 38.1 *km*, which would be ideal for reaching the third level of success. Finally, its cost is $360.00, which is much more expensive than the other balloon options.

Pros	Cons
High minimum burst altitude	Highest mass
High maximum burst altitude	Highest cost

Table 4. HAB 3000 Pros and Cons

3.2.2. Balloon Design Trade Study

Metrics

Four metrics will be considered within the balloon selection trade study: minimum estimated burst altitude, maximum estimated burst altitude, mass, and cost. With this in mind each category was given a specific weighting, in order to prioritize the most important parameters that would give the group the best possible choice.

Minimum Burst Altitude: The minimum burst altitude is the most significant metric when it comes to the balloon choice. This is because it is necessary to choose a balloon which will not burst at target altitudes; if the balloon bursts, then data cannot be collected and the mission is a failure. For these reasons, a weight of 0.35 is assigned to this metric. Based on the following table, it will be critical to choose a balloon with a minimum burst altitude score of at least 2 for level 1 success, 3 for level 2 success, and 4-5 for level 3 success. These minimum burst altitudes were listed on the balloon provider's website, and were tested using varying payload masses of approximately 1 *kg*.

Minimum Burst Altitude [km]	35-40	30-35	25-30	20-25	15-20
Score	5	4	3	2	1

Table 5. Minimum Burst Altitude Scoring

Maximum Burst Altitude: The maximum burst altitude is another significant parameter when it comes to deciding which balloon to use. It is ideal to have a maximum burst altitude that is significantly higher than the actual target altitude; this would suggest that the balloon is capable of going even higher without bursting. For this reason, this metric was given a weight of 0.3. The following table depicts the scoring definition for this parameter. It will be critical to choose a balloon with a maximum burst altitude score of at least 2 for level 1 success, 3 for level 2 success, and 4-5 for level 3 success. These maximum burst altitude were listen on the balloon provider's website, and were tested using a payload with mass of approximately 3 kg.

Maximum Burst Altitude [km]	35-40	30-35	25-30	20-25	15-20
Score	5	4	3	2	1

Table 6. Maximum Burst Altitude Scoring

Mass: Mass is a significant parameter when it comes to balloon choice because it directly effects the downward force acting on the balloon system. A heavier balloon will require a greater lift force to increase its altitude, which will require more force to be generated. It is difficult to generate large amounts of lifting force in the low-pressure and low-density environment of the stratosphere, and so it is desirable to require as little lift as possible. The minimum mass listed is only 1,000 g, since lighter balloons are not capable of maintaining altitudes required by this project. With this in mind this parameter was given a weight of 0.15.

Mass [kg]	1.0-1.4	1.4-1.8	1.8-2.2	2.2-2.6	2.6-3.0
Score	5	4	3	2	1

Table 7. Balloon Mass Scoring

Cost: The cost of the chosen balloon is a significant parameter due to the single-use nature of the mission; the payload and balloon will not be recovered. Per customer request, the total cost per launch shall be no more than $2,000. For this reason, this metric was given a weight of 0.2. The scoring table for the cost metric can be found below.

Cost [$]	61-120	121-180	181-240	241-300	301-360
Score	5	4	3	2	1

Table 8. Balloon Cost Scoring

Scoring

Using the above tables from the metrics section, (tables 5 - 8) the following trade study matrix was created and analyzed. Table 9 displays that the HAB-TX-1500 balloon will best fit the mission requirements needs in terms of facilitating the desired altitudes, as well as minimizing mass and cost. The HAB 1000 trails by only 0.15 points, and will be considered if the total mass of the payload is sufficiently low.

Category	**Weight**	**HAB 1000**	**HAB-TX-1500**	**HAB 3000**
Min Burst Altitude	0.35	4	4	5
Max Burst Altitude	0.30	4	5	5
Mass	0.15	5	4	1
Cost	0.20	5	5	1
Total Score	**1.00**	**4.35**	**4.5**	**3.6**

Table 9. Balloon Selection Trade Study Matrix

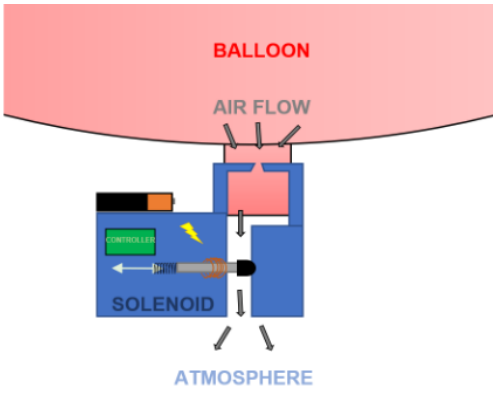

Figure 7. Proposed vent with a solenoid valve.

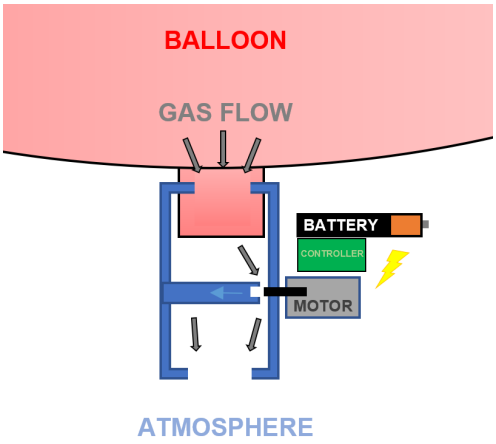

Figure 8. Proposed vent with electric motor.

3.3. Vent Design Process

3.3.1. Solenoid Valve

Two main types of solenoid valves will be considered in this section: direct acting valves and pilot-operated valves. Solenoid valves operate by energizing an electromagnet[15]; this generates a substantial magnetic field, which pulls the flow-halting device out of the flow path. This allows venting to occur. Once the electromagnet is no longer energized, the spring returns to its usual position and the flow is halted. This configuration would need a significant power source to generate the electric field and also a controller to operate the solenoid when needed. This is an active valve, meaning that knowledge of the balloon's pressure and surrounding atmosphere is needed.

Direct acting solenoid valves are mostly used in small-size (diameters typically under 25 *mm*), low pressure environments. This valve is able to open with zero pressure. It is faster than other solenoid valves in terms of valve connection and disconnection. Power consumption for this valve can be relatively high, ranging from 5 to 20 W. One of the main problems with this design is that end-of-life venting will require a significant amount of power; it will be necessary to terminate flight when there is still enough power to sufficiently vent the balloon.

Pilot-operated solenoid valves are typically used in large diameter and high pressure conditions. Pilot pressure is required for this type of valve in order for it to be opened. Power consumption for this valve is low (0.1-0.2 W). Due to the high-pressure requirement of this valve, though, it will not be considered further within the design space. The valve used in the HYFLITS design has a similar design to this one. Similarly, a servo spins and either opens or closes the gap to allow air to flow or be contained respectively. The difference it that the HYFLITS has a valve that operates vertically and is constantly drawing power to push up against the opening. In this design, it will be improved so that there is no waste of power.

Pros	Cons
Reliable actuation	Requires significant battery power
Valve housing is typically included	Requires logic controller

Table 10. Solenoid Valve Pros and Cons

3.3.2. Electric Motor

The primary type of valve used with electric motors utilizes a linear motion. Linear electric valves are used with globe, diaphragm, pinch, and angle valves[13]. These type of valves use a sliding stem that opens or closes a valve. Linear type actuators require tight tolerances, since any leakage will pose a large problem. As seen in Fig. 8, the valve operates by simply pushing or pulling a valve in front of the gas flow with an electric motor. These valves are highly reliable and can be precisely controlled. Electric motors such as servos offer the benefit of intermediate position control. This would allow a logic controller to place the valve in a partially open or partially closed state, which will be useful during end-of-life venting.

These valves are actively controlled; this means that a logic controller with knowledge of the local conditions must also be placed on board. While there is a wide variety of electric motors, the varieties available to use in terms of size and weight have limited closing power. This could be a potential issue as higher pressures may be needed to generate the required force. Another quality to consider is the actual valve mechanism used with an electric motor. To utilize this configuration, a unique housing and valve design would need to be integrated with the motor. This design introduces greater possibility for leaks to occur. This contrasts with the previous design, since valve-solenoids are typically sold as single units with their housing.

The main benefit to using electric motor valves is that many of them require power only while they open or close; this is desirable over the solenoid valves because they require power throughout the entire duration they are acting against the spring.

3.3.3. Venting Control Trade Study

Metrics

In considering the venting control trade study, the following metrics were investigated: mass, power, cost, and reliability. These metrics will be explained and analyzed in the following sections.

Mass: Mass is a critical element for every trade study, since any excess mass will make lift generation significantly more difficult. The mass of solenoid valves and of electric motor valves were investigated independently. While these valves come in a very wide range of sizes, typical masses of valves that may be feasible in this design were research extensively. It was found that solenoid valves have a typical mass of around 0.1 kg, and electric motor valves have a typical mass of around 0.3 kg. These are rough estimates, and will be narrowed down at a future date. Since these masses are relatively low compared to the payload and balloon mass, the weight for this metric will be only 0.15; metrics such as power, cost, and reliability will be much more significant for this design.

Mass [kg]	0.00-0.15	0.16-0.30	0.31-0.45	0.46-0.60	0.61-0.75
Score	5	4	3	2	1

Table 11. Venting Mass Scoring

Power Consumption: The operational lifespan of the balloon is dictated in part by power from the batteries. Therefore, reducing power consumption will extend the operating time of the balloon system. A valve that uses more power will require a more powerful battery, which will increase weight. Reducing power usage needed for the valve would allow more power to be used in the orbiting system and sensing devices. Power will be one of the more significant parameters when it comes to venting decisions, and as such earns a weight of 0.3.

The main difference when it comes to the two valve types, in terms of power, is that the solenoid valve requires power throughout the entire venting process. The electric motor valves, on the other hand, require power only while shifting the flow-halting device; in other words, the electric motor valves require power over much smaller time duration than the solenoid valves. In order to determine how much more total power the solenoid valve requires, it would be necessary to know the amount of time it takes for the balloon to vent to neutral buoyancy. For this reason, power consumption will be scored quantitatively based off of the typical wattage of each option.

Power Consumption [W]	0.0-2.1	2.1-4.0	4.1-6.0	6.1-8.0	8.1-10.0
Score	5	4	3	2	1

Table 12. Venting Power Scoring

Cost: Cost is a significant metric for the system since the project is aiming to minimize the cost per launch; per customer request, the cost per launch should be at most $2,000. Valves vary significantly in cost based on quality of construction and complexity. Cost is of roughly the same significance as the mass and power consumption metrics. For this reason, the cost metric for this design space earns a weight of 0.2.

While each type of valve comes in very wide price ranges, it was generally found that solenoid valves are slightly less expensive than similar electric motor valves.

Cost [$]	0-10	10-20	20-30	30-40	40+
Score	5	4	3	2	1

Table 13. Venting Cost Scoring

Seal Reliability: Reliability of the venting system does not relate the lifespan of the valve, but rather how much confidence can be instilled in it to function without significant leakage. Since leakage will make it significantly more difficult to achieve desired altitudes, this metric earns a weight of 0.4.

Many manufacturers produce solenoid valves that would easily be implemented into the balloon system. Electric motors, on the other hand, would need to be integrated into a valve system which could add larger uncertainty towards the confidence in the seal.

Valve Leakage Likelihood	Highly unlikely	Unlikely	Uncertain	Likely	Highly Likely
Score	5	4	3	2	1

Table 14. Seal Reliability Scoring

3.3.4. Scoring

In considering the metrics outlined in the previous sections, a trade study matrix was developed in order to analyze the optimal venting system. It was found that a solenoid valve would be best suited for this mission due to its low mass, low cost, and high seal reliability. The electric motor, however, trailed by only 0.3 points. This suggests that if any complications arise while developing the solenoid valve, the electric motor may be reconsidered. Shortly after completing this trade study, however, it was determined that the same venting system from the HYFLITS mission would be used. This was determined since the low-mass HYFLITS valve has flight heritage and is reliable.

Category	Weight	Solenoid Valve	Electric Motor
Mass	0.20	5	4
Power Consumption	0.20	2.5	5
Cost	0.20	4	3
Seal Reliability	0.40	5	4
Score	**1.00**	**4.3**	**4.0**

Table 15. Venting Options Trade Study Matrix

3.4. Tether Design Process

3.4.1. Initial Tether Design Trade Study

Static Fixed-Length Tether: The static fixed length tether is the simplest of the three designs under consideration. This design will require a tether length to be determined prior to launch, based on the given mission profile. As shown in Figure 9 the tether may be as long as 10 m to meet the orbiting requirements of the payload with the largest anticipated balloon diameter. Given a maximum potential length of 10 m it may be stated that launch operations will require a minimum of 10 linear meters to prepare the vehicle for launch. In the event that the balloon is launched under high winds it may not be possible for one person to complete the launch independently. Additionally, when transporting the system to a launch site the tether will have to be stored, likely on a spool. Manually removing the tether from its storage device will add time and complexity to the launch. However, this tether design has the lowest likelihood of introducing knots, snags, and tangles (i.e. proper deployment) to the tether during the launch procedure. Once launched, the tether will remain at the predetermined length and will not consume any power or resources from the systems onboard. Additionally, since there is no deployment during launch, this style of tether is the easiest to manufacture.

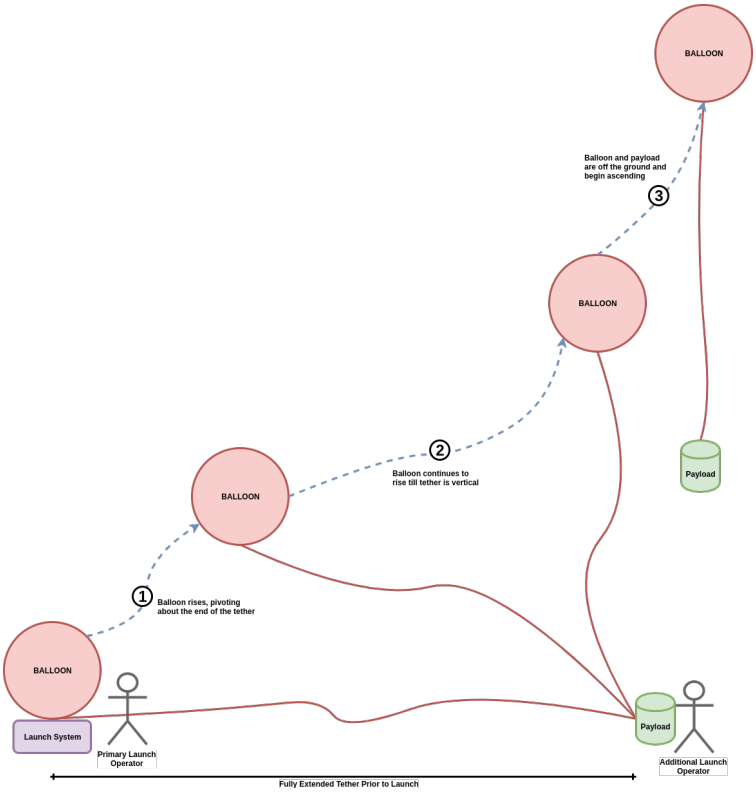

Figure 9. Static Fixed-Length Tether Deployment

Pros	Cons
Minimal chance of tangling	Difficult to launch
Easy to manufacture	Fixed length in flight

Table 16. Static Fixed-Length Tether Pros and Cons

Passively Unspooled Tether: The passively unspooling tether uses a fixed length tether like the static fixed-length tether, but it deploys to its final length passively during the launch process. The length of the tether will be predetermined for a given mission profile. Once the tether length has been determined the tether will be installed onto a spool deployment system. This deployment system will allow for the tether to deploy automatically as the balloon rises during the launch without any operator management. The spool additionally will serve to transport the tether, removing a step from the launch procedure when compared to the static fixed-length tether. Due to the compact nature of the spool tether deployment, the launch process will be manageable by a single person and will not require a large launch site. Despite the advantages in launch logistics that are offered by this solution, it does present some additional risk with respect to tether tangling during deployment of the tether at launch. This risk is fairly low however, as the spool deployment method has decades of documented success in applications such as sewing machines and fishing pole reels. After launch there is no opportunity to adjust the tether as it is of a predetermined and fixed length.

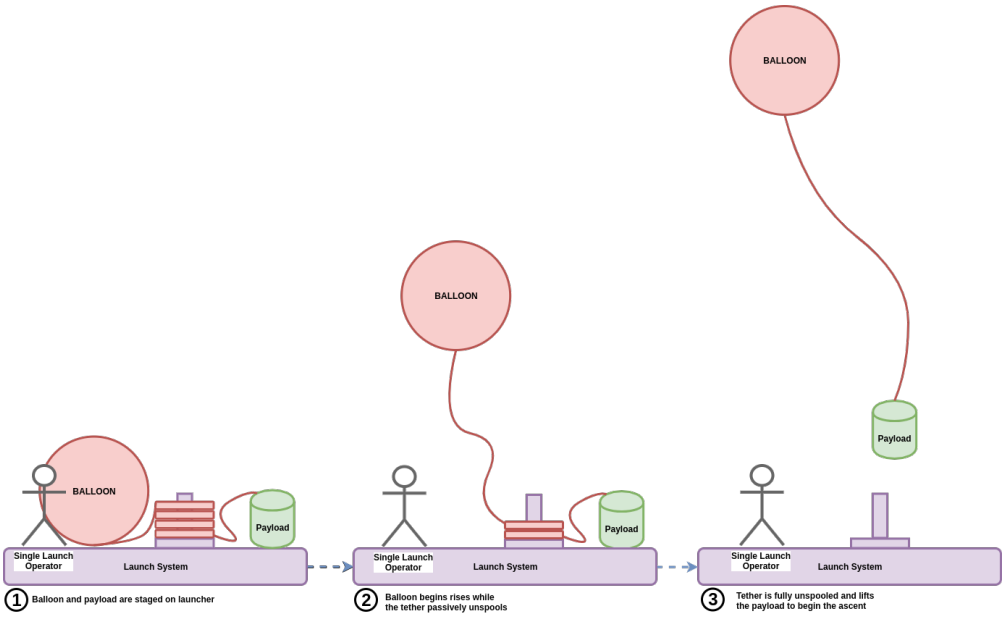

Figure 10. Passively Unspooled Tether Deployment

Pros	Cons
Small launch footprint	Potential to tangle
Simpler in construction than winch	Fixed flight length
Integrated transport and launch spool	
Easier to launch	

Table 17. Passively Unspooled Tether Pros and Cons

Dynamically Unspooled Tether: The dynamically unspooled tether consists of a method to fully deploy the tether on command after the balloon has been launched. Of the three options this is the most space efficient and the easiest to launch; the tether does not add any hazard to launch operations. After a successful balloon launch, the tether would be unspooled to the target length through the use of a winching device. The use of an onboard winch also permits the tether length to be adjusted mid-flight if desired. However, the inclusion of a winch onboard adds additional mass to the system and will consume some of the limited electric power from the batteries to operate. Additionally, winch controls will need to be developed, which adds to the software and telemetry complexity. This method has a fairly low likelihood of getting tangled as the tether will remain taught due to the weight of the payload, however the addition of a winch provides another point of mechanical system failure. The primary failure concern will be turbulence during winch deployment, as a decrease in the force exerted on the tether may cause the winch to free spool, causing a jam. In the event the winch fails to deploy at all, the mission would be limited to a single data collection on descent as the orbiter would not have freedom to orbit.

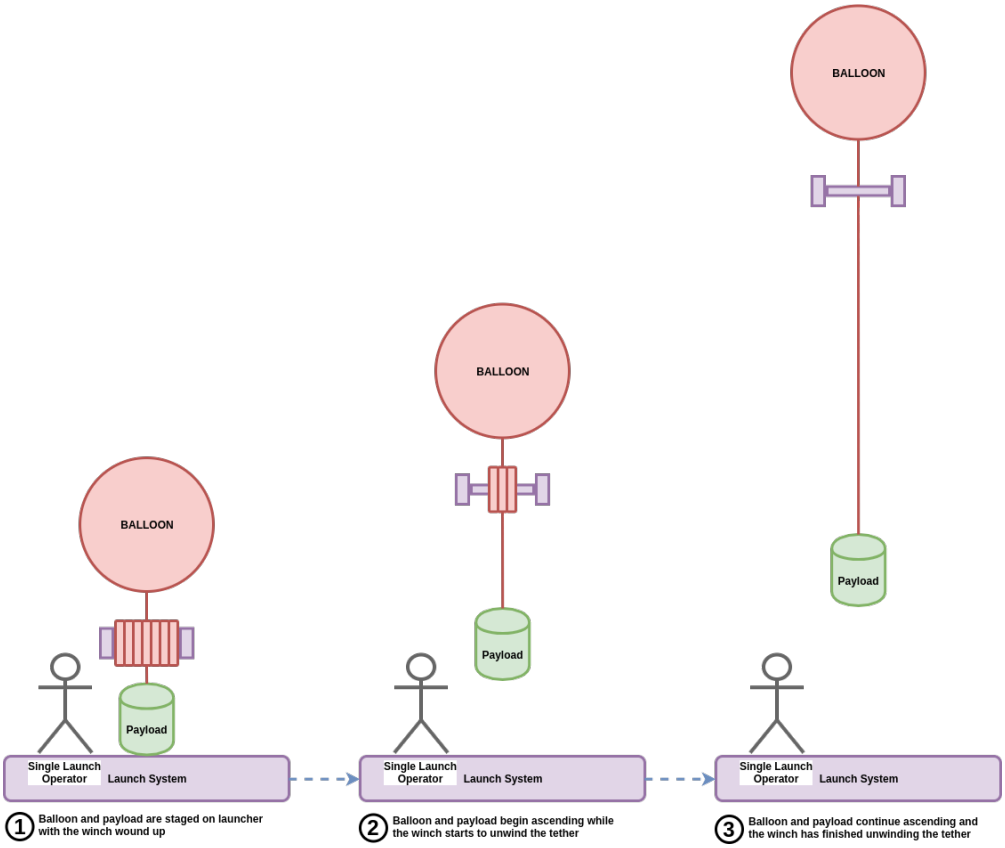

Figure 11. Dynamically Unspooled Tether Deployment

Pros	Cons
Low tangle likelihood	Adds mass and complexity
Easy to launch	Uses onboard power
Dynamic tether lenght during mission	

Table 18. Dynamically Unspooled Tether Pros and Cons

Metrics

The tether metrics analysis is purely qualitative, due to the subjective nature of the tether trade study. While there will be numerical analysis in a later section to select an appropriate material, the most challenging design choices that accompany the tether are currently non-numerical. A variety of commonplace processes are used as stand-ins for expected performance, and all three designs present the opportunity for rapid prototyping, testing, and refinement further in the design process.

Ease of Launch: Per customer requirement the balloon and orbiter system must be easy to launch. Ideally launch operations will require no more than one person, but may require two launch operators depending on the chosen design. The primary contributor to the number of launch operators required for a standard launch is the size of the launch area. If a given design permits launch entirely from a man-portable launch platform it can be operated by a single operator. However, if a tether needs to be extended (fully or partially) additional launch operators may be required to facilitate the launch, especially during inclement weather. For these reasons, the ease of launch metric earns a weight of 0.5. This is the most significant metric for the tether design space. The five scoring categories for ease of launch are outlined below.

Two-Phase Launch - 5: The two-phase launch is the highest score possible in this category. To meet this score

requirement the launch may be completed from a self contained launch platform by a single operator in two distinct phases. The first phase consists of installing the balloon to the launch platform and filling the balloon to the desired volume. Phase two releases the balloon, after triggering the release the launch operator is has completed the launch.

Two-Phase+ Launch - 4: The two-phase+ launch is identical to the two-phase launch except it requires the operator to trigger the deployment of the tether after balloon release. This is primarily a concern for the active winch deployment method, but depending on the final design of the launch platform it could also describe the passively unspooling launch.

One+ Operator Launch - 3: This launch can be easily completed by a single operator under standard launch conditions. Standard launch conditions require low winds and a large launch site. In the event of launch during inclement weather or in an enclosed launch site another launch operator may be added to help ensure mission success.

Two Operator Launch - 2: The two operator launch will require two operators to ensure mission success regardless of launch conditions.

Three Operator Launch - 1: This launch will require three or more launch operators to successfully launch the balloon and payload under all circumstances. This is in clear violation of customer requirements and will be avoided at all costs.

Ease of Launch	Two-Phase	Two-Phase+	One+ Operator	Two Operator	Three Operator
Score	5	4	3	2	1

Table 19. Ease of Launch Scoring

Mass: Due to the limited mass budget, it is critical to minimize dead weight on both the balloon and payload. Any additional weight will require more helium to lift to the target altitude and will require the controlled ascent subsystem to lift more mass, which will slow the ascent and consume more power. For this reason, the mass metric earns a weight of 0.2 for this design space. The categories are divided by mass added to the system, since both the static tether and passively unspooled tether require no additional mass on the system, they have achieved the maximum score. Standard hobby-sized winches weigh anywhere from 50 *g* to 100 *g*. In this preliminary state, it is assumed a typical hobby winch with a mass of approximately 75 *g* is to be used for the active unspooling launch.

Airborne Mass [g]	0-24	25-49	50-74	75-99	100+
Score	5	4	3	2	1

Table 20. Tether Mass Scoring

Tangle Likelihood: A tangled tether has the potential to ruin the mission by limiting the payload to a reduced orbit. While this is a very important parameter, it is closely related with ease of launch. If launch goes smoothly, there will be a lower likelihood of tangled tethers. For this reason and because ease of launch is already weighted heavily, the tangle likelihood metric earns a weight of 0.1. Tether designs are ranked based on the likelihood of a tangle during launch and deployment. The following is used to describe the chance of tangles for a given design:

No Tangles - 5: To achieve a maximum score in the tangling category there will be no chance of tangling the tether during launch or deployment. This requires a manual deployment of the tether on the ground by a launch operator.

Low Likelihood Tangles (Fixable) - 4: Tangles are permitted so long as there is a low chance that there will be a tangle, if a tangle occurs it will be fixable by the launch operator.

High Likelihood Tangles (Fixable) - 3: Tangles are permitted. There is a high chance that there will be a tangle, though if a tangle occurs it will be fixable by the launch operator. This is preferred over the low likelihood non-fixable as it delays launch but does not impact mission success.

Low Likelihood Tangles (Non-Fixable) - 2: Tangles are permitted so long as there is a low chance that there will be a tangle, if a tangle occurs it will not be fixable by the launch operator and may impact mission success.

High Likelihood Tangles (Non-Fixable) - 1: Tangles are permitted so long but there is a high chance that there will be a tangle, if a tangle occurs it will not be fixable by the launch operator and may impact mission success.

Tangle Likelihood	No Tangles	Low (Fixable)	High (Fixable)	Low (Non-Fixable)	High (Non-Fixable)
Score	5	4	3	2	1

Table 21. Tangle Likelihood Scoring

Transportability: Transportability reflects ease of transport and the transition from transport to launch. Transportation systems that also function in a launch capacity are preferred over those that require uninstallation from a transportation system prior to launch. Furthermore, systems that must be uninstalled and reinstalled onto another launch device are less preferred that those that require only uninstallation. For these reasons, the transportability metric earns a weight of 0.2.

Transportation is Launch System - 5: The tether will be installed into the launch system and transported in that configuration. The tether is ready to be launched with no additional steps.

Transportation is Launch Compatible - 4: The tether will be installed into a separate component of the launch system. The separate component will need to be integrated into the launch system prior to launch.

Uninstallation Only - 3: The tether will need to be uninstalled from the transportation system to launch. Once removed from the transportation system it is ready to launch.

Direct Reinstallation to Launch System - 2: The tether will be transported independently from the launch system. Prior to launch the tether will be uninstalled from the transportation system and reinstalled directly onto the launch system

Indirect Reinstallation to Launch System - 1: Tangles are permitted so long as there is a low chance that there will be a tangle, if a tangle occurs it will not be fixable by the launch operator and may impact mission success.

Transportability	Launch System	Launch Compatible	Uninstallation	Direct Reinstallation	Indirect Reinstallation
Score	5	4	3	2	1

Table 22. Transportability Scoring

Scoring

Considering the metrics outlined in the previous sections, a trade study matrix was created and analyzed. It was found that the statically unspooling tether is the best of the considered designs. The combination of high transportability, low likelihood of fixable tangles, no additional mass, and single operator launch represent the best combination of desired performance characteristics.

Category	Weight	Static Tether	Passively Unspooled Tether	Dynamically Unspooled Tether
Ease of Launch	0.50	1.5	4.5	4.0
Mass	0.20	5.0	5.0	4.0
Tangle Likelihood	0.10	5.0	4.0	2.0
Transportability	0.20	3.0	5.0	4.0
Score	**1.00**	**2.85**	**4.65**	**3.80**

Table 23. Tether Design Trade Study Matrix

3.4.2. Tether Design Refinement

Onboard Deployment

Figure 12. "COTS" Radiosonde Payload with Onboard Deployment Spool

Upon customer request, research and analysis was conducted with focus on the viability of passive airborne tether deployment methods. This request stemmed from a predicted tether length in the tens of meters, which posed a serious risk for complications with the environment during initial system launch. It was found that a simple spool based deployment system is frequently used when launching Commercial Off The Shelf (COTS) sounding payloads, similar to the Radiosonde RS41 in Figure 12.

These sounding payloads traditionally have a mass of approximately 100 g and reliably deploy tethers with lengths in excess of 50 m. This design was set aside as further analysis on the lifting body reduced the HALO tether length to 4.96 m, which the customer decided was suitable for a ground based tether deployment. Due to the significant increase in the mass of the HALO system compared to the sounding payloads (1500 g vs 100 g), testing would be in order to ensure deployment would not be too rapid.

Ground Based Deployment

From the analysis done during CDD it was determined that the passively unspooling tether provided the best solution to the tether problem. Storing the tether on a ground based spool prior to launch makes it easy to manage both in the staging process, for example at the CU Aero Building, and during launch operations. During launch the prewound tether will be connected to both the payload and the balloon prior to filling the balloon with helium. With a maximum tether length of roughly 5 m full deployment should be rapid enough to prevent snagging in nearby trees, provided the launch team chose an appropriate launch site and time. Launch should be conducted with winds not in excess of 5 *knots* and in an open field. More obstructive launch sites may be used at the discretion of the launch team if winds permit.

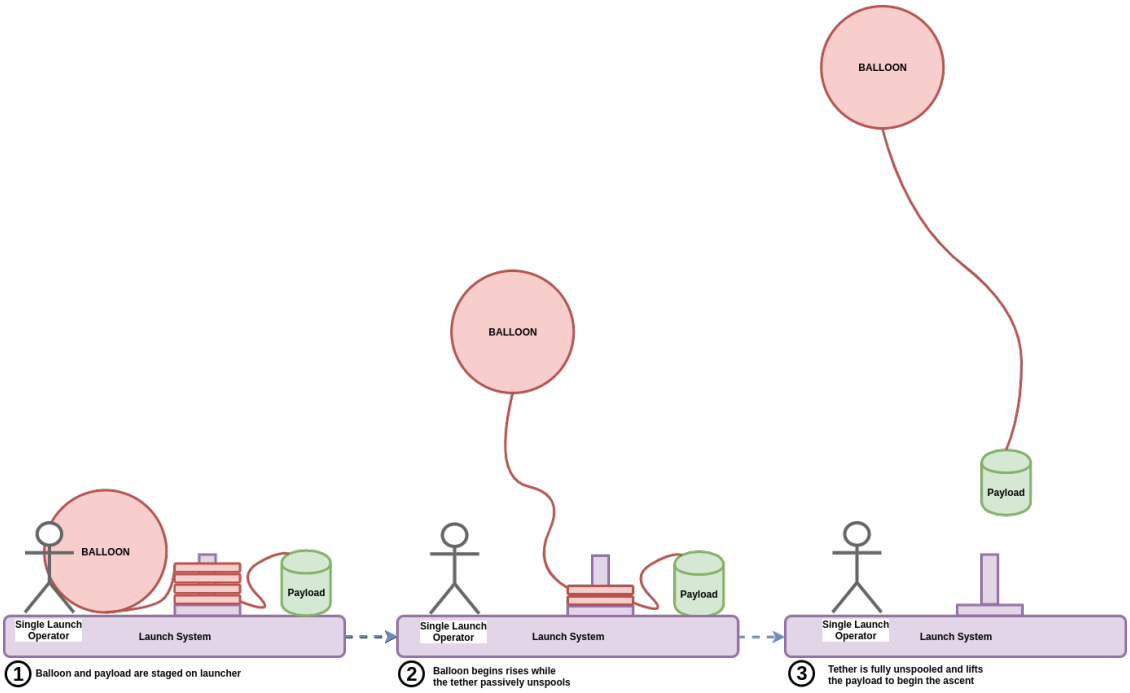

Figure 13. Chosen Passive Tether Deployment System

3.4.3. Final Tether Design

Tether Materials and Components

The tether will be composed to two separate tether lines. The first tether provides the mechanical strength to bear the tension loads as the payload orbits. The second is a non-load bearing tether that carries the communication lines from the sensor suite to the vent subsystem on the balloon. Also inline with the tether is a small parachute, which comprises the controlled descent and arrest system (CDAS).

Load Bearing Tether

The load bearing tether provides the mechanical strength to support the payload during orbiting procedures. This tether will be composed primarily of high tensile strength Kevlar twine, with a dynamic capacity of roughly 150 *lbs*. Kevlar was chosen as the primary tether material as it remains flexible and unaffected by the extremely low temperatures that will be experienced during the flight. On either end of the tether is a swivel from a fishing line application. These are rated to 50 *lbs* from the manufacturer and will both prevent the tether from twisting during orbit and also ensure the tether meet the 50 *lb* impulsive requirement from the FAA. Fishing swivels were adopted here in conformance with best practice determined by organizations such as NOAA and NCAR, as the FAA has failed to provide a time for the force to be applied, thus incompletely defining the impulsive requirement. The CDAS will also be installed inline with the load bearing tether. Figure 14 shows the planned attachment of the load bearing tether to the payload, with the Kevlar tether represented with yellow twine.

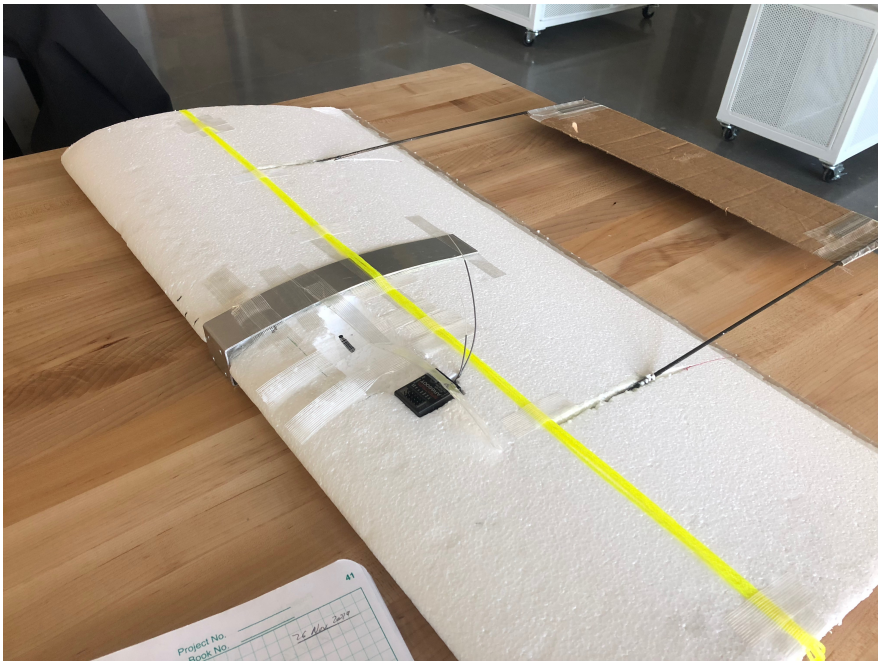

Figure 14. Example of Tether Attachment to the Payload from the Preliminary Orbit Acquisition Test

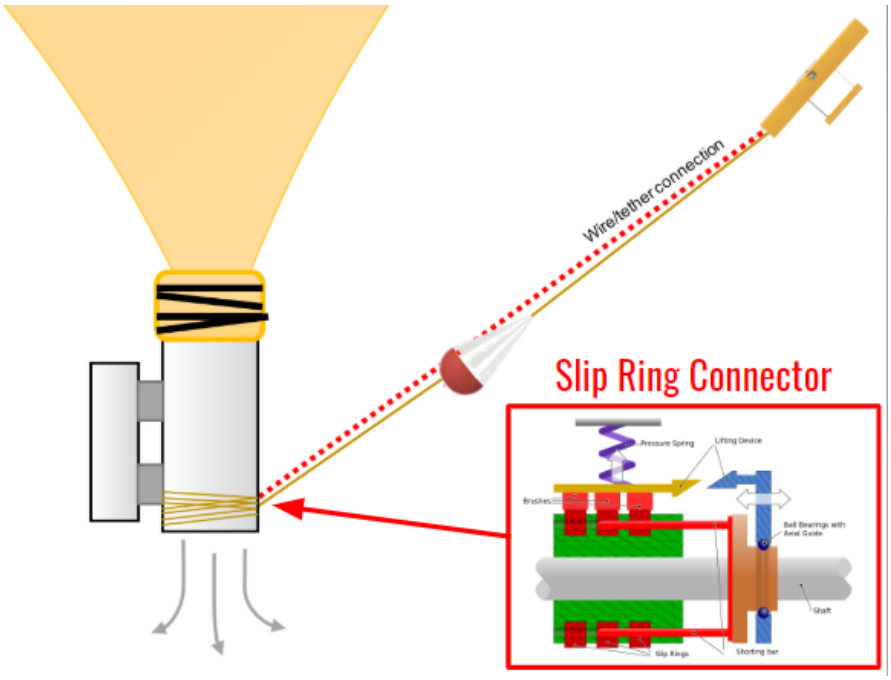

Figure 15. Tether Affixed to Balloon Vent

Non-Load Bearing Tether

The communication lines dictate the use of a non-load bearing tether that runs parallel with the load bearing tether. This tether element consists of the power and communication lines that permit the sensor package in the orbiter to send commands to the vent subsystem on the balloon. The balloon side of this tether will have a slip ring mounted to the vent, which will allow rotation of the communication lines to prevent twisting during orbiting phases of flight. To ensure that this tether is not placed under load it will be 15% longer than the load bearing tether.

Controlled Decent and Arrest System (CDAS)

The Controlled Decent and Arrest System in installed inline with the load bearing tether, between the tether and the balloon. It consists of a single model rocket style parachute and will deploy passively in the event of balloon failure. Mounting the parachute inline with the load bearing tether ensures that the parachute remains closed during flight, as the tension parachute will experience is the same tension that the tether will experience. The CDAS parachute is mounted as close to the balloon as possible to minimize the relative wind experienced by the parachute, as the tether sweeps a smaller arc at a lower velocity closer to the balloon.

Figure 16. Example CDAS Parachute in the Deployed State

3.5. Lifting Orbiter Design Process

The main objectives of this project are to record data outside of the balloon's wake and to control multiple autonomous ascents and descents between 25 *km* and 35 *km*. In order to achieve these objectives, a system which orbits below the balloon needed to be developed. Additionally, there must be a method of autonomously controlling the overall altitude of the balloon based on sensory measurements. The orbiter must be capable of providing a force great enough to move out of the balloon wake, and the lifting capabilities must be great enough to bring the entire balloon system to an ascent or descent rate of roughly 2 $\frac{m}{s}$. This will prove to be difficult due to the relatively large drag force caused by the large surface area of the balloon at high altitudes. Further, it was critical that the sensory measurement devices are moving in a stable manner as not to corrupt any recorded turbulence data. The following sections seek to explore designs capable of achieving these feats.

3.5.1. Lifting Orbiter Design Alternatives

Wing with Mounted Propeller

With this design, the orbiter will take the shape of an airfoil with a mounted propeller. In conjunction with a tether attachment, this will allow the airfoil to maintain circular motion around the wake of the balloon. Further, the angle of attack of this airfoil will be autonomously controlled in order to affect lift forces on the entire balloon system. This autonomous control will be actuated by a servo that will change the airfoil angle of attack based on altitude measurements from the GPS device. In order to ascend, the airfoil will increase the angle of attack from level to a desired angle to increase the lift on the payload. After the peak is reached, the wing would rotate to a negative angle of attack and provide negative lift, taking the balloon down to the valley of the flight profile.

The lift generated from this airfoil, as well as airfoils described in later designs, will be approximated using Equation 1.

$$L = \frac{1}{2}\rho V^2 S C_L \tag{1}$$

In this equation L is the lift generated by the airfoil, C_L is the lift coefficient of the wing, ρ is the ambient air density, V is the airfoil speed, and S is the airfoil area. Since air density at altitude may be less than 1% of air density on the ground[5], it will be difficult to generate this lift. Similarly, the drag on the balloon will be needed to be accounted for which can be found through Equation 2 below.

$$D = \frac{1}{2}\rho V^2 S C_D \tag{2}$$

To find the velocity that the airfoil will need to fly at to maintain a circular motion, Equation 3 can be used in conjunction with the horizontal force component of the tether to balance the forces. The propeller will provide the needed thrust to balance the wing drag and prevent orbit decay.

$$F_{radial} = m_{payload} \frac{V^2}{r_{orbit}} \tag{3}$$

In this design and the final design, propellers are being used. In order to conduct a proper force analysis, the thrust of the propeller must be analyzed. This will be done by modeling the propeller blades as airfoils which produce lift and push the plane along in its path. These airfoils will be modelled in a CFD program such as XFLR5 to get the respective coefficients of lift and drag to complete this analysis.

A series of calculations would need to be conducted in order to determine the required area for the wing. These calculations will be covered in more detail in Section 6.4. This ends up becoming the final design chosen with slight modifications such as adding a tail and elevators and well as changing the tether mounting location. A diagram indicating the initial setup is shown in Figure 17.

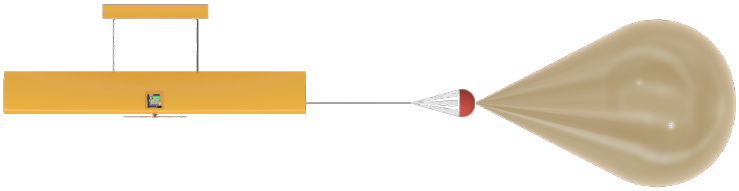

Figure 17. Wing with Mounted Propeller Design

Pros	Cons
Uses less power for lift	Difficult to initially acquire orbit
Can be modelled similarly to a plane	Will require a complex control system
All components are located in one place	Hard to generate lift / requires large wings

Table 24. Wing with Mounted Propeller Pros and Cons

Lifting Wing on a Rotational Tether

This design is centered around a high mounted motor. A tether will extend from the motor to the airfoil, actuating the necessary rotational motion of the orbiter. Similarly to the previous design, the angle of attack will then be autonomously controlled by a servo in order to generate positive or negative lift with regard to altitude measurements. The main advantage of this design is that wind perturbations will have a less significant effect; the spinning motor will recover circular motion much more quickly than the wing with a mounted propeller.

The main difficulty with this design is that the high mounted motor will naturally twist the balloon throat; it will be necessary to determine whether this twisting will significantly harm the balloon.

Similar to the first design, Equations 1-3 will be utilized when approximating the necessary orbiter rotational speed.

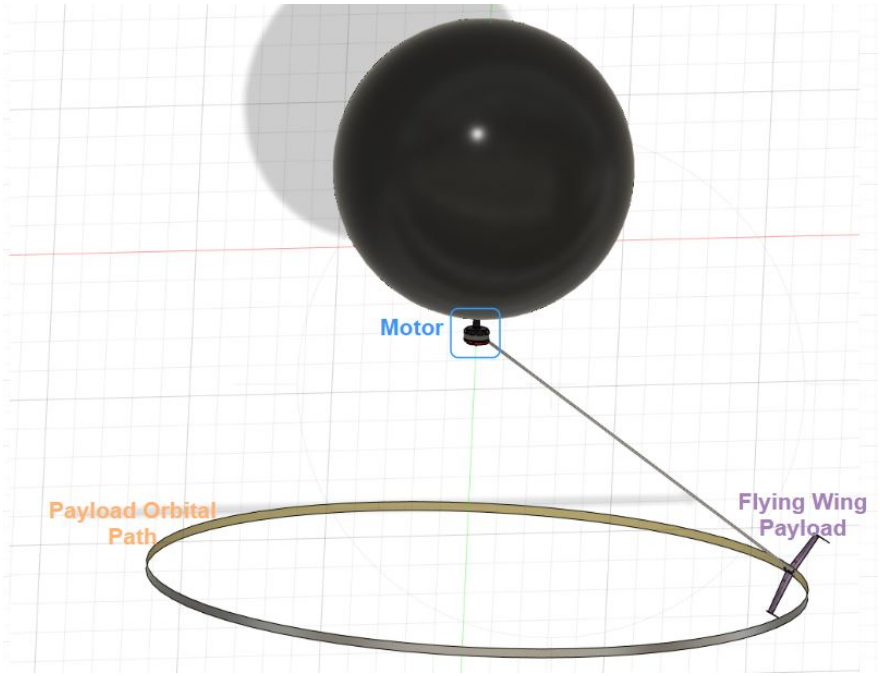

Figure 18. Lifting Wing on a Rotational Tether Design

Pros	Cons
Easy to restart motion if perturbed by wind	Complex control system
Easily modelled	Requires large wings
No propeller analysis	Motor will be high mass
	May twist balloon throat

Table 25. Lifting Wing on a Rotational Tether Pros and Cons

Separate Orbiter and Altitude Control Motors

This design is a direct continuation of the previous design. The primary difference is that this design implements a separate lifting force via a tethered propeller and motor system. This propeller and motor system will be tethered to the high mounted motor as shown in Figure 19 which will eliminate the need for lift force from the orbiter. This vertical tether could be replaced by a solid rod if deemed appropriate. The second tether will attach the orbiting payload to the high mounted motor as in the previous design. The motor will rotate the tether which will then move the payload outside the wake in a circular orbit.

This design comes with significant trade offs. Its biggest advantage is that the lifting source is acting directly upwards/downwards for more lift. The airfoil in this design is primarily for stability, and is not required for lift generation. This, in turn, means that the wing will not need to be nearly as large as in the previous two designs. This propeller and motor system will contribute significantly to the mass budget, and must be evaluated thoroughly for feasibility. If necessary, mass could be reduced by removing the airfoil and only orbiting the sensor suite.

Similarly to the first design, the propeller analysis will have to be modelled as sections of an airfoil to approximate the necessary propeller rotational speed. Figure 19 displays the proposed separate orbiter and altitude control system design. A wing is displayed in this figure, and is not designed to generate lift. If deemed necessary, however, it could generate lift by autonomously controlling its angle of attack, as in the previous designs.

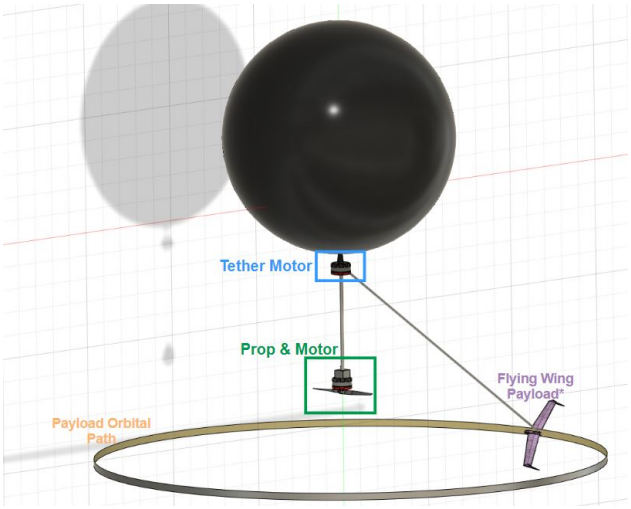

Figure 19. Separate Orbiter and Altitude Control System Design

Pros	Cons
Separate components can be simpler to work with	Two motors could yield high mass and power consumption
Primary lifting force parallel to Z axis	High RPM speeds that some motors can't handle
Easy to start orbiting and rising	Tethers could intersect and tangle

Table 26. Separate Orbiter and Altitude Control System Pros and Cons

In conjunction with this design, preliminary research on different motor types was conducted: specifically, high kV and low kV motors. Their brief specification for further investigation are located below.

High kV Motor	Low kV Motor
Faster RPM w/small props	Low RPM w/larger prop
Low Torque	High Torque
Mass Heavy	Light

Table 27. Motor Choice

Lifting Orbiter Trade Study

Metrics

In this section, the scoring system will be based on potential levels of success. Any metric with a score of 5 will be ideal for achieving the highest level of success, level 3. Any metric with a score of 4 will be capable of reaching the highest level of success, but ideal for the 2nd level of success. A score of 3 will be capable of reaching the 2nd level of success, but ideal for the 1st level of success. A score of 2 will be capable of reaching the 1st level of success, but not ideally. A score of 1 indicates a design option which will likely not be chosen, as it would require significant trade-offs in order to be suitably implemented.

This is not a perfect scoring system by any means, but it will serve as a baseline for determining the true meaning of an option's score. It is especially difficult to rate qualitative metrics on this scale, though an attempt will be made. For the lifting orbiter trade study, the following metrics were deemed relevant: control system complexity, mass, power consumption, and cost.

Control System Complexity: Control system complexity is an integral factor when considering the best lifting orbiter design. The Wing with Mounted Propeller and Wing on a Rotational Tether designs both require an effective control system; they must be maintaining specific orbiter angles of attack while remaining stable under wind perturbations. If anything goes wrong with these control systems and the payload does not properly orbit, then no lift will

be generated and the mission will be a failure. The third design, however, does not require a very advanced control system because the orbiter is not the primary lifting force. Even if the orbiter fails, the balloon will still be able to lift itself to target altitudes. For these reasons, the control system complexity parameter will earn a weight of 0.1.

Requires a Complex Control System?	**No**	**Yes**
Score	5	3

Table 28. Control System Complexity Scoring

Mass: Mass is a significant parameter for every aspect of this mission, since a higher overall mass will require a higher lifting force to effectively control the altitude. This becomes a pivotal system for weight constraints for all other systems. For this reason, the mass parameter has earned a weight of 0.3. The mass of each system will be predicted using typical masses of motors and propellers, as well as an approximated mass of the payload.

The first two designs will have very similar masses; they both require a large airfoil, a motor, and servos to actuate changes in angle of attack. While the third design does include two motors, it will not require a very large wing to operate.

Mass [kg]	0.00-0.60	0.61-0.90	0.91-1.20	1.21-1.5	1.5+
Score	5	4	3	2	1

Table 29. Lifting Orbiter Mass Scoring

Power Consumption: Power consumption is one of the more critical parameters for the lifting orbiter system. Power is required not only for data collection and transmission, but also for driving any propellers and motors - this is expected to be the main power consumer of all systems within the mission. For this reason, power consumption earns a weight of 0.4 for this design space. While this is a necessary parameter to quantify when evaluating the proposed lifting orbiter designs, this proves difficult to measure at this early stage. In light of this, general approximations were made as to the power consumption of each design.

The first design should theoretically require the least power, due to its nature of including only a single propeller on the airfoil. The second design should require the median amount of power, since a motor is driving the circular motion of the tethered-orbiter entirely. The third design will certainly require the most power, as a more powerful motor is implemented for the purpose of generating the desired lift for the balloon system.

Power Consumption [W]	0.0-4.0	4.1-8.0	8.1-12.0	12.1-16.0	16.1-20.0
Score	5	4	3	2	1

Table 30. Lifting Orbiter Power Consumption Scoring

Cost: Cost is also a significant parameter for almost every aspect of this mission, since it is desired by the customer that a single launch will cost no more than $2,000. Further, development and testing for the entire mission must cost no more than $5,000. The altitude control surfaces will be the main source of weight for the payload, and as a result will largely be the main consumer of cost. As a result, this metric earns a weight of 0.2. The HYFLITS balloon and sensor package cost approximately $1,000 per launch. This means that approximately $1,000 more can be spent in developing HALO; the cost scoring stems from this budget constraint.

It is estimated that the first two designs will fall into a score of 4, as they require most of the same parts. Their estimated cost will be somewhere in the $401-$600 range. The third design is estimated to be slightly less expensive despite the addition of a second motor, since the wing will be of a significantly smaller size.

Cost [$]	0-400	401-600	601-800	801-1000	1000-1200
Score	5	4	3	2	1

Table 31. Lifting Orbiter Cost Scoring

Scoring

Based on the above metrics, a lifting orbiter design trade study matrix was developed and analyzed. The Separate Orbiter and Altitude Control system scored the highest with a 3.95; it is predicted to have a simple control system, low mass, low cost, and relatively low power consumption. The score of 3.95 suggests that level 3 success should be achievable. Both of the other two designs trailed only by a small margin which means that if any complications arise with the separate orbiter and altitude control system, these other designs may be reconsidered; this happened to be the case. By not correctly anticipating propeller and motor difficulties, the third design won. After more in depth analysis, though, the models showed that the effective "wobble" that the motor would cause on the balloon neck would cause the propeller to spin sideways not aligned with the vertical axis anymore, which wouldn't generate the needed lift. Additionally, the high RPM of the propeller was not properly analyzed. It was soon calculated that the drag on the propeller blades would cause an excessive amount of torque that the motors couldn't handle. Due to the close scoring of these designs, though, it can be seen that the Wing with Mounted Propeller design was just under the third design. It was easy to switch over to this design and find that it would be more feasible to achieve the needed levels of success. Thus, the Wing with Mounted Propeller design won the trade study. This design was carried out will be fleshed out in the following subsection.

Category	Weight	Wing with Mounted Propeller	Lifting Wing on a Rotational Tether	Separate Orbiter and Altitude Control Motors
Control System Complexity	0.10	3	3	5
Mass	0.30	4	4	4.5
Cost	0.20	4	4	4.5
Power Consumption	0.40	4	3.5	3
Score	**1.00**	**3.9**	**3.7**	3.95

Table 32. Lifting Orbiter Design Trade Study Matrix.

3.5.2. Lifting Orbiter Design

Tether Attachment

In beginning the design of the orbiter subsystem, it was crucial to decide how the orbiter would actually be attached to the tether/balloon system. Through careful consideration, two primary ideas came to the forefront. These two concepts, referred to as Manta Ray and Popsicle attachment, can be found in the following diagrams.

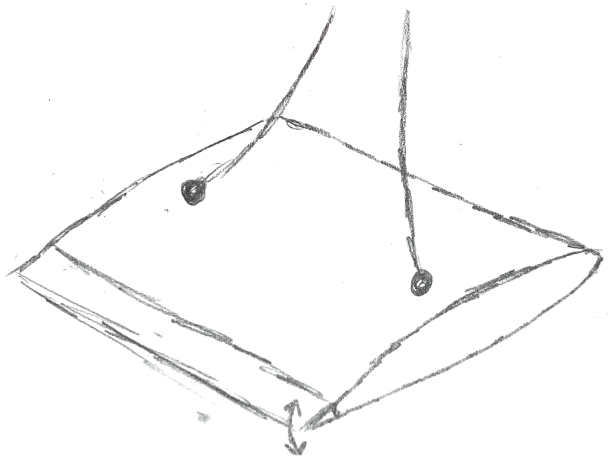

Figure 20. "Manta Ray" Attachment: Fixed Yaw and Roll

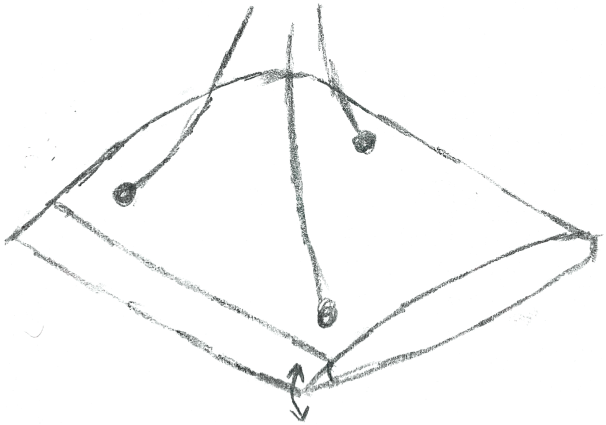

Figure 21. "Manta Ray" Attachment: Fixed Pitch, Yaw, and Roll

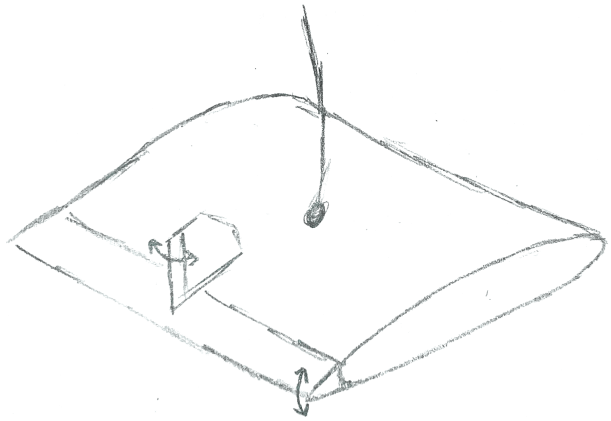

Figure 22. "Manta Ray" Attachment: No Tether Impact on Pitch, Yaw, and Roll

Figures 20, 21, and 22 show proposed tether attachment points for the "Manta Ray" design. In each case the mounting of the tether the effect of imposing different limits on the degrees of freedom available to the orbiter. Figure 20 limits the roll and yaw of the orbiter while permitting pitch to be variable through the motion of an elevator. Figure 21 uses a triply mounted tether, which has the effect of limiting pitch in addition to roll and yaw. In this case the rear control surface functions exclusively as a flap to alter the lift generated by the body for different phases of flight. The final diagram (Fig. 22) shows a single centrally located tether mount. In this configuration pitch, roll, and yaw are all unconstrained by the tether, so the addition of a rudder would be necessary ensure control of the orbiter.

The other design proposed, and eventually chosen, was the "Popsicle" design where the tether attaches to the side of the wing much like a popsicle stick is attached to the popsicle. This configuration is shown in Fig. 23. When orbiting in this configuration, the centripetal force will constrain the roll and yawing maneuvers leaving only the pitching moment to be controlled.

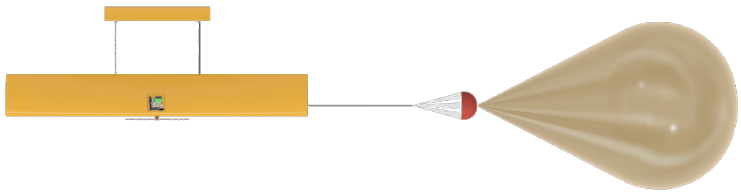

Figure 23. "Popsicle" Attachment

These different attachment methods have unique pros and cons. The Manta Ray attachment style maintains a lift vector which is in line with the tension force from the tether; this case is ideal for long tethers with a nearly vertical orientation. The Popsicle attachment style maintains a lift vector which is perpendicular to the tension force from the tether; this case is ideal for shorter tethers with nearly horizontal orientations. In order to decide which attachment style was ideal for the HALO mission, a complete design analysis was conducted for each. This design analysis will be outlined throughout the following subsections. It quickly became clear that the Manta Ray attachment was inferior due to its necessarily large tethers and large wing areas; for this reason, the Popsicle attachment analysis will be emphasized throughout this section.

Orbiter Structure

The lifting orbiter subsystem must be capable of generating lift in the positive vertical direction on ascent, and in the negative vertical direction on descent. For this reason, it was determined that a symmetric airfoil would be ideal due to its symmetric lift curve. This notion was further narrowed down through aerodynamic analysis using XFLR5, a CFD airfoil analysis tool. A trend quickly became apparent that among symmetric airfoils, thinner ones had preferred lift slopes for the expected flight Reynolds numbers. This lead to the selection of the NACA 0012 airfoil illustrated in Figure 24; this is the thinnest airfoil which would also be capable of fitting the electronics package with ample insulation. This selection was based on the ideal chord length of 0.4 m, which will be elaborated upon in the upcoming aerodynamic analysis subsection.

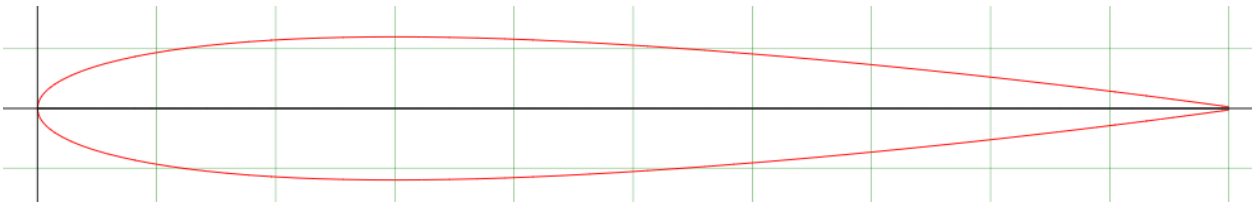

Figure 24. Illustration of a NACA 0012 Airfoil

Symmetric airfoils require an angle of attack to generate lift. For this reason, it was determined that a pitch-stabilizing tail would be necessary in order to maintain an optimal angle of attack. Optimal angles of attack would be those with high lift coefficients but with a sufficient angular margin to avoid stall. This optimal angle of attack was determined to be 6°; this will be elaborated upon in the upcoming aerodynamic analysis subsection.

Since this mission is heavily mass-constrained, it followed that the orbiter would be made primarily out of low-density foam. This lead to the selection of extruded polystyrene foam, which has a density of 16 kg/m^3. As a contingency, an ultra-low-density foam was researched with a density of 8 kg/m^3. Since there is no high-level structural data for this ultra-low-density foam, it would only be tested and implemented in the case where extruded polystyrene is too dense for the mission; it was later determined that extruded polystyrene was absolutely sufficient.

Now with an orbiter archetype chosen, it was time to consider the effects of low Reynolds numbers.

3.5.3. Reliability and Research of CFD at Low Reynolds Numbers

In developing the design of the lifting orbiter subsystem, the chief concern resided in the science of Reynolds numbers. A Reynolds number is defined as the ratio of inertial forces to viscous forces in a fluid, and is defined for an airfoil by the following equation.

$$Re = \frac{\rho V c}{\mu} \tag{4}$$

For flight at an altitude of 35 km, air density (ρ) drops down to approximately 0.0082 kg/m^3. This is less than 1% of the air density at sea level, which is why the expected minimum Reynolds number of around 4,000 poses a significant concern. This concern is rooted in the fact that Reynolds numbers significantly affect the aerodynamic properties of an airfoil. This relation is well visualized using Fig. 25 [36].

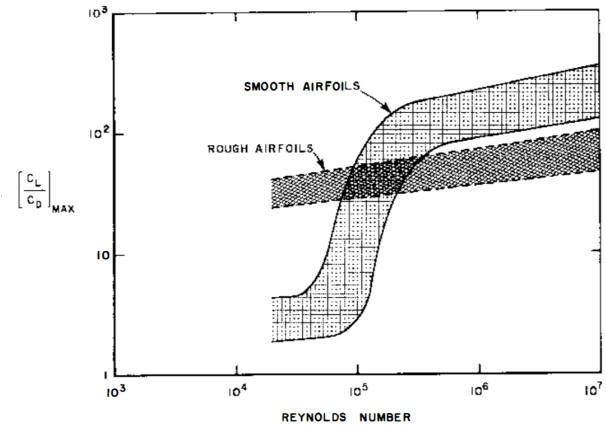

Figure 25. Effect of Reynolds Number on L:D Ratio

The important takeaway from this plot is the trend that rough airfoils operate with higher lift:drag ratios than smooth airfoils at low Reynolds numbers. It is incredibly difficult to objectively differentiate rough airfoils from smooth airfoils, and as such the orbiter was designed in accordance with smooth airfoil data. Note that on Fig. 25, the minimum tested Reynolds number is roughly 30,000. The lack of experimental data for expected Reynolds numbers is fairly widespread, and invited the necessity of alternative approximation methods. With the significance of Reynolds numbers in mind, a careful aerodynamic analysis was then conducted. In order to develop this aerodynamic analysis model, and to classify any success of aircraft flight at high altitudes around 35 km, multiple programs were investigated for airfoil flight at low Reynolds numbers.

Given the altitude and small nature of the aircraft, the Reynolds number of a wing at this altitude is much less than that of a modern aircraft, and in a similar nature to that of insects (on the order of 10^3; note that the expected Reynolds numbers are approximately 4000 as a minimum, and around 20,000 at a maximum). CFD models were therefore necessary to gauge the success of flight through varied vital parameters (namely that of C_L and C_D). Initial attempts to model a symmetric airfoil at this altitude were undertaken in variety of CFD programs: ANSYS fluent, XFLR5, SolidWorks Fluid Sim, and AVL. Results were met with data that appeared non-comparable between programs (namely CFD results from ANSYS in comparison to XFLR5). This was attributed to the uncertain nature/reaction of the selected airfoils to Low Reynolds number. ANSYS fluent had a variety of modifiable parameters attributed to varied low Reynolds number developed models (Turbulence and k-E model as some examples). XFLR5 had a singular turbulence model applied to its flow analysis (e^N model). This led to uncertainty in model results and whether flight models provided any accurate data, and which CFD program was reliable.

Extensive research was conducted around Low Reynolds number flight, and appropriate turbulent model application at these Reynolds numbers. Multiple research papers show flight analysis of low Reynolds numbers and UAV scale bodies and their comparison with CFD models. Kurtulus 2015 explored Reynolds numbers flow of 1000 for a NACA 0012 airfoil in ANSYS Fluent, which consistently displayed varying uncertainty's for convergence of C_L and C_D at high angles of attack. This resulted in extreme errors of nearly ± 0.8 for C_L and C_D values at angle of attacks of 25 deg or greater. Noticeable errors and fluctuations in C_L and C_D values begin to occur at angles of attacks of approximately 12 degrees, which lined up with results obtained by 5 other research papers. Predicted angle of attacks for feasible designs therefore would be limited to roughly ten degrees or less to maintain consistency in C_L and C_D, which is currently above the designed airfoil's necessary angle of attack. Note, comparison of XFLR data and Kurtulus are contained below in Figure 26. A minor over approximation is given by XFLR consistently. This allows the reasonable assumption that values obtained from XFLR5 are representative of low Reynolds number flight. This allows for greater investment in the following XFLR5 plots. The Reynolds numbers for the following plots comes from a wing chord of 0.4 *m*, orbiter velocity of M = 0.06, and atmospheric properties for the critical altitudes of 25 *km*, 30 *km*, and 35 *km*. The chord length of 0.4 was chosen since this chord length was low enough to have a reasonable wing aspect ratio, and high enough to be able to fit the electronics sensor package within the main wing section.

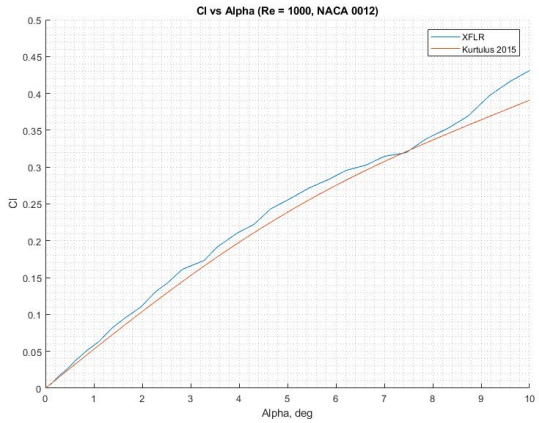

Figure 26. Comparison of XFLR and Kurtulus 2015

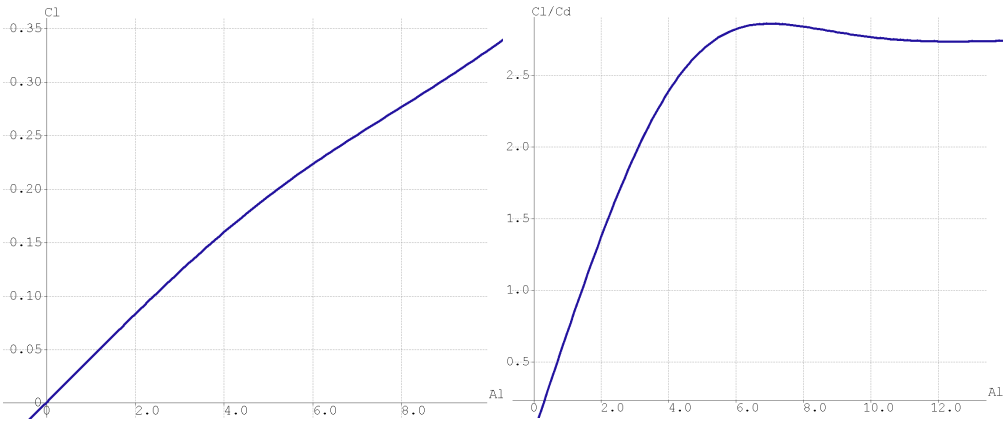

Figure 27. XFLR5 C_L of NACA 0012 at 35 km, Re = 4242

Figure 28. XFLR5 C_L/C_D of NACA 0012 at 35 km, Re = 4242

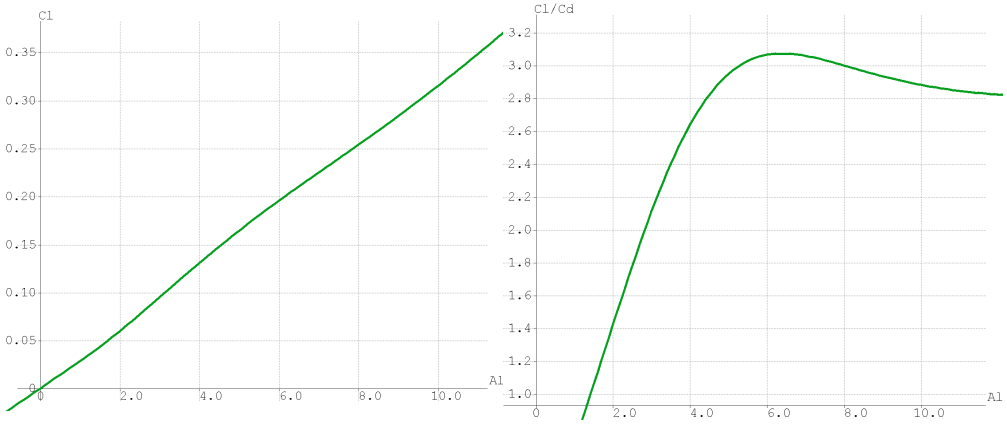

Figure 29. XFLR5 C_L of NACA 0012 at 30 km, Re = 9809

Figure 30. XFLR5 C_L/C_D of NACA 0012 at 30 km, Re = 9809

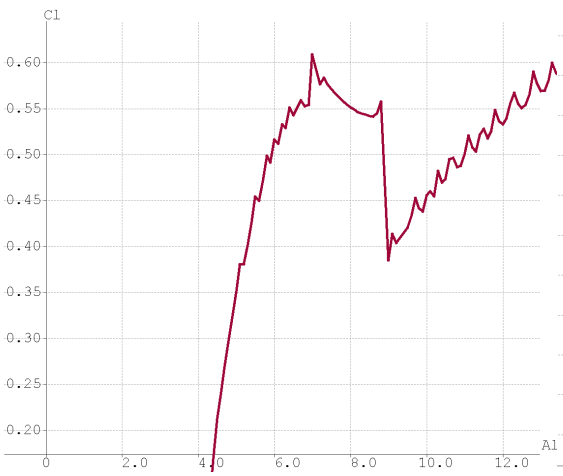

Figure 31. XFLR5 C_L of NACA 0012 at 25 km, Re = 21892

Figure 32. XFLR5 C_L/C_D of NACA 0012 at 25 km, Re = 21892

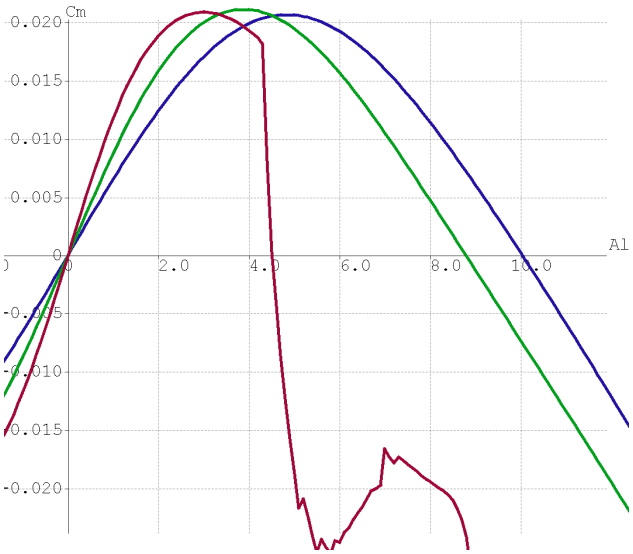

Figure 33. XFLR5 C_m of NACA 0012 at 25 km (red), 30 km (green), 35 km (blue)

3.5.4. Force Balancing and Aerodynamic Analysis

After achieving neutral buoyancy with the orbiter hanging below the balloon, there will be no horizontal forces on the system. Looking at the vertical forces, the buoyant force from the helium in the balloon will be counteracting the weight of every component attached to the system (balloon, helium, tether, parachute, vent, and orbiter). After the orbiter is turned on, it will begin orbiting to transition the balloon to a steady state, rising at 2.0 $m/s \pm 20\%$. The vertical and horizontal forces must still cancel to not cause additional accelerations. This free-body diagram is shown in figure 34.

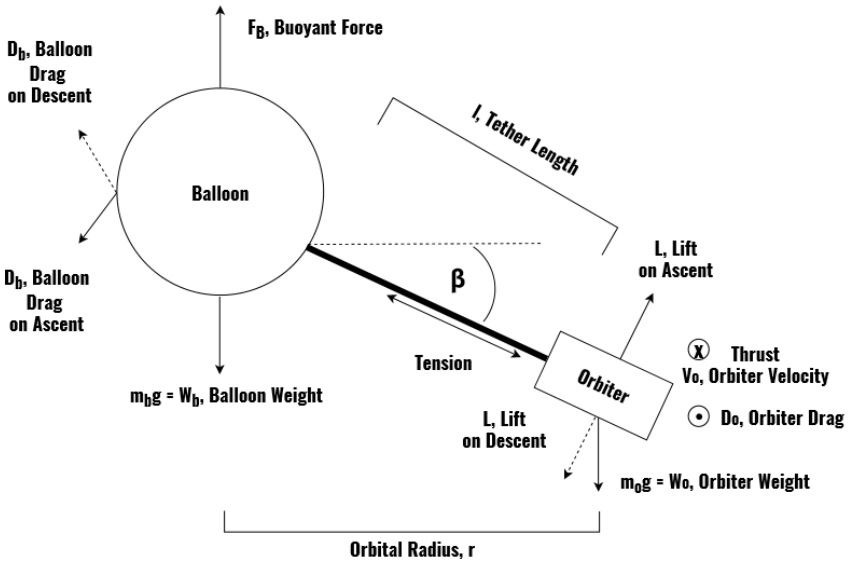

Figure 34. Free-Body Diagram for the Orbiting System

While in steady state, beginning with the vertical forces, the orbiter will now have a drag force that acts in the opposite direction of the velocity upward or downward (depending on if it is ascending or descending). The lift generated by the orbiter must counteract this drag force to allow the balloon to ascend or descend with a constant velocity with no additional forces. This lift force will change based on the angle, β, that the orbiter will have with respect to the horizontal. This lift will also change based on the velocity that the wing is flying at as well as the size of the wing. These variables will all need to be accounted for when designing how large to make the wing. In the lateral direction, it is assumed that the balloon is in steady state and is traveling with the crosswind so that the only lateral forces on it are wind gusts (which will be neglected for now). In order to keep the orbiter revolving around the balloon wake, it must have a propulsion device on it to cancel out the drag as it flies. Thus, a propeller is mounted on the front that will provide the thrust equal to the drag to maintain the plane's velocity. Since the plane will be at an angle of attack, this propeller will also be generating a small amount of lift in the direction of travel as well, but it is small compared to the lift of the plane.

Having understood the basics of the relevant forces in play, it became possible to begin with the actual orbiter design. This process begins with a calculation of the drag force on the balloon, D_b. In order to determine the drag force on the balloon, it is necessary to be aware of the amount of helium inside of the balloon. This was determined using Kaymont's balloon-burst calculator[37] below.

Figure 35. Kaymont High Altitude Balloon Burst Calculator

The above burst calculator is very useful for several reasons. It allows for valuable inputs of payload mass, balloon mass, and target ascent rate. For these inputs, the program outputs approximations of burst altitude and initial fill

volume. To start this calculation, approximate values of payload mass and balloon mass were input. Further, the target ascent rate was set to 0 m/s in order to obtain the equivalent ground-fill volume. This is because venting will allow for neutral buoyancy at the designated altitude of 30 km. This neutral buoyancy will correspond to an ascent rate of 0 m/s, since the buoyant force from the balloon is not large enough to ascend; all ascent velocity will be courtesy of the lifting orbiter. In reality, there will be more than 2.92 m^3 of helium within the balloon at the initial fill stage. After venting occurs, however, the volume of the balloon will be equivalent to predicted volumes if the initial fill volume was actually 2.92 m^3.

Using this effective initial fill volume of 2.92 m^3, the ideal gas law was employed to calculate the volume of the balloon as follows.

$$PV = mRT \tag{5}$$

Eqn. 5 begins this balloon drag approximation. Treating R as a constant, it is possible to rewrite this equation in the following manner.

$$R = \frac{P_1 V_1}{mT_1} = \frac{P_2 V_2}{mT_2} \tag{6}$$

Eqn. 6 was then used to relate atmospheric ground properties as well as the ground fill volume to atmospheric properties at altitude and the balloon volume at altitude.

$$V_2 = \frac{P_1 V_1 T_2}{T_1 P_2} = \frac{4}{3}\pi r_2^3 \tag{7}$$

Eqn. 7 can then be used in order to calculate the balloon radius from its volume, assuming a perfect sphere. Temperature and pressure values were obtained from the MATLAB function *atmoscoesa*, and V_1 was set to 2.92 m^3.

$$S_b = \pi r_b^2 \tag{8}$$

Having obtained the radius of the balloon, Eqn. 8 is used to calculate the cross-sectional balloon area; this is the area which will determine the magnitude of the drag force acting against the motion of the balloon. This drag was then calculated with the following equation.

$$D_b = \frac{1}{2}\rho V_b^2 S_b C_D \tag{9}$$

In the above equation S_b was determined through the process above, ρ was obtained using *atmoscoesa*, V_b is allowed to be from 1.6 to 2.4 m/s, and C_D was obtained from the following NASA figure [4].

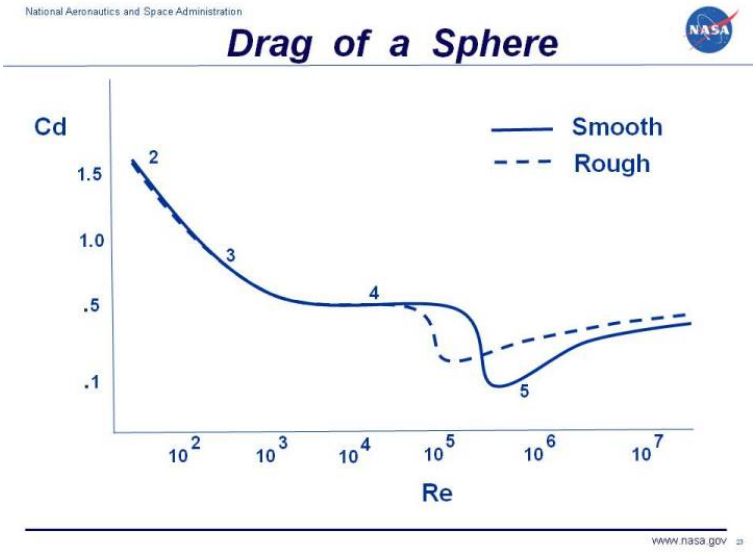

Figure 36. Drag Coefficient of a Sphere

From the above figure, it was obtained that the drag coefficient for the balloon would be approximately equal to 0.55. This is the value that was used for balloon drag calculations. This balloon drag value was calculated at several critical altitudes: 20 km, 25 km, 30 km, and 35 km. Since the 35 km altitude has the highest balloon area and therefore the greatest lift required, all design parameters were based on the requirements for this altitude.

In the 35 km altitude case, solutions were found by making calculations for a span of β angles ranging from 1°to 89°. For each potential beta angle, wing and tail areas were solved by coupling the following two equations.

$$\frac{l_t S_t}{c_w S_w} a_t \alpha_t = c_{m,ac,w} + a_w \alpha_w Kn \tag{10}$$

Eqn. 10 was used to balance the pitching moment about the orbiter system. In this equation, many of the variables were treated as constants. l_t, distance from wing a.c. to the leading edge of the tail, was determined through boom deflection analysis to be a maximum of 1 m. l_t should be lower than this, however. If l_t is higher, then tail area S_t will necessarily be lower and less lift will be generated by the tail. For this reason, l_t was set to a value of 0.5 m. c_W was determined to be 0.4 m due to the required purposes of the wing. Lower chords are ideal due to more ideal aspect ratios, though the wing must have enough volume to incorporate the sensor package with minimal active heating. A chord length of 0.4 m balanced these objectives nicely. a_t, the lift slope of the tail, was determined to be approximately 0.0382 using XFLR5. This can be seen in Fig. 27. α_t and α_w were both determined to be 6°; this value was chosen in order to main a high C_L without stalling. Stalling can be distinguished by a peak in the plot of Fig. 28. $c_{m,ac,w}$ was determined to be 0.019 by looking at the moment coefficient produced by XFLR5 at a 6°angle of attack. This moment plot can be found in Fig. 33. Pitch stiffness Kn, the distance between the center of gravity of the orbiter and the aerodynamic center of the wing, was initially set to 0 m since the placement and mass of the electronics package would likely result in the orbiter center of gravity being near the aerodynamic center. After narrowing the design space, this Kn was altered according to previous area solutions.

This pitch moment equation was then coupled with the following lift equation in order to solve for wing areas for each iteration of changing β.

$$\frac{1}{2}\rho V_o^2 [C_{L,w} S_w + C_{L,t} S_t + \sin(\alpha_w)(C_{D,w} S_w + C_{D,t} S_t)] = L = \frac{D_b}{\cos(\beta)} \tag{11}$$

Eqn. 11 was derived from a vertical force balance on the orbiter. It is necessary that the orbiter generates enough vertical lift in order to counteract the drag on the balloon as it ascends at a velocity between 1.6 m/s and 2.4 m/s. This balloon velocity would ideally be as close to 2.4 m/s as possible, in order to achieve a longer mission duration and therefore more useful data. V_o, orbiter velocity, was set to a maximum of 20 m/s for the maximum altitude in order to optimize wing area and therefore mass. This 20 m/s maximum was set by the customer. It was later determined that, due to the constricting mass budget, the maximum attainable ascent velocity would actually be closer to 1.8 m/s. This is sufficient, since it is still within bounds provided by the customer. The first two terms in this lift equation, involving $C_{L,w}$ and $C_{L,t}$, come straight from the typical aerodynamic lift equation (Eqn. 1). The second two terms, involving $C_{D,w}$ and $C_{D,t}$, come from the lift provided from the propeller. The propeller must necessarily provide a thrust equal to the drag on the orbiter. Some of this thrust will be in the vertical direction, since the orbiter is at an angle of attack of 6°. Combining Eqns. 10 and 11, it was possible to solve for possible wing and tail areas for each iterated β angle.

For each wing and tail area, relevant design parameters are then extracted in conjunction with the following equations.

$$b_w = S_w / c_w \tag{12}$$

Eqn. 12 was used in order to calculate the wingspan from the wing area and wing chord.

$$AR_w = b_w^2 / S_w \tag{13}$$

Having solved for wing span, Eqn. 13 was used in order to calculate the aspect ratio of the wing. Typical values for wing aspect ratio lay around 8, and any values deviating greatly from this value were removed from the solution set.

$$b_t = \sqrt{AR_t * S_t} \tag{14}$$

In order to solve for the tailspan, an Aspect Ratio (AR) of 8 was chosen for the tail.

$$c_t = \frac{S_t}{b_t} \tag{15}$$

Having solved for the tailspan, the tail chord was solved with the above equation.

With these relevant wing and tail characteristics, the next logical step is to calculate the mass of the orbiter for each of these proposed solutions. Orbiter mass was determined first by multiplying the wingspan by the side-view area of the wing and multiplying the tailspan by the side-view area of the tail in order to obtain foam volumes. These volumes were then multiplied by the selected foam density of 16 kg/m^3. Then the mass of the foam which would be replaced by the sensor package was subtracted, and the mass of all remaining components was added. These remaining components consisted of the two carbon fiber booms with a linear density of 0.05 kg/m, the motor, and the propeller. Motor and propeller masses were initially approximated at roughly 100 g collectively, and were later tweaked after the propeller analysis and selection.

Having calculated the mass of this orbiter system, the next step was to calculate the orbit radius for each prospective solution (at each β angle). After carrying out radial and vertical force balances, the equation for orbit radius simplified down to the following equation.

$$r = \frac{m_o V_o^2}{(m_o g - D_b)\cot(\beta) - D_b \tan(\beta)} \tag{16}$$

The next step in this process was to eliminate any solutions which did not fulfill the requirements of the mission. If the orbit radius was lower than the predicted balloon radius, the orbit period was less than 1 s, or if the orbiter mass exceeded the mass budget of 1.52 kg, then the "β angle solution" was thrown out. The remaining solutions had properties which can be found below.

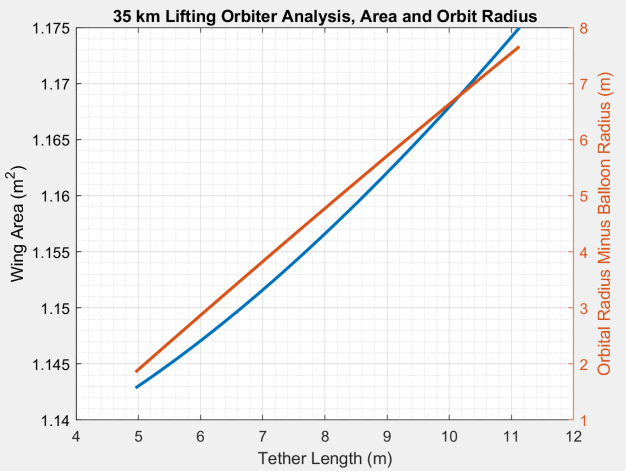

Figure 37. Orbiter Design Space, Area and Orbit Radius Focus

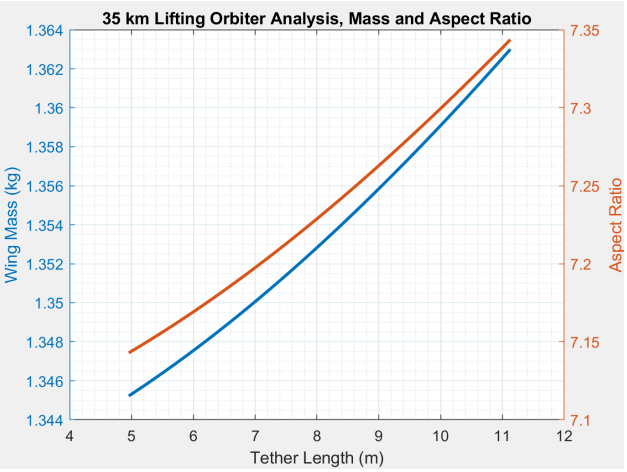

Figure 38. Orbiter Design Space, Mass and Aspect Ratio Focus

From these feasible solution spaces, the lowest-mass system was selected. This is to minimize the chance of balloon burst as the maximum altitude of 35 km is achieved. This minimum-mass solution yielded the following set of orbiter characteristics.

l_{tether}	β_{25km}	S_w	AR_w	c_w	b_w	S_t	b_t	c_t	$m_{orbiter}$
4.96m	8.40°	$1.14m^2$	7.14	0.40m	2.86m	$0.13m^2$	1.00m	0.13m	1.35kg

The final wing design can be seen in the following figure.

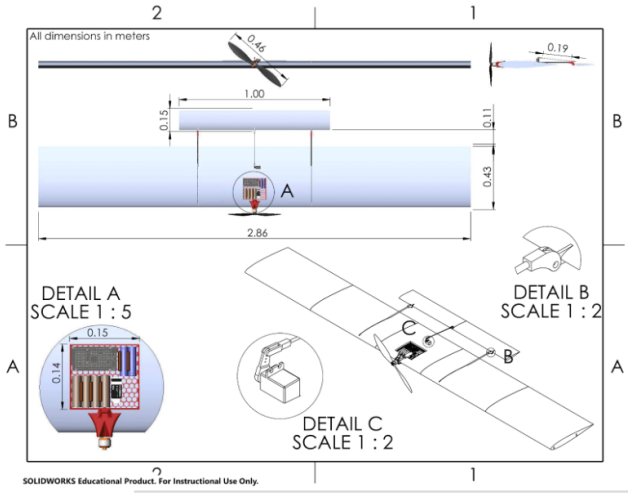

Figure 39. Orbiter Dimensions

3.5.5. Propeller analytical model

One driving parameter paramount to project success is the propeller. The propeller chosen as the main thrust component must work at all altitudes and provide an adequate amount of thrust for both steady state and accelerating function. The main consumer of power on the payload is expected to be the lifting orbiter motor which drives the propeller. Note that as RPM of a motor decreases from its no-load value, it is due to increased torque on the motor, which is linearly proportional to current. As a result, the propeller must have a balance between RPM and torque, enough to generate the necessary thrust on the propeller but also be within reasonable power consumption range.

A propeller, in function, is an airfoil cross section driven vertically to move air with significant momentum through the propeller cross sectional area. This results in a component of lift and drag that can be resolved in two different directions, namely the normal and tangential directions. The tangential components represent thrust, while the normal components amount to the torque generated by the propeller. The model developed attempted to solve for this torque by analyzing only key sections of a propeller.

As flow approaches the inner hub of propellers, flow can become unpredictable in nature and provide uncharacteristic results of the propeller. This inner section also generates negligible torque and lift, considering the low pitch and twist of propellers close to the hub. On the other end of the propeller, tip speeds exceeding Mach .85 can have undesirable effects, including extreme laminar flow bubbles and complete flow separation, causing substantial increase in drag. As a result, a model was developed looking only at .5 to .8 blade radii away from the hub, the main contributor of both thrust and torque, and ensuring that the outer tip did not reach .85 tip Mach speed. This model can be visualized using the following figure.

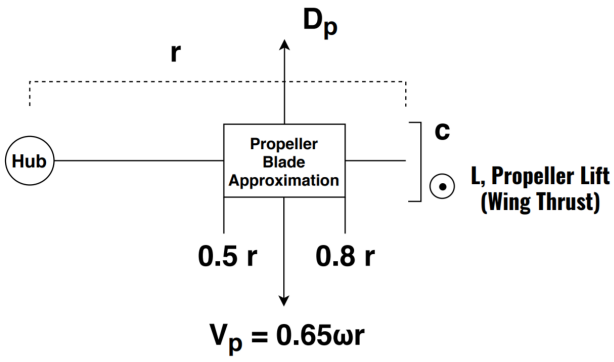

Figure 40. Simplified Propeller Free Body Diagram

Within this propeller thrust approximation, the first step is to acknowledge that the propeller must provide enough thrust to counteract the drag acting on the orbiter.

$$D_o = T_{prop} \tag{17}$$

Drag on the orbiter can be solved using the aerodynamic drag equation below.

$$D_o = \frac{1}{2}\rho V_o^(S_w C_{D,w} + S_t C_{D,t}) \tag{18}$$

In Eqn. 18, all values have been determined at this point; relevant drag coefficients are extracted from XFLR5 plots throughout Figs. 27 to 32.

$$T_{prop} = \frac{1}{2}\rho V_p^2 S_p C_{L,p} n \tag{19}$$

Eqn. 19 then solves for the thrust of the propeller as if it were an airfoil. n represents the number of propeller blades, which was set to 2 in order to maximize propeller efficiency. In order to evaluate this expression, propellers were simulated as NACA 4412 airfoils in XFLR5 to obtain lift and drag coefficients. These lift and drag coefficient plots can be found throughout the following plots.

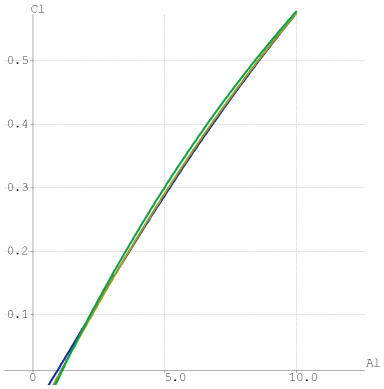

Figure 41. Propeller C_L at 35 km (blue), 30 km (gold), and 25 km (green)

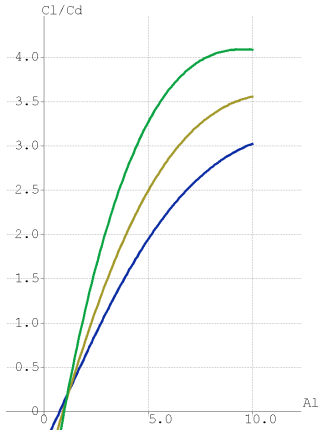

Figure 42. Propeller L/D at 35 km (blue), 30 km (gold), and 25 km (green)

To choose a propeller under this approximation, propeller pitches and diameters were varied in typical increments of 0.5 *in*. For each of these considered propellers, a required V_p, or propeller velocity at 0.65 r, was calculated at the 35 *km* altitude. These propeller velocities were then related to necessary motor torque using the following equation.

$$\tau = 0.65r \times D_p \tag{20}$$

Eqn. 20 can be coupled with the typical aerodynamics drag equation found in Eqn. 2 in order to solve for the necessary torque provided by the motor.

It was then concluded that an 18x8 propeller, that is a propeller with an 18 *in* diameter and an 8 *in* pitch, would be the ideal propeller for this mission. APC Propellers makes a suitable thin electric propeller of this size with a low mass of 85.9 g. For this propeller, the estimated maximum required torque was found to be roughly 0.011 $N * m$ with a maximum required RPM of approximately 5194.

This allowed for a choice of motor, which was determined to be the Turnigy D2822/14 Brushless Outrunner 1450kV. This motor, provided by HobbyKing, is capable of of producing a maximum torque of 0.33 $N * m$ and is rated at 1450 kV. This 1450 kV rating means that the motor can spin at 1450 rpm per volt. These characteristics surpass those required for this mission for a low motor mass of only 37 g.

3.5.6. Boom Deflection

The tail is connected to the main body of the orbiter through the use of twin carbon fiber booms, which will experience some deflection under load, which will have the effect of changing the angle of attach of the tail. To mitigate undesirable effects on the lift profile as a result of boom deflection, a suitably stiff boom system must be designed. Each of the two booms consists of a hollow carbon fiber tube, which is assumed to deflect uniformly under

load per the principles of beam deflection. Equation 21 describes the second moment of area for a tube of nominal diameter d and thickness t and is shown in Figure 43.

$$I_y = \frac{\pi}{2}\left(\left(\frac{d}{2}\right)^4 - \left(\frac{d}{2} - t\right)^4\right) \tag{21}$$

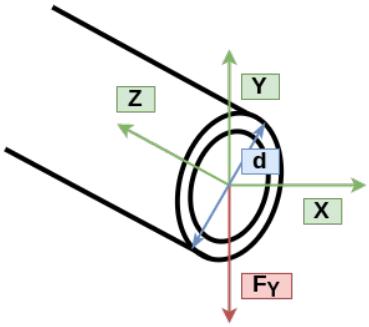

Figure 43. Cross Section of a Tube for Deflection Analysis

The current orbiter design has twin tail booms, so the deflection can be represented as shown in Equation 22.

$$\sigma = \left(\frac{F_y * l^3}{3EI_y}\right)\left(\frac{1}{2}\right) \tag{22}$$

With Young's Modulus of 228 *GPa*, tube diameter of 5 *mm*, tube thickness of 1 *mm*, boom length of 0.5 *m*, and predicted tail lift force of 7.5 *N*, the tail deflection is found to be 13 *mm*. Over the 0.5 *m* length of the tail this results in an induced angle of attach of roughly 1.5 degrees. Figures 89 - 91 in the Appendix contain a design space for 1, 2, and 3 boom tail designs with varying wall thicknesses and diameters. The 5 *mm* twin boom with the thinnest available wall thickness of 1 *mm* provides suitable resistance to deflection while minimizing mass penalties.

3.6. Thermal Design Process

Thermal control is critical to the function of the orbiter. The mission profile includes traveling to altitudes where temperatures drop as low as -56.50°C[5]. The most pressing requirement of the thermal system is to maintain a high enough temperature for any batteries to remain functional. Batteries fail at low temperatures because they rely upon chemical reactions that begin to react too slowly to generate a functional current at extremely cold temperatures. The temperature that this phenomenon starts to occur in specialized lithium batteries is around -20 °C. The second driving factor for the thermal control system is that it must use insulation to match the shape of the chosen lifting orbiter design without adding excess weight to the system. A trade study will be conducted on the following designs with the goal of choosing the design that will improve the success rate of the mission as a whole.

3.6.1. Thermal Insulation Trade Study

Because the lifting orbiter must be a certain size and shape to provide the required lift for mission success, choosing the right insulation material is the first step in conducting a thermal analysis of the system. It was deemed infeasible for the mission to utilize a combination of different foams for the wing and electronics bay insulation because the final project must be easily producible for the costumer. For this reason, the chosen insulation must be capable of providing insulation for the electronics and provide the structure for the lifting wing. That limitation greatly affects this insulation trade study.

Insulation Trade Study Metrics

Three main metrics will be considered within the thermal selection trade study: thermal conductivity, cost per cubic centimeter, and density of the various foam materials. With this in mind, each category was given a specific weighting, in order to prioritize the most important parameters that would provide the best possible insulation choice.

Three main foam materials were considered in this trade study which include: polyurethane foam, extruded polystyrene (XPS), and phenolic foam. The thermal conductivities, costs per square centimeter, and densities of

these materials were researched and compared.

Thermal Conductivity: Thermal conductivity is a very significant metric when it comes to the choice of insulation material. This is such an important metric because it inversely relates to the amount of heat transfer that will occur between the atmosphere and the internal payload. In other words, a lower thermal conductivity will ultimately result in a lower heat transfer. Because the lifting orbiter payload will also need to be a functional aerodynamic body, reducing the bulk of the insulation could be critical to mission success.

Thermal Conductivity [$\frac{W}{mK}$]	0.020-0.023	0.024-0.026	0.027-0.029	0.030-0.032	0.033-0.035
Score	5	4	3	2	1

Table 33. Thermal Conductivity Scoring

Cost Per Cubic Meter: The cost metric is significant when considering which insulation material to choose because the because the lifting orbiter will be entirely composed of the insulation material. The mission statement also requires that the overall payload construction remain under $2,000 per launch. For this reason, cost per cubic meter is one of the most important aspects of the chosen insulation material with the lowest values being preferred.

Cost [$\frac{\$}{m^3}$]	2500-3000	3000-3500	3500-4000	4000-4500	>4500
Score	5	4	3	2	1

Table 34. Insulation Cost Scoring

Density [$\frac{g}{cm^3}$]: The density metric is significant when considering which insulation material to choose because the lifting orbiter will be entirely composed of the insulation material. The mission also had a strict mass constraint via FAA regulations. For this reason, density is arguably the most important aspect of the chosen insulation material with the lowest values being preferred.

Density [$\frac{g}{cm^3}$]	0.030-0.031	0.031-0.032	0.032-0.033	0.033-0.034	0.034-0.035
Score	5	4	3	2	1

Table 35. Insulation Density Scoring

Insulation Trade Study Scoring

The weighting of each thermal category was decided based upon the expected importance of each parameter. The orbiting wing had to be made of the lightest foam used in this study, not the best. This is because the orbiter needed a very large wing to generate enough lift to complete the mission and the entire system had to stay below a certain mass to remain under FAA regulations. It was deemed infeasible for the mission to utilize a combination of different foams for the wing and electronics bay insulation because the final project must be easily producible for the costumer. For this reason, the most important parameter was decided to be density because the lifting wing has a fixed size needed to generate the required lift for project success. Therefore the lowest density foam would have the lowest weight and thus reduce the required lift and size of the system. The most important parameter was thus decided to be density. For that reason it was given a weight of 0.6. Cost is also important for mission success because each flight was required by the costumer to remain under 2000 dollars. Since the entire lifting wing is made of the insulation material, the cost per cubic meter would greatly affect the whole system weight. For this reason, cost received a weight of 0.30. Lastly, the thermal conductivity was given a weight of only 0.10 even though it is inversely correlated to heat transfer because it can be supported by active thermal control. The price of the other two at that volume was also infeasible. For this reason, the chosen foam insulation for this mission is extruded polystyrene.

Based on the results of the trade study illustrated in Table 36, extruded polystyrene was determined to be the best foam material to use as insulation for the payload. Extruded polystyrene scored very well in the important density category, and is inexpensive. This makes it the optimal insulator for the lifting body orbiter design.

Category	Weight	Polyurethane	Extruded Polystyrene	Phenolic Foam
Thermal Conductivity	0.10	4	1	5
Cost [$\frac{\$}{m^3}$]	0.30	5	2	1
Density [$\frac{g}{cm^3}$]	0.60	1	5	1
Score	**1.00**	**2.50**	**3.70**	**1.50**

Table 36. Initial Insulator Material Trade Study

3.6.2. Thermal System Design Alternatives

There were two main conceptual design alternatives considered for the thermal control system. The first of these designs is passive thermal control. The second is a combination of passive and active thermal control. It is important to note that a method of pure active thermal control was not considered because it is not feasible. Any material used to cover the electronics bus will function as an insulator and thus add passive control. For this reason, only passive control and a combination of active and passive control will be considered as viable designs.

Passive Thermal Control: Passive thermal control is the simpler of the two designs and relies entirely on passive insulation and heat generated from essential electronics that have functions separate from heating. An example of these electronics would be an electric motor for the orbiter that drives a propeller. Being able to implement this design would have bee very simple and easy. This sytem would have required less electronics like heaters in the payload which would in turn require fewer batteries and cut weight and complexity. However, it would also require thicker insulation. Unfortunately, after running some lift vs drag calculations, the lifting orbiter team came up with a max thickness of 4.8 centimeters. These values were plugged into the thermal model, which will be described later, and resulted in a failure to keep the electronics in their operating range. This result meant that active heating in the form of heaters would need to be implemented in the electronics bay.

Active Thermal Control: An active thermal control system allows for the addition of a heater within the payload that would reduce the amount of insulation required to keep the internal temperature above the target temperature. This design is thus able to meet the requirements set down by the lifting orbiter.

One pro of this design is that the active heating can be triggered on and off to keep the payload in an exact temperature range.

One con of this approach is that it is more complex and that the heaters will draw power from the batteries which means that either more battery capacity will be needed, or the flight time will need to be shorter. However, it is a tradeoff that must be made to meet the lifting body requirements.

3.6.3. Thermal Model

Would the thermal system be able to satisfy the functional requirement of allowing the mission to survive the atmospheric conditions (FR 3.0)? How much active heating would be needed with the new design? Before these questions could be answered, an in-depth model had to be developed to represent the electronics bay within the lifting orbiter system throughout hte mission.

One concern with electronic survival is that lithium batteries have reduced capacity at temperatures around the bottom and top of their operating range which is illustrated in Figure 44.

4.3.5 Temperature Dependency of Capacity	Cells shall be charged per 4.1.1 at 23℃ ± 2℃ and discharged per 4.1.2 at the following temperatures.		
	Charge	Discharge	Capacity
	23℃	-10℃	70% of P_{ini}
		0℃	80% of P_{ini}
		23℃	100% of P_{ini}
		60℃	95% of P_{ini}

Figure 44. Manufacturer Provided Discharge Temperature Dependence for Electronics Battery

Charge Temperature	Discharge temperature		
23°C	-10°C	23°C	40°C
Relative Capacity	60%	97%	97%

Figure 45. Manufacturer Provided Discharge Temperature Dependence for Motor Battery

The batteries cooling to a temperature below this range is a concern because the atmospheric temperature can get as low as -56.5 $°C$. The electronics bay will also be located on the orbiter which will be orbiting under the balloon at a maximum velocity of 20 $\frac{m}{s}$. This orbiting velocity will elevate the magnitude of forced convection heat transfer and cool the system quicker. Both of these conditions are a concern for decreasing the battery temperature to a point where it can no longer operate as intended. If the batteries reach a temperature near their operating range, their performance will decrease. If the battery temperature reaches a temperature below their operating range, they will not be able to supply functional power. If either of these conditions occur, the orbiter will not have adequate power to operate as intended. For this reason, a predictive thermal model had to be created in order to determine whether the HALO mission would be able to meet the functional requirement of surviving the atmospheric conditions (FR 3.0).

Heat Transfer Model

The thermal model was designed to include the following kinds of heat transfer: conduction, convection, radiation, and electronic equipment heat generation. These forms of heat transfer and how they will interact with the system as a whole can be visualized in Figure 46 below.

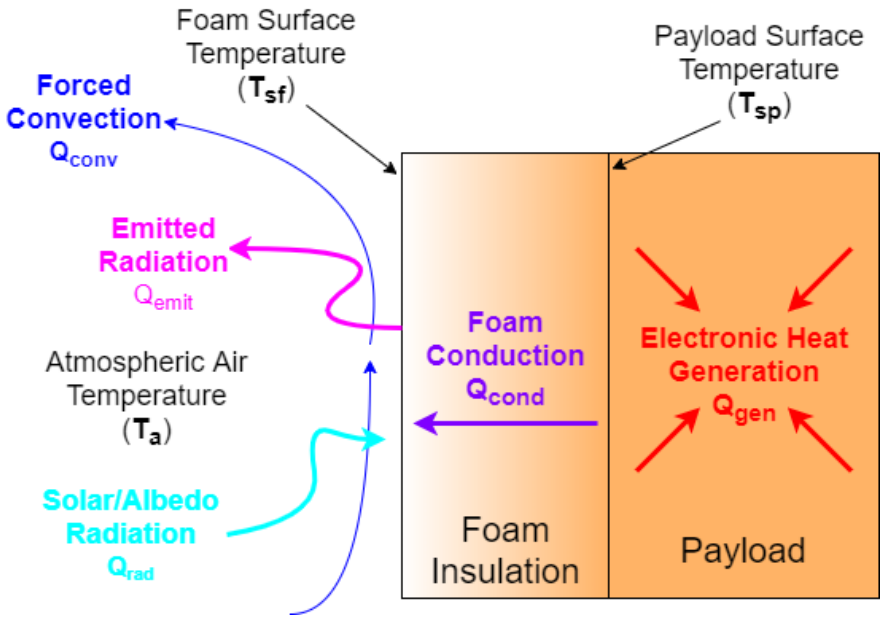

Figure 46. Types of Heat Transfer in System

Conduction in the HALO mission can be broken into two main categories: conduction through the foam insulation and conduction through the electronics bay. The conduction through the foam was calculated using Equation 23. In this equation, 'k' is the thermal conductivity of the medium, 'A' is the area, 'd' is the distance between two points, and T_2 and T_1 are the temperatures of the two points. The thermal conductivity value of extruded polystyrene is 0.034 $\frac{W}{mK}$ [7]. The payload was assumed to conduct via the thermal conductivity value of air at different altitudes which were derived from the engineering toolbox and stay between 0.020 and 0.030 $\frac{W}{mK}$ for the mission altitude and temperature range[5]. The payload was assumed to conduct instead of naturally convect because of the tight space restricting air movement.

$$Q_{cond} = \frac{kA(T_2 - T_1)}{d} \tag{23}$$

Forced convection was the dominant form of heat transfer between the outer foam and atmospheric air. The

velocity of the air was assumed to be the fastest case with 20 $\frac{m}{s}$ flow over the wing. The velocity of the air directly behind the propeller was additionally assumed to be 25.4 $\frac{m}{s}$ because the propeller accelerates the flow. Only the outer foam was assumed to interact via forced convection and the magnitude of the heat transfer was solved for using Equation 24 below. Calculating the value of h_{conv} is a lengthy endeavor that can be viewed in 'CalcdTdt.m' MATLAB script in the appendix.

$$Q_{conv} = h_{conv} A (T_{atm} - T_1) \tag{24}$$

Radiation heat transfer took various forms in the thermal model. These forms included: outer-foam emitting radiation, absorbing albedo radiation, and absorbing solar radiation. The outer-foam emitted radiation was calculated for each element according to Equation 25. This was completed using the Stefan-Boltzmann constant ($\sigma_b = 5.67 * 10^{-8}$ $\frac{W}{m^2 K^4}$) and the emissivity (ϵ) of extruded polystyrene (0.9)[38].

$$Q_{emit} = -\epsilon \sigma_b A T_1^4 \tag{25}$$

The outer-foam absorbing solar radiation was assumed to be on top of the payload and the magnitude of heat gained was calculated using Equation 26 below. The magnitude of solar radiation was assumed to be 1.0 of the solar constant (1367 $\frac{W}{m^2}$) because the mission will take place so high in the atmosphere, and thus there will be little radiation shielding[26].

$$Q_{solar} = S A \alpha \tag{26}$$

The outer-foam absorbing albedo radiation was assumed to be on the bottom of the payload and the magnitude of heat gained was calculated using Equation 27 below. The magnitude of albedo radiation was assumed to be 0.30 of the solar constant (410.1 $\frac{W}{m^2}$) based on average albedo radiation from the Earth and was equal to[26].

$$Q_{albedo} = 0.3 S A \alpha \tag{27}$$

Lastly, heat generation occurs in the payload due to the electronics equipment. The electronics equipment was assumed to generate the amount of heat equal to their power draw which was calculated using the voltage and input current. For example, a GPS that draws 0.5 W of power would generate 0.5 W of heat. The power draws, and thus heat generation magnitudes of all the electronics equipment, will be discussed in the electronics section yet to come.

Based on the unique shape of the system (NACA 0012 Airfoil), and the location dependent heat generation of the electronics, it was decided that a finite element matrix would be suited to handle the thermal modeling requirements of HALO better than a low fidelity model. To complete this task, a three dimensional matrix consisting of finite cubes was constructed that modeled the shape of the system. Each cube was assigned properties of either foam or payload which could be assigned a specific classification such as outer foam, battery, or GPS. Based on the classification, the cube element could undergo different types of heat transfer discussed above or have different values of mass, thermal conductivity, etc. Figure 47 below represents a cross sectional cut of the three dimensional model generated using this method where the yellow represents the electronics bay.

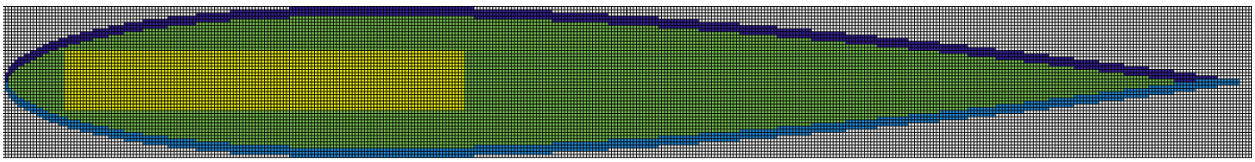

Figure 47. Types of Heat Transfer in System

The sum of the heat transfers can then be used to calculate the change in temperature for each element using Equation 28 below. 'c' is the thermal capacity ($\frac{J}{K}$) of whatever element is being analyzed and 'm' is the mass of that element. Using these values, along with Q_{net}, the change in temperature per second of each element can be calculated. The change in temperature per unit time for each of the elements was then integrated through the MATLAB function ode45().

$$\frac{\delta T}{\delta t} = \frac{Q_{net}}{cm} \tag{28}$$

The model continues to integrate time steps until a stable solution converges. The model currently works by assigning every element a temperature close to what the predicted final temperature will be to save convergence time.

Electronics Bay Dimensions and Location

The next step in designing the new thermal system was to determine the dimensions and location of the electronics bay within the orbiter wing. This was the next step for the thermal model because the functionality of the orbiter is the primary driver of mission success. For this reason, the thermal system was designed in order to fit within the required orbiter specifications. The orbiter is composed of a lifting wing designed around a NACA 0012 airfoil which is illustrated in Figure 24. The electronics bay had to be designed to fit within this airfoil. These specifications were largely constrained by the required aerodynamic performance of the orbiter as well as the size of the electronics equipment described in the previous sections.

The height of the electronics bay was chosen to be at a minimum value to fit all of the electronics equipment. The electronics bay was designed in this way using the knowledge gained from the low fidelity model that it is best to maximize insulation thickness. A thinner electronics bay would allow for a thicker foam insulation layer on the top and bottom. This in turn results in a lower heat transfer from the electronics bay to the atmosphere which will keep it at a higher temperature in the cold environment. Minimizing the height of the electronics bay was a primary thermal goal because the maximum orbiter airfoil thickness is constrained by aerodynamic performance and has a maximum height of only 4.8 *cm*. The tallest piece of electronic equipment is the batteries which constrained the height of the bay to a minimum of 1.85 *cm*. The location of the electronics bay in the height dimension was chosen such that the it is centered between the top and bottom of the symmetrical NACA 0012 airfoil. This was chosen because it maximizes the foam thickness on both the top and bottom and also aligns the center of mass along the chord line.

Next, the width and length dimensions and locations of the electronics bay were chosen to satisfy two main conditions while also providing adequate foam insulation thickness. The first condition was that the volume of the electronics bay must be large enough to contain all of the electronics. The second condition was that the center of mass of the electronics would help align the entire orbiter center of gravity at the aerodynamic center of the lifting wing which is located at quarter chord. These two requirements were met by designing a box that is 12.8 *cm* in length and 13.4 *cm* in width and starts at a length distance of 2 *cm* from the tip of the airfoil. For width, the electronics bay is centered at a location exactly along the center-line of the orbiter. These dimensions and locations resulted in the electronics bay layout illustrated in Figure 48 below.

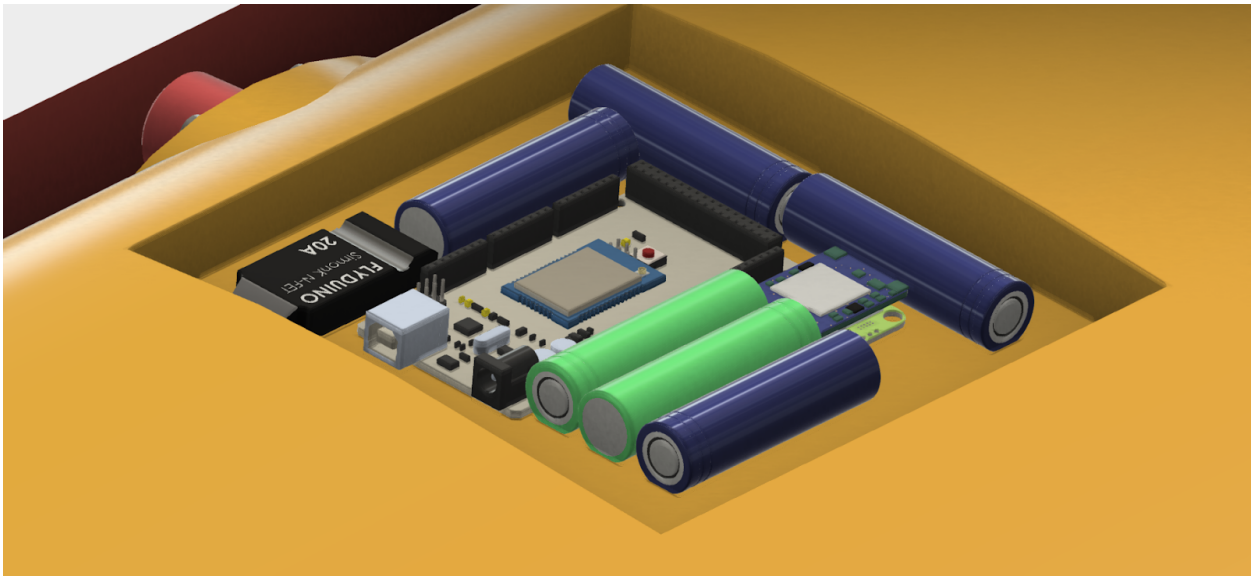

Figure 48. Digital Model of Electronics Bay

The model was then simulated using a worst case altitude of 25 km where the atmospheric temperature is at its lowest (-56.5 °C). The model was integrated using only essential electronic equipment heat generation to see if the payload could survive the conditions. The model indicated that the internal payload temperature converged around -25 °C. This was deemed an unreasonable internal payload temperature because it is too low in the battery operating range. Because it is so low, the total battery capacity would be greatly reduced to less than 60% of the original capacity . For this reason, it was decided that active heating would need to be added to the system.

The model was run using different magnitudes of heat generation until the average payload temperature converged

around an accepted value of 0 °C. This temperature allows the batteries to operate at around 70% to 80% of the nominal capacity. The required magnitude of active heating to keep the batteries at this temperature was determined to be 1.56 Watts based on the model.

After some research, it was determined that wirewound resistors would be the best option to accomplish this. Wirewound resistors are a good solution for active heating because they are cheap, light, and easily implementable. The specific wirewound resistor that was chosen to generate the 1.30 W heat is the Ohmite 20J50RE. This resistor has a resistance of 50 Ω which generates 0.218 W when subjected to the 3.3 V Arduino ESC voltage based on Equation 29. For this reason, six of these resistors were used for a total of 1.31 W generated. Using more resistors has the additional benefit of more surface are for heat transfer to occur between the heater and the electronics bay air. They could also be placed to surround the batteries and concentrate the heating where it is most needed.

$$P = \frac{V^2}{R} \tag{29}$$

After running the model at low temperatures, it was discovered that the resistor would overheat the payload during the first portion of the mission unless the resistors could be switched on and off. In order to accomplish this on and off capability, a relay circuit was designed that will be directly powered by the Arduino Mega. The Mega will monitor a TMP36 temperature sensor, and when the temperature reads below 10 °C, the Arduino will activate a switch on the relay circuit (n-Channel MOSFET) containing the resistor. By opening or closing the circuit, current supplied to the resistor can be added or removed. The relay switch using an n-Channel MOSFET relay switch is illustrated in Figure 49.

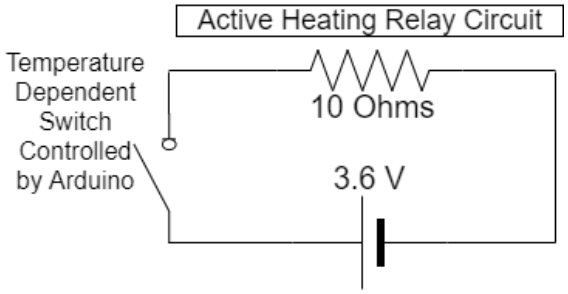

Figure 49. Relay Switch for Active Heating

Using the model with all the described conditions and active heating results in Figure 50 below. This figure illustrates that the electronics bay stays around an average temperature of 0 °C which was deemed viable for battery performance. Battery performance was determined to be viable at 0 °C because it results in 70% to 80% of the nominal capacity. For this reason, the thermal model indicates that the payload can survive the atmospheric conditions and satisfies FR 3.0. This model was tested and verified using a hypobaric chamber test and a thermal chamber test. These results and implications will be discussed in the 'Verification and Validation' Section later in the paper.

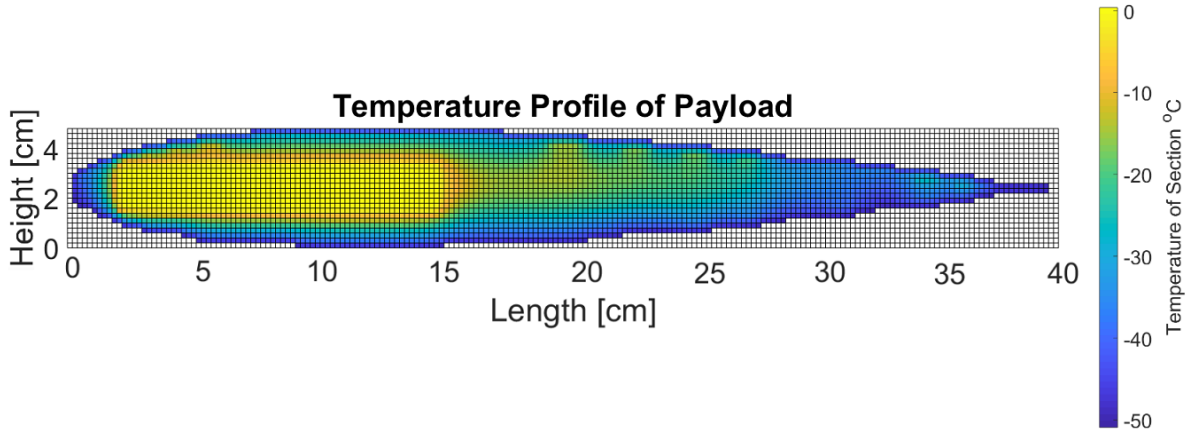

Figure 50. Final Electronics Bay Thermal Model

3.7. Baseline Design

The overall design consists of the latex balloon, HYFLITS valve system, the lifting orbiter system, and the sensor package, as seen in Fig. 51. The balloon utilized for the launch will be the HAB TX-1500 which will lift the entire mission package to our test altitude. This balloon will also provide the lifting force needed to attain neutral buoyancy at the target altitude.

The venting system utilized will come from previous HYFLITS missions. It will be powered and operated through a hard line that runs alongside the tether.

The HALO system will begin oscillations within the target altitude through the orbiting motion of the affixed flying wing. This wing will be driven by an on-board propeller. By creating lift, the wing will decrease the weight felt on the balloon and will allow the balloon to rise in altitude. The flying wing will have a tail that is actuated by a servo. This will allow the wing to change elevations which, by creating negative lift, will pull the HALO system to the bottom of the target altitude.

Inside of the flying wing will be the sensor package. This includes sensors to gather positional and environmental data. These sensors will allow the system to effectively operate autonomously based on environmental factors. This will also allow turbulence data to be collected on the leading edge of the flying wing.

The balloon will be affixed to the venting system. This system replicates the same venting mechanism that was utilized on previous HYFLITS missions. The venting system is followed by the tether, which consists of a Kevlar load bearing structural tether and a non-load bearing communication tether. The load bearing tether also includes the CDAS model rocket parachute. The primary payload is suspended on the other end of the tether, and consists of a wing, tailerator, motor / propeller combo, and sensor package.

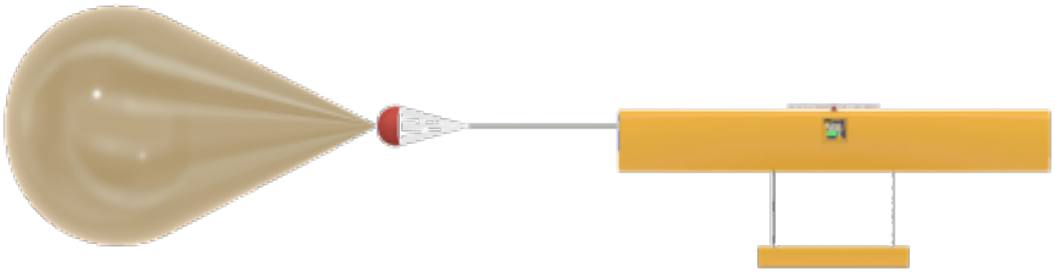

Figure 51. Full System Diagram

4. Manufacturing

Author(s): Tyler Faragallah, Kelly Crombie, Ryan Lansdon

4.1. Manufacturing Scope

4.1.1. Lifting Orbiter

The lifting orbiter was manufactured 100% in-house, with the exception of the electronic components. The main body of the wing and tail were CNC cut with a hot wire cutter from blocks of expanded polystyrene foam. The tail was supported by carbon fiber spars that were embedded in the wing and secured with generic two part epoxy resin. The same spars were embedded longitudinally and provided spanwise resistance to flexing. The motor mount, electronics bay, and tail hinge components were all 3D printed out of PLA, using a fused deposition modeling type printer. The components were all permanently assembled in place using the same epoxy resin that was used to secure the carbon

spars in place. All the 3D printed parts were designed to be printed without needing support material during the print process, which ensures an accurate part is produced without the need for detailed touch-up work.

4.1.2. Tether

The tether was made of an assortment of commercially available off the shelf components, which were then assembled into the tether subsystem. The tether subsystem can be further broken down into the structural tether that connects the payload to the balloon and the communication tether, which supports no weight but allows the electronics in the payload to communicate with the vent on the balloon.

Load Bearing Tether

The load bearing tether is made of a length of 150 pound test Kevlar kite twine. This is tied on one end to the vent/balloon and is tied to the top of the CDAS parachute on the other end. Another length of the same Kevlar twine is tied to a 50 pound test fishing swivel which is also tied to the CDAS parachute suspension lines. The end of this Kevlar length terminates at the payload and is wrapped multiple times around the span of the wing before being bonded in place using epoxy and fiber tape.

Data Tether

The data tether begins on the vent where an electrical slip ring is mounted. The slip ring allows the data tether to move and rotate independently from the load bearing tether, mitigating tangling risks. Extending from the slip ring is a three wire communication line, which connects to the Arduino in the orbiter electronics bay. The data tether must be 10% longer than the load bearing tether to ensure that it never has to support any of the forces encountered during ascent and orbiting operations.

4.1.3. Software

Wrapping together all of Project HALO is a moderate reliance on software. With excellent wing design and analysis, the team expects the orbiter to be able to orbit with ease; however, there is a still a fundamental load placed on software to ensure all subsystems will run smoothly. The main concerns are thermal control, orbit acquisition, data transmission, and altitude control. Since the project will be entirely autonomous the software will need to have well designed loops to ensure it can handle various cases the conditions will present. Luckily, Project HALO heavily relies on a flight profile. The balloon will rise, vent, orbit, then descend. Since the underlying structure of flight is already determined, the code can be designed to handle each case in a step-like manner. Below are a few flow charts outlining various subsystems and cases the code will be handling.

Figure 52. Key For Electronics Flow Charts

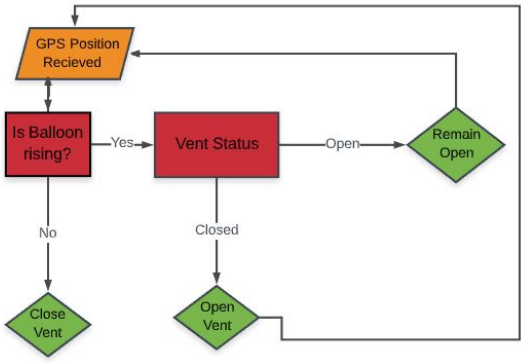

Figure 53. Venting for neutral buoyancy

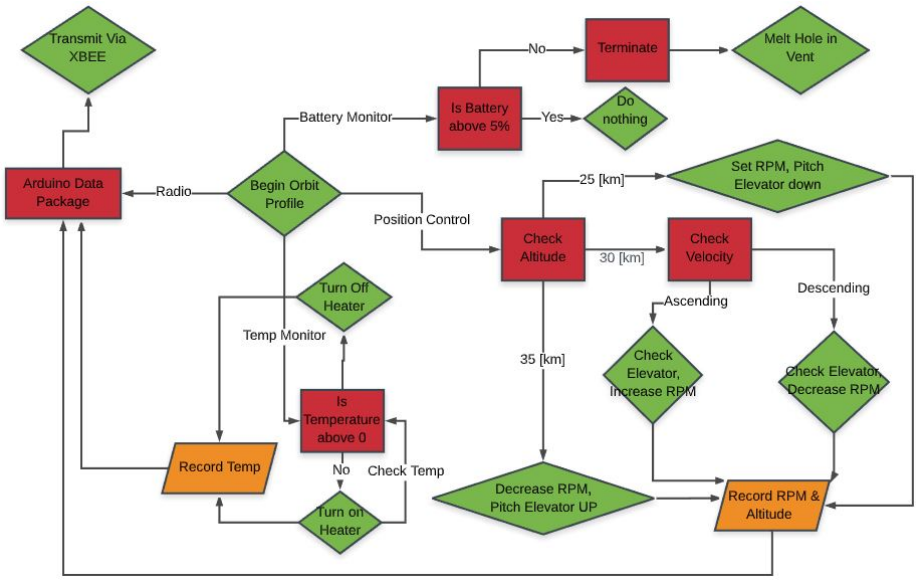

Figure 54. Simplified Orbital Loop Flow Chart

In addition to the simplified flow charts, project HALO has developed some brief sample code for all the basic Arduino capabilities. The code is provided in the full archive document with detailed instructions on how to run it and what to expect the code to do. Below is a brief outline of what code is available for each subsystem.

1. Motor / ESC: We currently have a set of code for calibrating the ESC to any desired settings. This is done through the serial monitor directly to the computer. This same code can also be used for manual testing. The code allows you to input a throttle percentage and then will send the signal to the ESC and hold it until you send another signal. A perk of this code is you can quickly turn off the code with a 0 command. The orbit acquisition code has not been developed yet.

2. IMU: Code has been developed in order to parse IMU data to extract only the parameters relevant to β angle calculation. Namely, the angular rates can be extracted and converted to a β angle.

3. GPS: For the GPS we developed code to read in and parse the data using the help of some libraries. Using libraries from Adafruit we can jump straight to getting the altitude, latitude, and longitude. We can also store these into float variables which we later use to control our vent and tail servos and motor.

4. Servos - Vent & Tail The team developed working code to actuate a servo via serial monitor. Code was also developed to set the vent and tail servo to open/ closed and up/down depending on the GPS altitude. Controlling the servos is extremely easy in Arduino the only thing to note is you need to be very careful with the orientation

of the servo. The control horn on the servo gear can be removed and replaced to get a better range of motion if you need it. After changing the control horn be sure to update your max and min deflection angles. For example, we discovered 43 degrees was the point where the vent closed and 130 was the point is was open without putting too much strain on the spring.

5. Radio: The Xbee, similar to the servo, is very simple to use. Code was developed to use an Xbee library which you can send strings of data with a simple ”write” function. Our code includes integration to send temperature sensor data over the radio live. We also developed a set of code for testing the radio which takes in data from the serial monitor and the Arduino sends to the radio which is then output by the radio.

6. Temperature Sensor: The temperature sensor code is just two-three lines which take in an analog input and then do some basic math to convert the signal into the temperature in Celsius or Fahrenheit. This code and shifting is dependant on the sensor, but the rough calibration is based on your input voltage. Since the Arduino Mega is a 5V system the math boils down to taking the signal multiply by 5V and divide by 1024 then account for the manufacturer offset. This will give you a temperature in Fahrenheit, you can then convert to Celsius with more math. Regardless, the team had it calibrated to within 2 degrees. The team calibrated against a wall thermometer so it was not the most accurate method. Further calibration should be done with a more finely controlled temperature and against a sensor with a higher accuracy.

4.1.4. Electronics

A table including all electronics in the electronics package can be found below.

Component	Chosen	Voltage [V]	Current [mA]	Mass [g]	Powered By:
GPS	Adafruit Ultimate	3.3	25	8.5	3.3V Arduino Pin
Controller	Arduino Mega	7.6	100	53	LG MU1 Barrel Connector
IMU	Sparkfun 9DoF Razor IMU	5	10	15	5V Arduino Pin
Radio	Digi XBee® SX 900	3.3	150	3	3.3V Arduino Pin
Motor	Hobby King D2822/14 1450kv	14.4	2000	38	Samsung 50E
ESC	HobbyKing 20A ESC 3A UBEC	14.4	20000	30	Samsung 50E
Controller Battery	2 x LG MU1 18650	6.7	NA	2x49 = 98	NA
Motor Battery	4 x Samsung 50E 21700	14.4	NA	4 x 69 = 276	NA
Temperature Sensor	TMP36	3.3	5	1	3.3V Arduino Pin
Heater	Ohmite WHC10RFET	5	variable	.2	5V ESC Pin
Relay Switch					Arduino Digital IO
Logic Shifter	SparkFun Logic Level Converter	5	10	8	3.3V & 5.5V Arduino Pin
Tail Actuator	HS-5055MG	5	3	9.5	Arduino Digital IO

Table 37. Electronics Suite Breakdown

Once all electronics were chosen for the project in accordance with functional requirements, the following schematic was developed showing the pinouts to be used for each component.

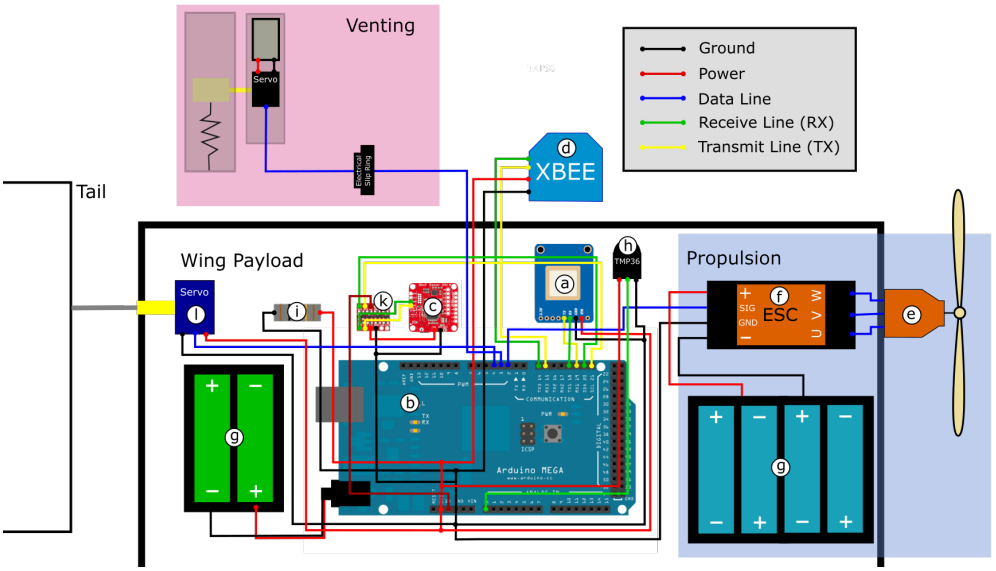

Figure 55. Electronics Schematic

- Sensors: Since all the sensors are relatively similar, this section serves as a general guide. The most useful way to hookup all the electronics is to solder header pins onto the body and then use female to male jumper pins to plug into the Arduino. This makes the process quick and easy. However, for long term manufacturing header pins can be used and then soldered into the PCB board discussed later.
- WireRound Resistors: For the resistors, the main thing to note is they come with large exposed metal leads. In order to ensure there is no shorting, these should be trimmed down significantly. Next, solder your preferred gauge of wire and be sure to use heat shrink over the end all the way up to the resistor so there is no bare metal exposed.
- LiPo Batteries: To manufacture the batteries the team opted to solder them. Many will recommend against doing so, but it is perfectly safe if you use proper technique and materials. They key to making the batteries safely is to use solder flux, nickel strips, and to use a wide head soldering iron tip. You will also need to keep the wiring diagram handy depending on the battery. The two cell setups we used are shown below. On the batteries, the flat side denotes the negative and the side with the vent cap is the positive. Since the batteries heat up very rapidly the safest method is to do the following:
  - Cut nickel strips to connect battery terminals
  - Solder wires onto each nickel strip
  - Create pool of solder on each end of nickel strip which will connect to the battery terminals
  - Apply flux to battery terminals
  - Position the nickel strip
  - Inser flat wide head solder iron directly into the solder and wait for it to melt.
  - Move solder iron within in the solder puddle and apply heat to the terminals for a few seconds then slowly remove while applying pressure to the nickel strip.

  While doing the above process monitor the temperature of the batteries and ensure they do not become uncomfortably hot to handle if they do you need to stop immediately and allow the battery to cool before handling. Additionally, when making the battery you will want to use an XT-60 connector which will allow you to connect to an ESC and a JST-XH connector which is what LiPo balance chargers use.

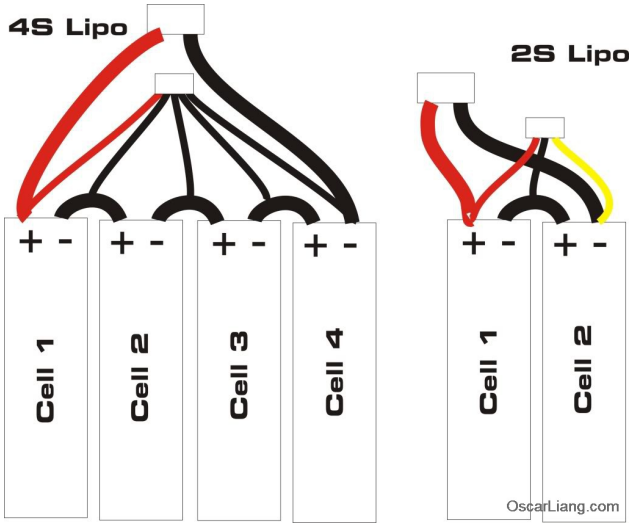

Figure 56. Wiring Diagram for 2 and 4 Cell Battery Packs

- ESC / Motor: For the ESC motor you will want to make a pair of quick connectors, solder, and a heat sink. Essentially, this allows you to connect and disconnect the two components which helps keep the components easy to transport and swap out when one breaks. For our project we chose spade connectors, but one you use a covered bullet connector because the spade connectors are exposed and could lead to shorts.
- Custom Arduino Mega Shield

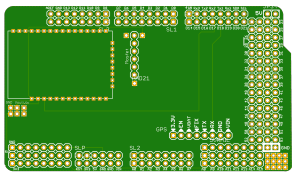

Figure 57. Front of shield

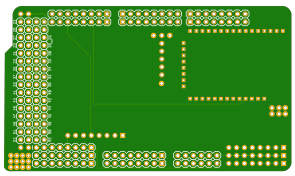

Figure 58. Back side of PCB Board

As the team began the manufacturing process we quickly realized plugging everything into the Arduino directly was slow and tedious. It also made wiring a mess and made it easy for things to come unconnected. We decided to make a custom PCB shield instead to fix this issue. Above are some pictures of the shield. It was created in Eagle in which we only use a 3 layer board with traces on the top and bottom. We made slots for the radio and GPS which connect to the proper Arduino ports via traces. We also added extra ground and 3.3 and 5 Volt rails for future project development.

4.2. Manufacturing Outcome and System Integration

4.2.1. Lifting Orbiter

The construction of the lifting orbiter proved to be one of the more challenging manufacturing tasks for the semester. The team was unfamiliar with the techniques and outcomes that result from the CNC hot wire foam cutting process. When combined with a CNC machine that has only the support of tribal knowledge passed between students and faculty there was a lot of trial and error to get the correct g-code, CNC machine parameters, and order of operations. However, the wing and tail sections were successfully cut, assembled, and to some degree tested prior to campus closure.

4.2.2. Tether

The load bearing portion of the tether was easy to manufacture, and working tether examples were used within the first 3 weeks of the semester to conduct the *CDAS Drop Test*. However, while the components had arrived the data tether was never assembled or tested during the semester, save for a small test to ensure that the vent could be opened and closed on command from the Arduino.

4.2.3. Software

The difficult components of the software was developed and tested, however the bulk of the mission essential code was not developed. Development and testing were ongoing for the GUI to read the live data transmitted from our payload. The final launch code would need to include an orbit acquisition loop, altitude oscillation loop, and a termination loop. Unfortunately, none of these control loops were written in Arduino and are only shown in our block diagrams. These control loops were never completed due to campus closure; they were to be developed alongside calibration tests which were yet to come.

4.2.4. Electronics

During the assembly of the electronics, the largest challenge was packing all the components as close together as possible. This was required to increase the effectiveness of the active heating system and to reduce its power draw. Additionally, it was found that there was not enough room to use standard micro-electronic style jumper wires between components, so a custom Arduino shield was developed. However, the order for the shield was interrupted due to campus closure.

4.2.5. System Integration

At the conclusion of the manufacturing portion of the semester each of the major subsystems: lifting orbiter, tether, software, and electronics, had be integrated to the point that there was a working prototype of each one. The next tests that were planned would have required the integration of major subsystems, working towards a fully integrated project tests at the end of the semester.

5. Verification and Validation

Author(s): Braden Barkemeyer, Jared Dempewolf, David Cease, Kyle Mcgue, Tyler Faragallah, Kelly Crombie, Jacob Marvin, Nolan Ferguson

5.1. Controlled Descent and Arrest System (CDAS) Verification

5.1.1. CDAS Test

The first test that the team was able to conduct was one that tested the abilities of the CDAS. This test involved attaching a 1.5 kg mass to the CDAS, and dropping it off of the CU aerospace building. This test would allow the team to verify the successful deployment of the CDAS (which is a parachute), as well as its ability to slow the descent speed of the system to a safe speed. This was chosen to be the first test as it was the simplest to set up, gain permission, and complete. In order to properly predict the behavior of this test, a set of differential equations were set up and, with the help of MATLAB's ode45 function, were solved and were able to record both the velocity and acceleration of an object dropped from a height, mirroring the group's set up of a system falling with a parachute deployed. As such the underlying differential term that was solved for was:

$$a = \frac{F}{m} = \frac{\frac{1}{2}\rho S\,(Cd + \delta)V^2}{(m + \delta)} \tag{30}$$

This equation gives us the aerodynamic motion of the system, with which both velocity and acceleration through descent can be calculated. It is important to note here that the term δ represents a compounded uncertainty in the aerodynamic properties that influence drag of the system (like parachute Cd), and were added in to help produce an upper and lower bound for the model. So from this model the group was able to produce Figures 59 and 60.

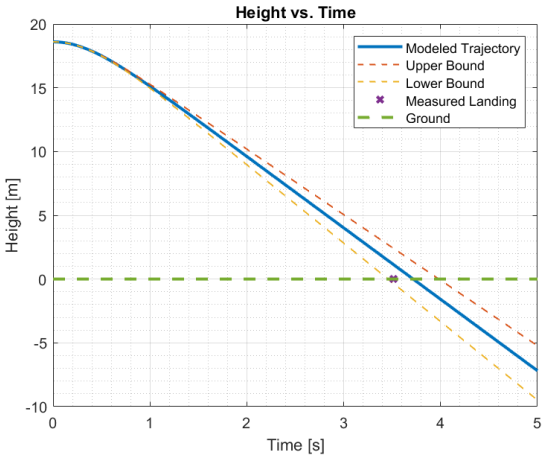

Figure 59. CDAS Test: Height vs. Time

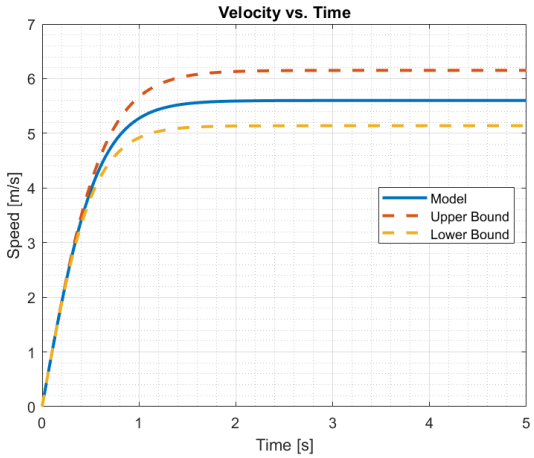

Figure 60. CDAS Test: Velocity vs. Time

From these plots it can be concluded that we should expect this test to take roughly 3.5 to 4 seconds and reach a terminal velocity after around 1.5 seconds, if the model is correct. If this is the case the group will have successfully proven that the method of satisfying the CDAS requirement will have been fulfilled, which would mean the team has properly addressed FR 7.0.

The experiment was completed and video-recorded. It was found that the CDAS reached the ground after approximately 3.5 seconds, which matches within the bounds of the model. The group was also able to use the video taken and, with the help of a tracking software, was also able to get the experimental velocity. With the tracking software a flight profile was obtained, for which the terminal velocity could be found. This average final velocity turned out to be roughly 5.9 $\frac{m}{s}$, again which is contained in the uncertainty bars on figure 60. It is also important to note that the difference between the ideal kinematics model (5.44 $\frac{m}{s}$) and measured experimental velocity ($\approx$ 5.9 $\frac{m}{s}$) is very marginal.

5.1.2. CDAS Implications

The implications of the CDAS test are that it can be said with confidence that the model created for it is sufficient in explaining and providing the basis to verify FR 7.0. This is important because it would indicate that in the event of a catastrophic failure, the group's project would descend at a safe rate and not injure any person or property. Also it is important to make a note that this model should be viewed as the worst case as the final project has a payload with a much larger surface area, which in turn would increase drag and significantly decreasing the descent velocity.

A very rudimentary way that the group has arrived at this conclusion is from studying another catastrophic event that has occurred. It is said that there was an accidental killing in baseball where the pitcher (Carl Mays) directly struck the batter (Ray Chapman) hard enough to fracture his skull. As such the group focused on this weird event to try and figure out the energy that is needed to have the potential to kill somebody if an object strikes the right place. From a quick Google search the estimated speed from a fastball during this pitcher's time is around 90 mph (= 40.2336 m/s) and the mass of an average baseball is around 150g. With these it is possible to use kinematics in order to try and find the energy that was exerted:

$$\frac{1}{2}mV^2 = KE \rightarrow \frac{1}{2}(0.15)(40.2336)^2 = KE = 121.42J$$

With this energy as the basis of human endangerment, a new velocity can be found. The group opted to study the velocity that would be induced from just the electronics package reaching terminal velocity, as it carries most of the mass and the foam would offer a less rigid and has an extremely high surface area. The previous equation re-solved for the group's electronics package can be found as:

$$\frac{1}{2}mV^2 = KE \rightarrow V = \sqrt{\frac{2KE}{m}} = \sqrt{\frac{2(121.42)}{0.6}} = 20.117m/s$$

This result is to say that a 0.6 kg electronics payload would begin to reach the endangerment region at a velocity of around 20.117 $\frac{m}{s}$. From above it has been seen in the CDAS results that the absolute maximum estimated velocity is

around 6.2 $\frac{m}{s}$, which is to say that there is a factor of safety of about three in terms of addressing the descent speed. It is also important to note here, that this velocity would represent that the electronics package has the size and shape of a baseball, which is not the case. As such the effects that would be experienced would be mitigated as the surface area, and compactness of the package is much greater. So this calculation should serve as an absolute worst case, which still allows the group a factor of safety equalling three.

5.2. IMU β Calculation Verification

5.2.1. β Determination Model

β angle determination is one of the key elements of the HALO mission. As is visible in Fig. 61, β is the angle from the horizontal where the tether meets the balloon. In order to determine whether the orbiter is flying within the balloon wake, this β angle will be actively checked and controlled; if β is too high and the orbiter is within the projected balloon wake, the motor will be actuated to a higher setting in order to decrease β.

In order to determine exactly what this β is, an IMU on the lifting orbiter will be measuring angular rates. This IMU will be oriented such that one axis points in the direction of motion. With this orientation, it is then possible to calculate β with a simple trigonometric relationship.

$$\beta = \arctan(\frac{w_x}{w_y}) \tag{31}$$

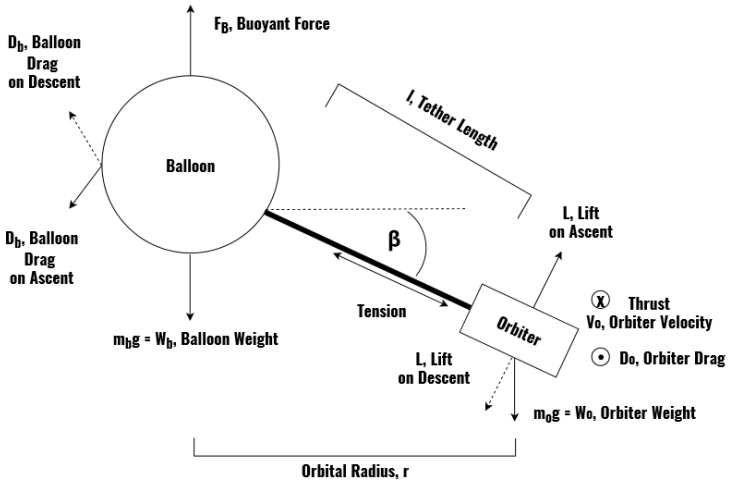

Figure 61. Free Body Diagram

With reference to the free body diagram illustrated above, w_x is the angular rate along the axis pointing towards the tether, w_z is the angular rate along the axis pointing into the page, and w_y is the orthogonal axis.

5.2.2. β Determination Test

In order to verify this β determination method, a low-level preliminary test was conducted. This consisted of hooking an IMU up to a laptop, setting it up to output its angular rates to a serial monitor, and manually swinging it in circles. These angular rates would be used to calculate a corresponding β angle for each successive data point. During the experiment, a video was recorded in order to visually measure β as a means for comparison. The results from this test can be seen in the following plot.

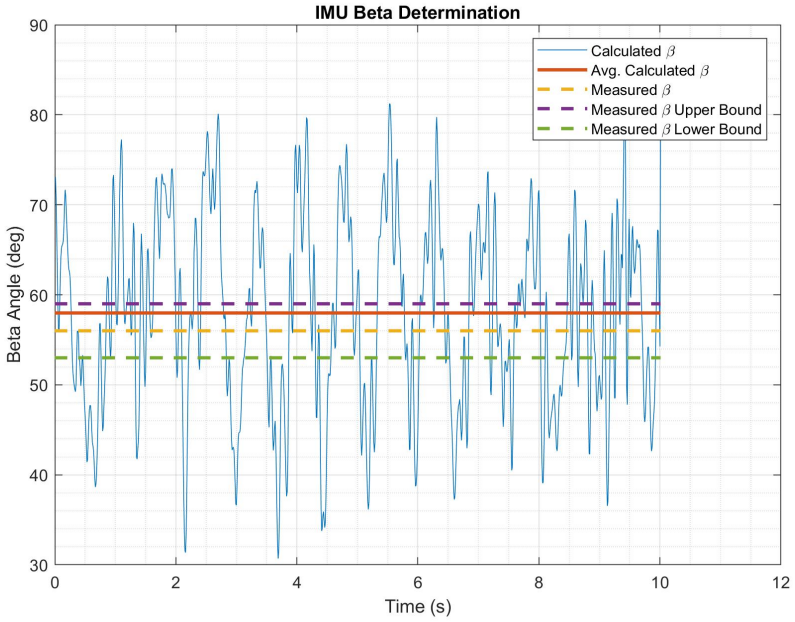

Figure 62. β Determination Test Results

5.2.3. β Determination Implications

Focusing on Fig. 62, it is clear that there is significant measurement noise involved with the experimentally calculated β angle indicated by the blue line. This was expected, since the IMU was manually swung in circles. The source of this noise likely came from human error, footsteps, or unsteady arms. The three dashed lines represent the β angle measured visually from the video; upper and lower bounds, as well as the mean angle are represented. The mean experimental β angle falls less than 2°away from the mean visually measured β angle, suggesting that this determination method is suitable for the mission. It will be reasonable for this mission to control the orbiter to more than 2°outside of the balloon wake, so this error is acceptable.

This was a low-level, preliminary test. This was deemed acceptable at the time, because this β determination would be further verified during the Orbit Acquisition and Moored tests. This test corroborated FR 1.0, that there will be a method of controlling the altitude of the balloon and payload.

5.3. Tether Strength Verification

5.3.1. Tether Strength Concerns

The tether must be strong enough to support the loads that will be created during the ascent and orbiting phases of the project. These are projected to be a maximum of 10 pounds, or 4.5 kg. In addition, the Federal Aviation Administration (FAA) requires that tethers on unregulated balloons break when subjected to a 50 pound (224 N) impulsive force. This is to ensure that the a payload and balloon does not get caught on an aircraft in the event of a collision. However, the FAA does not provide a time interval for the load to be applied during verification testing. Using known industry practices from NOAA and NCAR balloon flights, we developed the following test.

5.3.2. Tether Strength Test

The current method accepted by industry to meet the FAA requirement is the use of an overly strong tether with an engineered weak link inline with the tether to permit breakage under the 50 lb impulsive force. The weak links used in NOAA and NCAR balloon launches are pieces of ”50 pound test” fishing hardware, which have a published working load of 50 lbs. The tether was tied to a ”50 lb test” fishing swivel, which was hooked on a hanging scale. The hanging scale was suspended between two tables with the other end of the tether tied to an eye-bolt that passed through two 25 lb weights for a grand total of 50 lbs. The weights were lifted till there was 3 inches of slack in the tether before being

dropped to impart an impulsive load on the tether. The load experienced at failure was recorded using a high speed camera pointed at the scale, which enabled a frame-by-frame review of the force loading for each test instance.

Figure 63. Tether Test Setup

5.3.3. Tether Test Implications

We found that our chosen fishing hardware was not the weak link in our system, and easily survived the drop test. However, the kevlar tether routinely broke at the attachment knot that had been used to connect it to the fishing swivel. As shown in Figure 64 the recorded force never exceeded 42 lbs at breakage and never was lower than 36 lbs, which ensures that the tether will break upon impact with an aircraft while also supporting the payload with a safety factor of 3. Figure 64 also shows the statistical bootstrap analysis of the test data, which allowed the extrapolation of the experimental dataset into a viable statistical model. With the tether breaking below 50 lbs, it provides extra confidence that the HALO project will not be jeopardizing the safety of civil aviation during launches.

Further, this test corroborated the notion that the tether would not break under expected tension forces imparted by the orbiter, which are expected to reach a maximum value of approximately 10 N during flight.

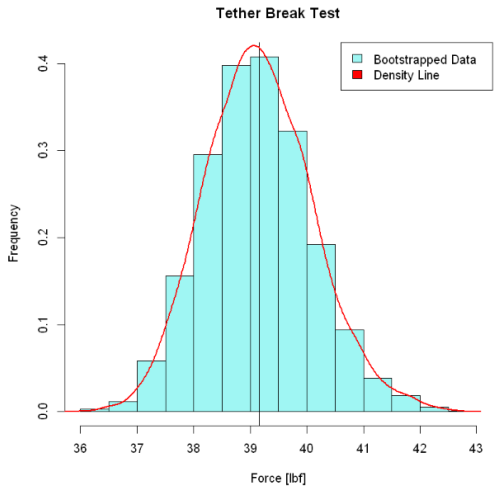

Figure 64. Tether strength testing results

5.4. Software Verification

Due to the high reliance on software it was quickly deemed a critical aspect of this project. Unfortunately, due to campus closure, we did not get to verify the main chunks of our software but we were able to prove feasibility with almost all our baseline components.

5.4.1. Radio Testing

The team conducted two tests of our radio.

One was a small scale range test in which we sent a fixes stream of data out through the radio, we then moved the receiver station away from the window until we lost the signal. Without any specified antenna setup we were able to reach across Colorado Ave from the electronics shop window despite debris.

The second test was a short range test in which we transmitted live temperature data while conducting the vacuum chamber test.

5.5. IMU Verification

The IMU was able to successfully communicate with the Arduino Mega, allowing transfer of values required for calculating the Beta angle. This was the fullest extent of on board beta angle testing. Note, however, a preliminary spin test, holding the IMU and spinning it in a circle, showed a beta angle average calculation within 3 degrees of the expected value. See section 5.2 for specifics.

5.5.1. Software Dry Run Test

Our first major test looked at how our system meshed together. In the dry run test we looked at actuating our tail and vent relative to altitude. While we could have included motor rpm, we did not include in the test since moving the motor and battery would have made the test harder to conduct. We conducted this test by looking at altitude change between the floors of the aerospace building and having the vent open or close and the tail move up or down.

5.5.2. Motor Testing

The team conducted two main tests of the motor. The first was a throttle test in which we stepped in from 0-100% in single increments, 10 percent increments, then larger random steps. The idea behind the test was to ensure the motor could respond quick enough. The team also conducted a test from 0-100% throttle in which we monitored the temperature of the ESC. This was done so that we could better collaborate our heat dissipated for the thermal model.

5.5.3. Software Implications

From all these tests we proved we can use all of our components. We got GPS data, thermal data, were able to control all our servos. We proved baseline controls using Arduino software. The main implications are that you really need to make sure you track your numbers and data type correctly in Arduino otherwise if you leave off decimals it can really mess with your control loops.

5.6. Thermal Model Verification

Thermal survival was a concern for our project because temperatures temperatures in the upper atmosphere can get as low as -56.5 degrees Celsius. To address this concern, a high-fidelity thermal model was created which was discussed in detail in the 'Design Process and Outcomes' section. The results of this model indicated we could meet our functional requirement of electronic survival. However, some tests needed to be run to verify the model. The two tests that were completed were a hypobaric chamber test and a thermal chamber test.

5.6.1. Hypobaric Chamber Test

A large concern with the model was that the resistors would not be able to dissipate heat to the payload in a low density environment. This is because there are less molecules in the air at low density and thus fewer molecules for heat to transfer through. Because of this, the purpose of this test was to verify that the heaters would be able to transfer heat in a low-density environment as well as validate one of the model's assumptions that heat transfer in the payload can be modeled as pure conduction.

The hypobaric chamber test was performed by placing the payload in a hypobaric chamber with the pressure cranked down to match the lowest expected atmospheric density (0.008 $[\frac{km}{m^3}]$). The temperature was 22.5 degrees Celsius in the room so using the ideal gas law, the hypobaric chamber pressure was reduced to 678.8 Pascals.

For this test, three thermal sensors were placed in the three locations indicated in Figure 65. The idea was that the temperature gradient between the locations would help indicate if heat was transferred throughout the payload in accordance with the model. In the plot, the black line indicates our predictive model while the colored lines indicate the data at the 3 thermal sensor locations. The 3 thermal sensor locations stayed within half a degree of each other which verifies that heat is still able to transfer through the payload. Likewise, the predictive thermal model average temperature stayed within 1 degree Celsius of the average data which verifies that the resistors were able to transfer heat to the payload air.

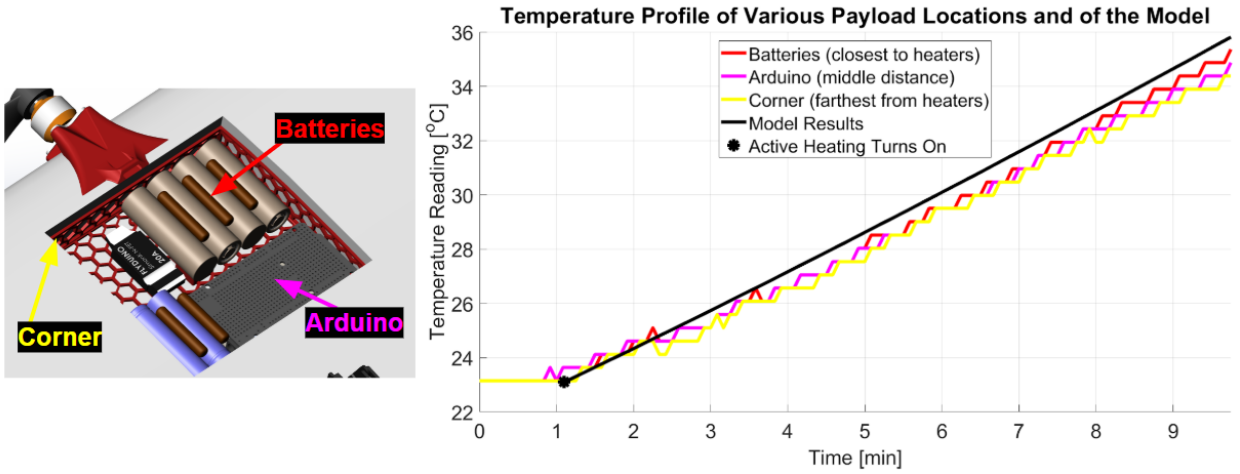

Figure 65. Hypobaric Chamber Test Results

5.6.2. Thermal Chamber Test

The thermal chamber test served as a preliminary test to see if the payload could establish the predicted thermal gradient between the inside and the atmospheric conditions. Because of this, the purpose of this test was to generally verify the model code and heat transfer equations by comparing the predictive model to real world data.

The thermal chamber test was performed by placing the payload in a cooler with dry ice. All of our electronics were present with the exception of the motor. Three temperature sensors were used. Two were located in the payload with one near the batteries and one near the Arduino (Figure 66). The third was placed directly at the outer surface of the payload. This sensor was used to determine how cold the atmospheric conditions in the cooler got and help to determine the temperature gradient between the inside of the payload and the outside.

In the plot (Figure 66), the black star indicates when the active heating turned on and then remained on for the duration. This was set to a trigger of 20 degrees Celsius for testing purposes. The green box indicates the electronics operating range. The black line near the top is the predictive model and the two colored lines at the top represent the data from the thermal sensors in the payload. Lastly, the blue line along the bottom is the temperature on the surface of the payload box due to the dry ice. The data outperformed the model by 4 degrees Celsius and established a temperature difference of 72 degrees Celsius. This keeps the payload well within the operating range and the 4 degree difference verifies the model behaves closely to real world conditions. Some of this error may be due to the fact that the cooler is a closed system is not fully representative of an atmospheric circulation.

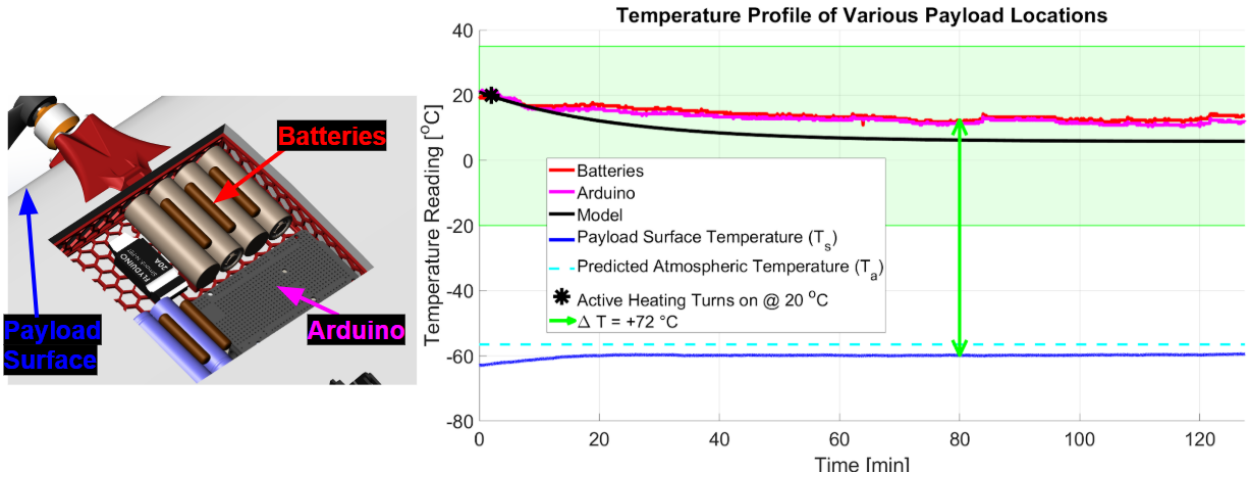

Figure 66. Thermal Chamber Test Results

5.6.3. Thermal Implications

In conclusion, the hypobaric chamber test was conducted to verify that the heaters would be able to transfer heat in a low-density environment as well as validate one of the model's assumptions that heat transfer in the payload can be modeled as pure conduction. The test was successful in those regards and establishes more confidence in the thermal model moving forward. Likewise, the thermal chamber test was conducted to generally verify that the model is predictive of real world conditions. It too was successful in that regard.

Both of these tests served to establish a higher confidence in the thermal model and a higher confidence that the mission would be able to meet Functional Requirement 3.0. This requirement states that the electronics must be able to survive throughout the mission duration.

One shortfall of the completed tests is that they did not include convective heat or radiation heat transfer that would be present in the actual mission. These would have been very hard factors to investigate and test without a full flight test. However, if a full flight test had been able to be performed, then the temperature data could have been used post-operatively to improve the model for future iterations. The benefit of the HALO mission type is that it will have many future launches and that the system can continue to be improved as more data is gathered. The model could be constantly improved.

5.7. Thrust Model Verification

5.7.1. Thrust Model

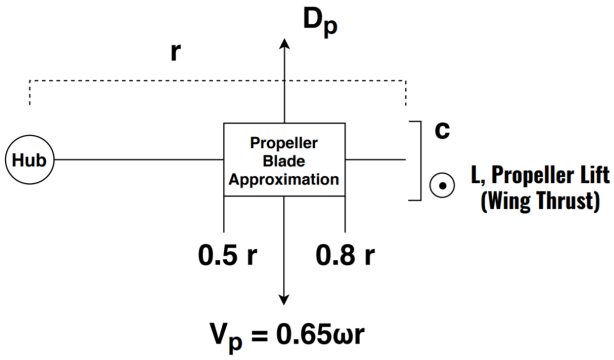

Figure 67. Blade Element Theory Approximation

Verifying that the orbiter is capable of reaching velocities suitable for this mission is critical; in order to do this, the utilized thrust model must be verified. The thrust model used for this mission consisted of a simple Blade Element Theory approximation. This consisted of treating the middle section of a propeller as a NACA 4412 airfoil and conducting a simple aerodynamic analysis.

5.7.2. Thrust Model Test

This thrust model was verified with the help of a static thrust test stand. The selected motor and propeller combination was attached to the stand, and motor inputs were stepped up from 10% to 100% in 10% increments. At each step, a corresponding RPM was measured with a tachometer. This data was collected and compared to the trend predicted from the Blade Element Theory model. The results of this test can be found in the plot below.

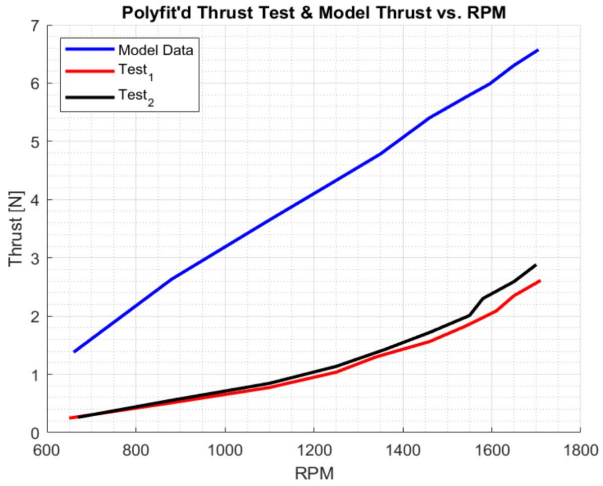

Figure 68. Thrust Test Results

5.7.3. Thrust Implications

Focusing on Fig. 68, it is evident that the predictive Blade Element Theory thrust model over-predicted the generated thrust by a factor of approximately 2. Unfortunately, due to campus closure, the source of this error could not be properly investigated. It would have been beneficial to repeat this test with different motors and propellers to gain a better understanding of where the model failed. Under the circumstances, no hard conclusions could be drawn from the gathered data. This test failed to verify FR 2.0, that the orbiter would be capable of orbiting beneath the balloon. Even if these results had been consistent for varying propeller sizes and the utilized thrust model always over-predicted by a factor of 2, success could still be found in the HALO mission. There are various potential solutions to this issue including: increasing designed motor RPM, increasing maximum allowed orbital velocity, or decreasing the maximum system altitude. Overall, this obstacle should not lead to critical failure for the HALO mission.

5.8. Data Range Verification

5.8.1. Data Range Test

The data range test ensured fulfillment of Functional Requirement number 4, that we are able to transmit collected data from the payload, to the ground station. Because the HALO system was not designed to be recovered, the data collected in flight needs to be received continuously in real time. Ascending over 30 km in altitude, any slight horizontal wind force would have the potential to drift the package dozens of miles off course from the launch site. We thus designed for a feasible transmission distance of approximately 100 km.

Because the proposed data range that would be tested was so large, the method of ensuring transmittable range was done using signal attenuation. To do this, the radios would be set at a nominal fixed distance apart, approximately 100 ft. The power passed to the radios would then be gradually reduced until the signal was lost, or until the data being received had significant lost packets. This is the method of validation used with HYFLITs, so there was confidence in

this test's ability to replicate real conditions. This test would was anticipated to validate two critical aspects of HALO during this test—namely that that the system would be able to communicate to the ground station during flight and than the GUI would be able to decipher data packets in real time.

The GUI pictured in Fig. 69 is the application developed in Matlab that allowed for processing of real time data. The GUI was designed to decipher and break down the components of the data transmissions such that it could be interpreted to determine the system's performance. Information such as altitude, location, and velocity are derived from GPS and thermocouple data is logged over time. An important aspect of the GUI is its ability to count lost packets. In each data packet is a unique ID that is iteratively increased. The groundstation GUI preemptively looks for this initializing ID number and determines if it is the next packet in the sequence, and as such is able to determine if there are any pieces of data missing.

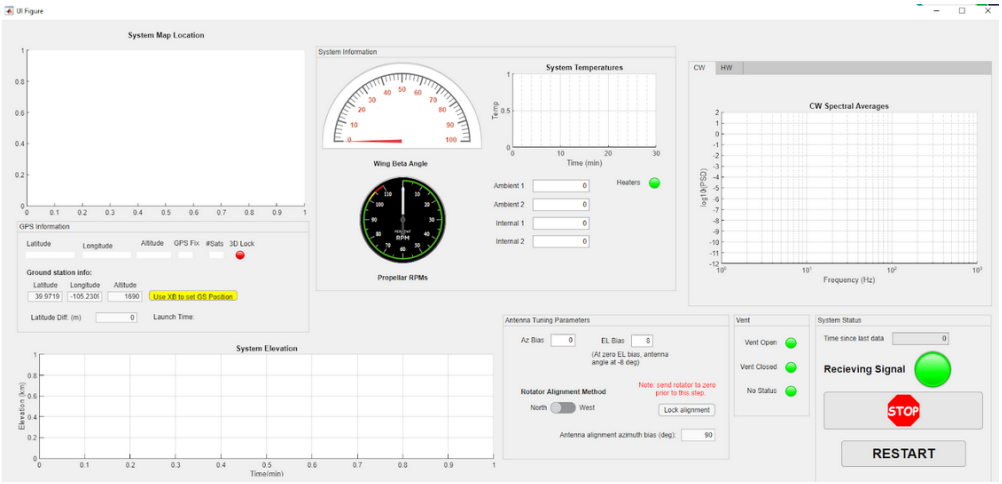

Figure 69. Matlab GUI developed to process real-time data transmissions.

5.8.2. Data Range Implications

The data range test confirms if the system is able to communicate while operating at its test altitude. Due to not being able to test, there are uncertainties with this test regarding atmospheric and wind disruptions. We have not been able to gain a bound on the amount of moisture or cloud cover present that would inhibit communication. Without validation of this test, the HALO system would be unable to receive data communications. The Matlab GUI is the method utilized to not only receive, but also process and analyze data in real-time. Without real-time analysis it would be impossible to tell if adjustments in transmission parameters needed to be made or if the test needed to be terminated altogether. This includes occurrences such as the system flying into controlled airspace, or ascending at a rate that is uncontrollable.

5.9. Low Altitude Orbit Model Verification

5.9.1. *Low Altitude Orbit Model*

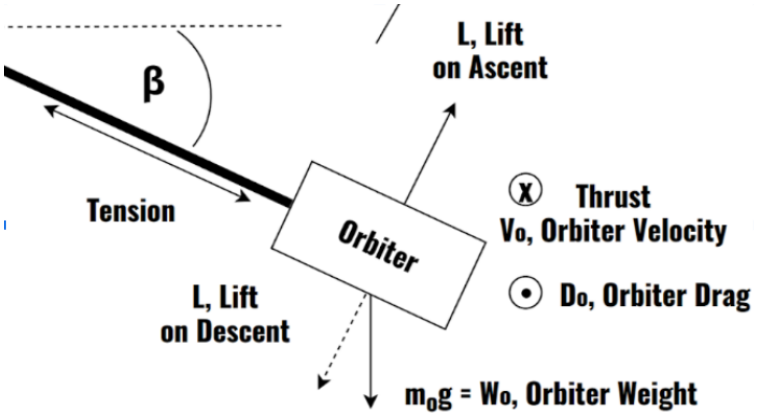

Figure 70. Free Body Diagram

Two of the tests that the team never was able to conduct were the Orbit Acquisition test and the Moored test. Both of these were the final tests to be performed before a final flight. They would both test the orbit acquisition, orbit stability, and software implementation as well as catch any unforeseen complications. These tests stem from the force balance conducted in figure 70.

From this, a force balance can be conducted which results in a balance in the X, Y, and Z directions as shown in equations below. In the above figure, the positive x-direction points right and the positive y-direction points up.

$$Tcos(\beta) - Lsin(\beta) = \frac{mv^2}{r} \qquad Lcos(\beta) + Tsin(\beta) = W \qquad D = F$$

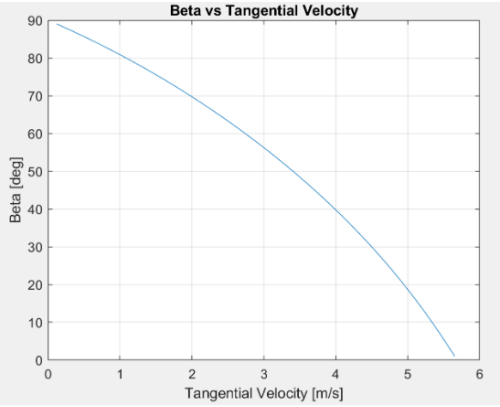

Figure 71. Relationship between the beta angle and the tangential velocity

These can then be combined to solve for a beta angle - tangential velocity relationship. This is plotted in Figure 71

From this, the team can use the desired beta angle to make sure that the orbiter is outside the balloon's wake and take the tangential velocity that relates to that to make the orbiter stay at that angle in a circular fashion around the balloon. To do this, the propeller would have to be countering any drag forces to keep that constant velocity and zero acceleration.

5.9.2. *Orbit Acquisition Test*

One of the tests that would either support or counter our model is the Orbit Acquisition test. This test, as shown in Figure 72 consists of tying the tether to a crane on the ground to simulate being suspended by the balloon. It would help satisfy FR 2.0: The payload must be capable of orbiting beneath the balloon. It would help mitigate the risks of not acquiring orbit and not having orbit stability. The wing would have all the components inside and would start in a vertical resting position. The motor would then ramp up and use the IMU to acquire the desired beta angle. This test would help verify that the wing stays stable at the desired angle and the error that might accompany that angle. If would also help verify our lift and drag coefficients from our models. This would be done by placing a load cell in-line with the tether and measuring the tension force. From this, the team would backward solve the force balance equations to get the needed coefficients to compare to the ones being used.

5.9.3. *Orbit Acquisition Test Implications*

If this test were conducted, the most important aspect that would be successful or not would be the ability to acquire orbit. Without this ability, the entire mission fails its objective. The second implication of this test is for the team to see whether all the software implementation was successful or not. At this stage, all the software should be working perfectly. If not, this is the test to catch it and make any corrections. This test would also allow us to trim the throttling sequence. Since it will be stepped, checked by the beta angle, and the stepped up again in a loop, the throttling jumps would have to be experimentally set for efficiency. Lastly, the test would have helped validate our models or correct them. The team would have received lift and drag coefficients from the load cell that would help tell how accurate the model is. This test was made to see if the team could successfully implement all of the system components. Of course there would also be errors accompanying this test. For example, the load cell accuracy of 0.1lb, the tail servo angle precision, any wind effects, and the atmospheric conditions will all be extraneous variables that can't be controlled. These errors would have to be accounted for when post-processing.

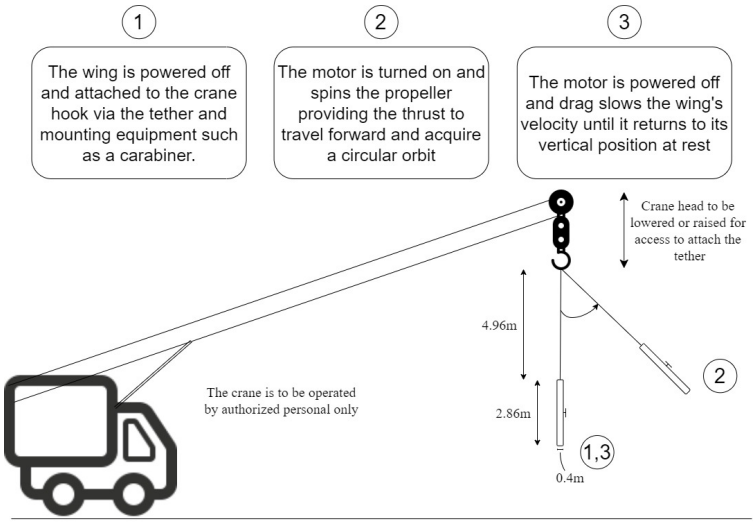

Figure 72. Orbit Acquisition Test

5.9.4. *Moored Test*

The final low-altitude test after the Orbit Acquisition test would have been the Moored test. This test is similar to the last one, though it incorporates the balloon. It is laid out below in Figure 73.

As seen, this test consists of the balloon moored to the ground by a weight. The wing is still mounted to the neck much like the last test. Here, the balloon is filled with helium to be positively buoyant to keep the tether taut. This test will satisfy FR 1.0: There will be a method of controlling the altitude of the balloon and payload. In this test, the wing will still be flying around the balloon in a circle, but now it will be actuating its tail servos to change the angle of attack. From this, the load cell attached in-line with the mooring tether will be able to sense the change in lift of the system due to those changes in angle of attack. This test was not able to be performed, but if it were, the team may have received results similar to those fabricated in Figure 74.

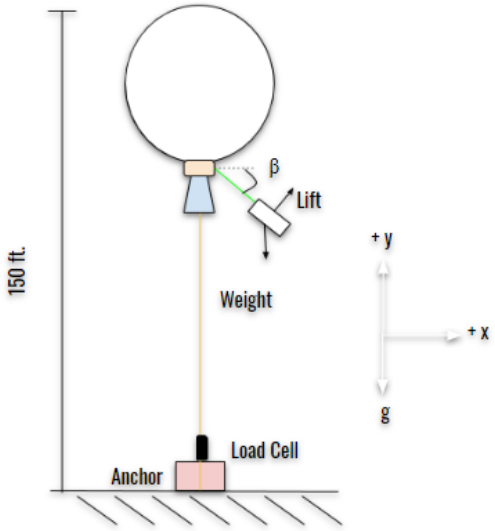

Figure 73. Moored Test

Figure 74. Expected Results

5.9.5. Moored Test Implications

The main implication of this test would be having the confidence that the orbiter could change the altitude of the system. From the load cell data, the team could see if this is the case. Additionally from that data, the team could again solve for the lift and drag coefficients and further support these values in the model. Again, this is one of the final tests, so it would also verify that all components were successfully integrated and work correctly. Additionally, since this is the only test with the balloon and orbiter together, it would be critical to observe the balloon dynamics when the orbiter is flying. Since this would be hard to model and since there is not much information on what might happen, this would be a crucial time to correct anything that may not work because of these dynamics. This test would also have the same error sources as the last test, so these would have to be accounted for in post-processing.

5.10. Neutral Buoyancy Verification

Verification of the ability to achieve neutral buoyancy to some degree was a necessity; this is the basis of improved data collection for the HALO mission, and separates it from the HYFLITS mission in function. Due to conflicting opinions about the nature of the HALO payload and its classification, verification of the Neutral buoyancy model with our originally designed flight test would not be possible. Solutions to this are elaborated on further in the model, Test, and Test implications sections.

5.10.1. Neutral Buoyancy Model

A neutral buoyancy venting model was created with the primarily with Archimedes principle and the Ideal gas law in mind, using pressure differential calculations to model venting from the Balloon payload. The ideal gas law was differentiated, and ordinary differential equation solver. Tuning the initial parameters, namely the altitude that venting would begin, led to favorable results for neutral buoyancy acquisition at an altitude of 30 Km in altitude. This initial height value was 22.5 Km approximately. At this altitude, the vent could be closed after a rigorous neutral buoyancy calculation. The model uses a steady ascent velocity prediction, with little to no assumptions about vertical velocity variations resent in the atmosphere. Results of this model are in the Appendix section dedicated to neutral buoyancy.

5.10.2. Neutral Buoyancy Test

The initial plan to verify the neutral buoyancy test was to have a full flight payload attached to a balloon, and fly in predicted conditions. However, with legal jurisdiction not allowing clear classification of the balloon and subsequently disallowing a standard flight test. As such, a revamped flight test designed purely for testing neutral buoyancy acquisition was created instead. Hardware placing the full payload into legal jurisdiction would be removed, in addition

with the lifting body as a whole. This new "skeleton payload", consisting only of core electronics and hardware inside a standard payload container, would fly in-place of the lifting orbiter. This payload would fly at the same predicted weight, presumably allowing neutral buoyancy to occur at the same location in altitude.

5.10.3. Neutral Buoyancy Test Implications

This would verify the Neutral Buoyancy model, and the ability to propagate throughout the atmosphere, despite apparent flight restrictions. Verification of this is verification of project objective 1, namely the ability to improve upon the data collecting capabilities of HYFLITS.

5.11. Full Flight Model Verification

5.11.1. Flight Model

The culmination of our project would have resulted in a final flight test. This flight test would mark the successful implementation of each of the HALO systems as HALO would complete its full mission as indicated by the CONOPS. Recall that to complete this final flight, the orbiter would conduct orbit oscillations between the altitudes of 25 *km* and 35 *km* while collecting and transmitting angular rates from the IMU and GPS data. All models mentioned up to this point will be further verified with this high-level test. Models specific to this final flight test can be found below.

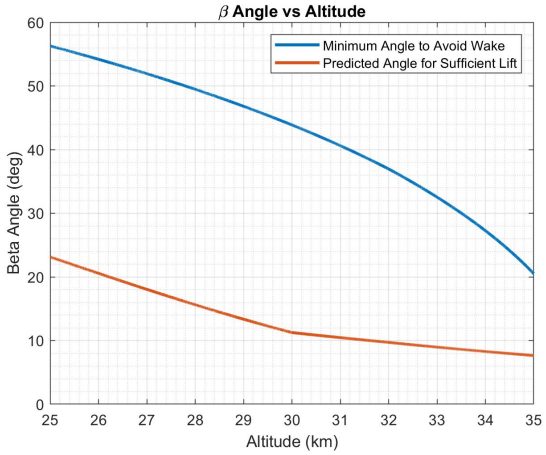

Figure 75. Final Flight β Model

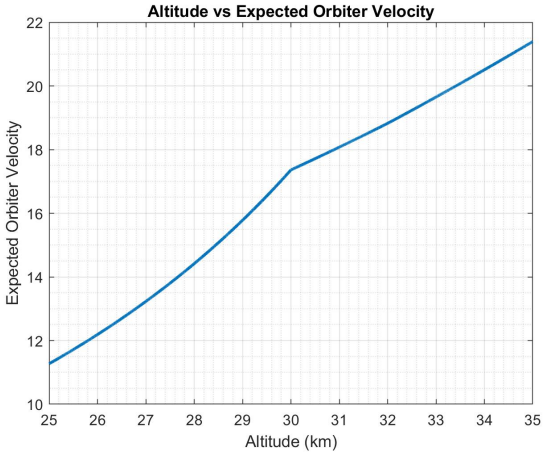

Figure 76. Final Flight Velocity Model

The above plots indicate the predicted orbiter β angles and velocities throughout the stratosphere. These models will be verified in conjunction with the Final Flight Test.

5.11.2. *Flight Test*

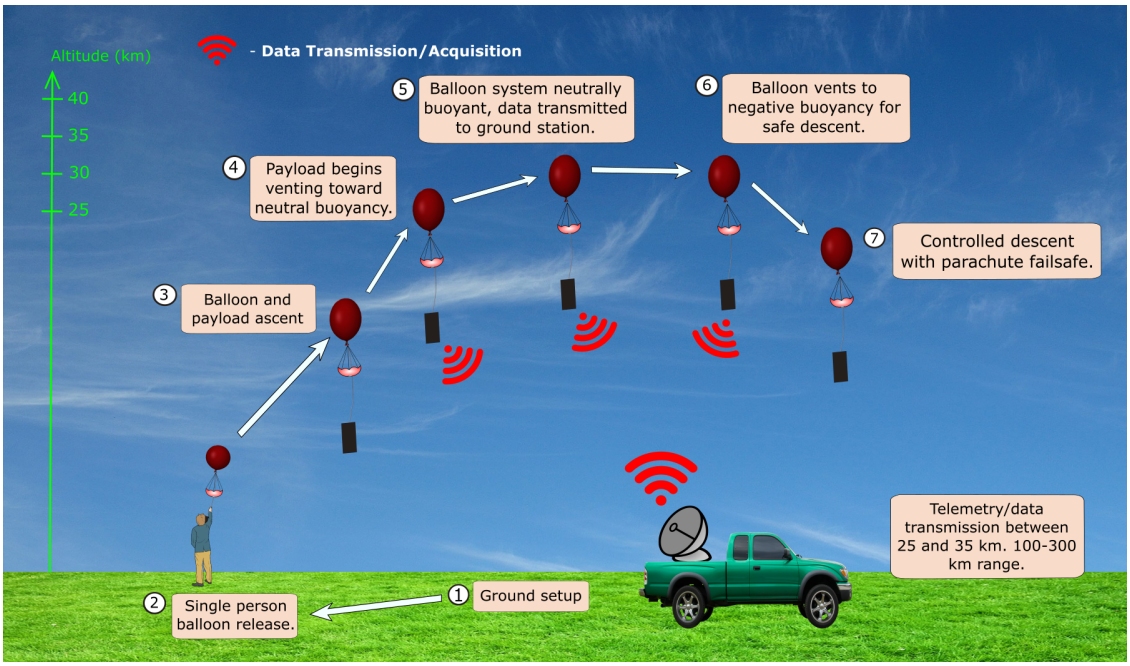

Figure 77. Final Flight Test CONOPS

5.11.3. *Flight Test Implications*

If this final flight test were successful, then all functional requirements would be verified. This would mean that a more effective method for collecting turbulence data had been achieved. For future iterations of the experiment, the turbulence sensor could be implemented on the wing for collection of actual turbulence data.

6. Risk Assessment and Mitigation

Author(s): Braden Barkemeyer, Jared Dempewolf

Like almost everything else in life, this project involves some necessary risks. There are always possible technical, logistic, safety, and financial risks that can spring up. As such, mitigation strategies must be developed for these risks. These acknowledged risks, as well as their respective mitigation strategies, can be found in the following sections.

6.1. Possible Risks to Project Success

In the following subsections, the group goes through possible risks that can be associated with project HALO. There are a total of 15 risks that were analyzed; most of these will be discussed in the follow subsections, and the remaining risks can be found in the Appendix.

6.1.1. *Unable to Conduct Actual Flight Tests due to External Factors*

Technical	The plane hasn't been cut The electronics haven't been connected The software hasn't been tested
Logistic	The launch space isn't reserved or is occupied The airspace is highly trafficked The balloon fails to meet a certain FAA regulation
Safety	Too much overhead traffic CDAS hasn't been tested
Financial	Increased cost of Helium
Likelihood	Likely
Severity	Catastrophic

Table 38. Final Flight Test Associated Specific Risks

6.1.2. *Unable to Initiate Orbit at Altitude*

Technical	Defect in concept/design Modeling step that was overlooked Elevator fails to actuate Motor/prop system fails to turn on Certain components fail to work due to cold temperatures
Logistic	Hard to accurately model on Earth High winds prevent any forward motion
Safety	Too cheap of components were used that they break when needed
Financial	Increased cost of Helium
Likelihood	Likely
Severity	Catastrophic

Table 39. Orbit Acquisition Associated Specific Risks

6.1.3. *Balloon Burst*

Technical	Balloon not designed for our height/payload Orbiter forces on balloon neck too large Balloon over gassed at launch and rises too quickly to burst Orbiter produces too much lift and exceed the maximum altitude
Logistic	Balloon goes out of stock Balloon is hit by a bird Balloon gets hit with a strong crosswind that causes unbearable stresses on the material
Safety	Balloon pop leaves the payload free-falling The balloon material will be scattered through the air and land in ecosystems where people/animals ingest it
Financial	Weaker balloon chosen due to budget cuts
Likelihood	Likely
Severity	Severe

Table 40. Balloon Burst Associated Specific Risks

6.1.4. *CDAS Failure*

Technical	The cords get tangles mid-flight The system plummets upside down preventing the expansion of the parachute The chords that connect to the parachute are the ones that break during the 50lbf
Logistic	Bad manufacturing of the parachute
Safety	The payload will fall too fast and kill someone/thing TThe falling object hits someone's property
Financial	Too cheap of parts/assembly
Likelihood	Likely
Severity	Major

Table 41. CDAS Failure Associated Specific Risks

6.1.5. *Vent Too Much Helium*

Technical	Defect in customer's venting system – can't reseal properly Error in the GPS altitude sensor The venting occurs too quickly and the balloon was buffeted by winds during this time so didn't have a chance to get to equilibrium Failure to model the venting rate properly
Logistic	Customer runs out of usable vents
Safety	The balloon may impact an aircraft and needs to descend immediately
Financial	Team HALO only has enough money for one flight and can't afford more helium
Likelihood	Highly Likely
Severity	Major

Table 42. Venting Associated Specific Risks

6.1.6. *Wing Stays in Wake*

Technical	Failure to operate the motor/prop Elevator fails to actuate Failure to model density effects correctly
Logistic	People mess with the assembled plane and break something
Safety	Motor continues to spin without cooling from the airflow, overheats, and explodes sending pieces plummeting downwards
Financial	Design must be paid for and built again to fix the problem
Likelihood	Likely
Severity	Severe

Table 43. Wake Associated Specific Risks

6.1.7. *Software Error*

Technical	Defect in concept/design Failure to code correctly Failure to account for problematic cases Software components go below the workable temperature
Logistic	Computer gets a virus Failure to acquire the correct software package
Safety	Motor could be sent a command that over-spins the propeller and it explodes The motor starts up during launch on accident and cuts someone
Financial	Have to buy new software or spend labor time fixing the problem
Likelihood	Likely
Severity	Severe

Table 44. Software Associated Specific Risks

6.1.8. Q_{diss} *Too Hot/Cold*

Technical	Defect in design Failure to model all sources of heat and how they dissipate Failure to add enough insulation A hole is found that lets out too much heat Software errors that fail to actuate heater
Logistic	Hard to model The manufacturer fails to provide the correct insulation values for the foam The manufacturer fails to provide the correct insulation values for electrical components
Safety	Failure to turn off the heater lets everything overheat and explode
Financial	All components melt and have to be re-purchased Have to purchase new components / have to purchase new sheets of better foam
Likelihood	Low Likely
Severity	Severe

Table 45. Thermal Control Associated Specific Risks

6.1.9. *Propeller Disturbances Propagate to Sensors*

Technical	Defect in concept/design The wing fails to orbit correctly and pushes the sensors into the wake of the balloon The speed of the plane fails to go at the correct speed and it goes too fast The orbiter generates less lift than expected and the balloon rises too slow Sensors are placed too close to the propeller
Logistic	Hard to model The wind moves upward and pushes the disturbances upward where the wing will soon be
Safety	The data becomes flawed and is then used to design hyper-sonic vehicles that fail to to incorrect data
Financial	The sensors may be damaged The mission will have failed and will have to be paid for again
Likelihood	Low Likely
Severity	Severe

Table 46. Propeller Associated Specific Risks

6.1.10. *Tether Breaking*

Technical	Becomes brittle at low temps Method of attachment unreliable Winds break it Bird flies into it
Logistic	Out of stock Not enough length provided
Safety	The system fails and leaves only the CDAS
Financial	Have to buy more / have to do more flights
Likelihood	Extremely Unlikely
Severity	Severe

Table 47. Tether Associated Specific Risks

6.2. Pre-Mitigation Risk Matrix

Using the data from the previous risk outlines, the team was able to place the pre-mitigated risks into a matrix in order to help visualize where each risk lies. Fig. 78 shows this data, and is located just below. As one can see, the risks seemed to be grouped in the middle-right of the table. This corresponds to risks that need to be addressed as the risks could have the potential to pose serious problems moving forward, especially the risks with at least high

likelihood or a severe impact on the success. Each of these previously mentioned sections contain risks that have the ability to not only hurt the teams ability to meet deadlines, but also provide the basis of failing to meet project success. For example the second risk that was talked about is the inability to initiate orbit at altitude. If this risk is not addressed, the entire project will not be able to address the customers needs and thus be a failure.

	Minimal	Minor	Major	Severe	Catastrophic
Near Certainty					
Highly Likely			6	3	
Likely		7	5, 8	4, 9, 10	1, 2
Low Likelihood				11, 12, 13	
Extremely Unlikely			14	15	

Figure 78. Pre-Mitigation Risk Matrix

6.3. Risk Mitigation

With the previous risk matrix being constructed, it was determined that risk mitigation strategies were required. This section was created to show the possible solutions to each risk, while providing an updated likelihood and severity. The following subsections will go through each risk again and acquire mitigated data.

6.3.1. Unable to Conduct Actual Flight Tests due to External Factors

If the team is unable to conduct flight tests, this would impact the final product. Flight tests are necessary to see a final product and catch any last minute problems that need to be changed. To mitigate this risk, all manufacturing deadlines were front-loaded. Since all the manufacturing objectives were completed ahead of deadlines, it left more room for leniency in a final flight day. This would mitigate the risk of having bad weather on that day. Another strategy was to talk to the necessary people ahead of scheduled testing days to get the time-frame and approval ahead of time. This would prevent any concerns about logistics interfering with the tests. With these strategies, the risk was lowered to a low likelihood of happening and a severe status.

6.3.2. Unable to Initiate Orbit at Altitude

One of the most important risks is the ability (or lack of) to obtain orbit. This was mitigated by adding additional tests that weren't planned. The orbit acquisition and moored tests both start with the wing close to the vertical position and starting from rest as it would in flight. This would allow the team to see the path of the orbiter in real time, running the test several feet away. By running both of these tests (they are similar but provide two times to catch any problems), the team would be more confident that the risk of acquiring orbit would be mitigated. In addition to these tests, the initial elevator deflection would be increased to make sure that the wing turns when is needed and will start orbiting in a circular fashion. This would also be confirmed to work in the previous tests. With these mitigation strategies in place, the chance of failure reduces to a low likelihood, and the severity decreases to major.

6.3.3. Balloon Burst

The team realised that the balloon bursting is definitely a risk that needed mitigating. The first solution was to purchase a Totex balloon. This would help increase the strength of it over other materials like Latex. The payload mass was always a concern, but it was minimized to allow the balloon to reach the maximum altitude without bursting. The height of oscillations was also reduced from the customer's request of 40km down to 35km where the models better predicted a safe trip. Part of this reduction was also on part of the balloon manufacturers. They gave an estimated bursting altitude, and the team built in a several kilometer buffer so that the balloon never reaches that altitude. These mitigation strategies helped reduce the chance of failure and risk to low likelihood and major, respectively.

6.3.4. *CDAS Failure*

To mitigate the risk of the CDAS (parachute) failing, the team had multiple options. First the team conducting a drop test with the intended parachute off the Aerospace Building. This allowed the group to visually inspect whether the system would successfully deploy and slow the descent rate. In order to apply this to the overall system the team further designed a connection method that would ensure the parachute would be automatically deployed open in the event of a catastrophic balloon failure. This mounting design would then be tested in another series of drop tests with a backup balloon. Finally the group will also incorporate multiple fail-safes, such as a battery monitoring system. This would ensure a CDAS deployment in the event of battery loss. With these mitigations the team is able to say the new likelihood would be a Low Likelihood and severity of Major.

6.3.5. *Vent Too Much Helium*

In order to help the risk of venting too much helium, the team decided to be very patient when venting at altitude. If the system vents too fast, the balloon will never reach the designated altitude. If it vents too slow, the balloon might get too high and burst. Through the process of venting, waiting for about five minutes, re-checking the altitude, and then deciding whether to vent again or not, the team could gain confidence in being neutrally buoyant in the desired range. Short venting periods and larger time intervals in-between allowed the team to be confident that the balloon was not just caught in an updraft. This helped mitigate the risk and push the probability of failure down to likely. It is still a major failure if it happens.

6.3.6. *Wing Stays in Wake*

Another issue that could arise is the problem that the wing could stay within the balloon wake, essentially making this project un-viable to improving the current HYFLITS missions. This can be mitigated by first adjusting the wing geometry to induce more lift generated. On top of this fix, it is possible to also address this problem with the use of a different propeller and motor combination which would produce more thrust to escape the wake. In order to test for this risk the group will be conducting orbit acquisition tests, which will help provide a flight profile that will then be examined to verify the wing rests outside of the wake. With these mitigation tactics the likelihood of this occurring drops to Likely and the severity to Major.

6.3.7. *Software Error*

If a software error were to occur, the entire mission would be in jeopardy and would again result in project HALO not improving upon the current mission. To mitigate the possibility of a software error the group will incorporate redundancies and purchase higher quality of components. In doing so the group aims to have systems and checks in place that will alert the group of an error, and allow the ability to adjust them using on-board software backup protocols. By using higher quality components to help reduce the possibility of a component failure and increase the factor of safety. The updated placement in the risk matrix for including these mitigations results in a likelihood of Low Likelihood and severity of Major.

6.3.8. Q_{diss} *Too Hot/Cold*

If the electronics being dissipated inside the electronics package is either too hot or cold, the components included could fail and render the flight useless. As such to mitigate this problem the group will first need to ensure that their thermodynamic model is correct. This will be done by conducting the electronics survivability tests, where this includes a dry-ice test and a hypobaric pressure chamber test. These tests will allow the group to verify their model by recreating the set up of each test. Also, if it is found that there is too much or not enough heat being lost, the group will be able to add or remove additional insulation. Finally active heating will be able to cycle on and off, and as such help the group maintain the internal temperature of the electronics box to stay within acceptable ranges. With these plans in place the group is able to reduce the likelihood to Extremely Unlikely and severity to Minor.

6.3.9. *Propeller Disturbances Propagate to Sensors*

In regards to Level III success, the propeller could propagate the surrounding air towards the turbulence sensor, and thus skew the data collected. To mitigate this the group plans on moving the turbulence sensor towards the leading edge closest to the balloon. This was chosen as the β angle induced would allow this position to sit slightly higher than the middle, where the propeller is placed. In addition, if this movement is seen to not be sufficient, the group also

has the ability to move from a puller to a pusher propeller. This would result in the turbulence sensor and propeller being on opposite sides. These strategies then allow the group to say the mitigated likelihood is Extremely Unlikely and severity of Minor.

*6.3.10. **Tether Breaking***

The main mitigation strategy for lowering the risk of the tether breaking was orbiting at a lower speed. By doing this, there is less tension in the tether and thus less chance of it snapping. This had to be balanced with the effect that a higher speed results in more lift, however. This risk was already extremely unlikely to happen, though by slightly decreasing the speed of orbit, the severity decreased on the matrix to major.

6.4. Post-Mitigation Risk Matrix

Finally, with the mitigation strategies accounted for, the group constructed another risk matrix in order to show where the risks lay after mitigation. This new risk matrix can be found in Fig. 79. As one can see most of the risks were successfully moved down in likelihood as well as in severity. It is important to note that each risk that is trapped in the yellow sections will require additional attention when the spring semester comes around, as they still have the possibility to derail the project. Moving forwards, however, these risks don't allude to significant difficulties that would be expected hinder the project success.

	Minimal	Minor	Major	Severe	Catastrophic
Near Certainty					
Highly Likely					
Likely		8	6, 9		
Low Likelihood	7		2, 4, 5, 10, 13	1, 3	
Extremely Unlikely		11, 12	14, 15		

Figure 79. Post-Mitigation Risk Matrix

7. Project Planning

Author(s): David Cease, Paolo Wilczak

7.1. Organizational Chart

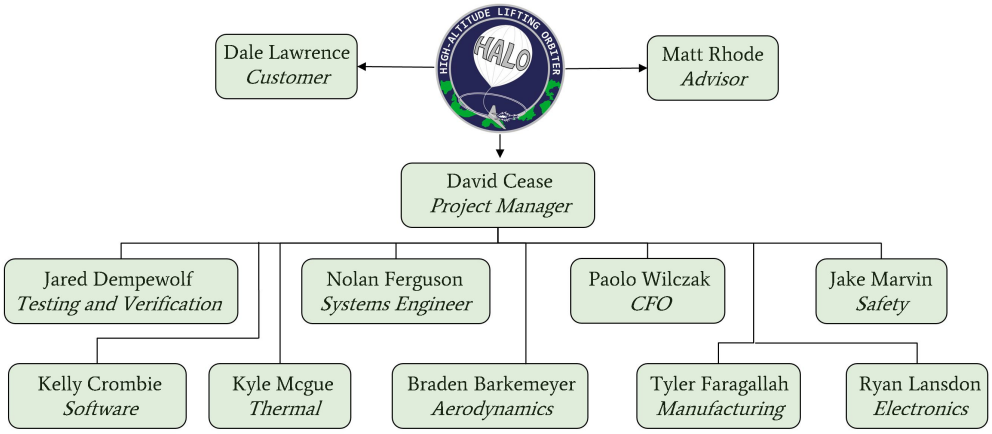

Figure 80. Organizational Chart

The Organizational Chart found above outlines the leadership roles of all team members. Every team member contributed to additional areas, normally picking up a secondary role. For example the project manager also worked on wing design and software, the safety lead also worked on vent design and data transmission, and the systems engineer also worked on thrust modelling and software.

7.2. Work Breakdown Structure

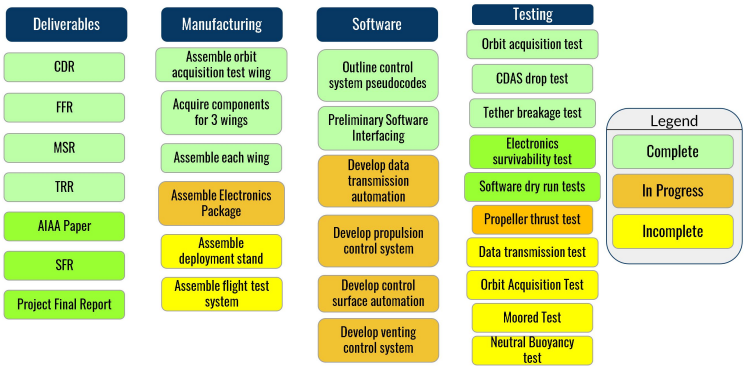

Figure 81. Work Breakdown Structure

Above is the Work Breakdown Structure for the HALO mission. Due to campus closure, not everything was able to be completed. Manufacturing was most of the way complete, since a deployment stand was not necessary per the cancellation of the final flight test. Software and testing were supposed to go hand-in-hand, since software would be calibrated based on test results. This is why software and testing each came to a standstill.

7.3. Work Plan

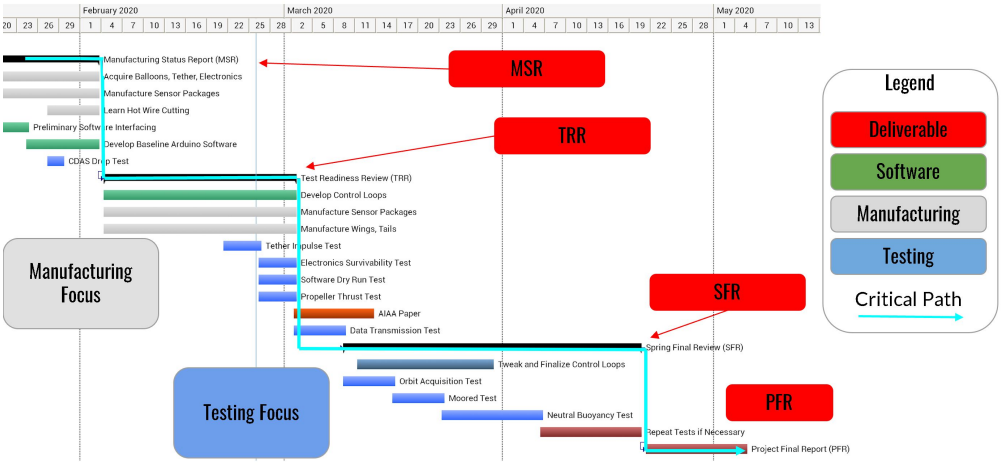

Figure 82. Work Plan

Above is the Gantt chart for the HALO mission. The critical path is highlighted in blue, and the legend on the right should be helpful in distinguishing different types of tasks. This work plan was designed to allow for approximately two weeks of margin; this was likely going to be overly ambitious, as the moored test and neutral buoyancy tests would likely leak into this margin.

The critical tasks in this chart are focused on testing, since manufacturing was largely straightforward. The top-level critical tests would include the environmental survivability tests, propeller thrust test, data transmission test, orbit acquisition test, moored test, and neutral buoyancy test. Unfortunately, due to FAA complications, the final flight test envisioned in the CONOPS was cancelled partway into the semester.

7.4. Cost Plan

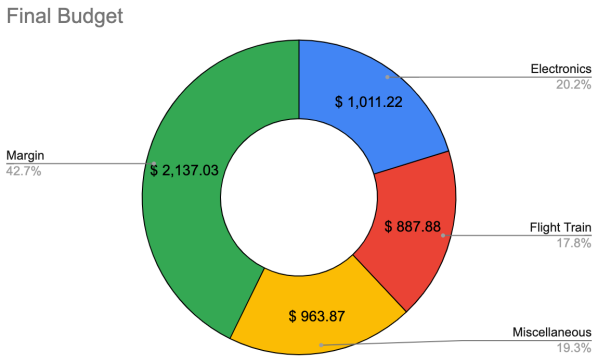

Figure 83. Final Project Budget

The group planned the project around a strict, $5,000 limit. The budget would be used for buying all the necessary materials for building the project as well as any additional materials needed for conducting the tests. The project is designed to be a single use system. Therefore, the components are meant to be cheap since they only need to work once. This aspect of the project allowed for a large margin in the budget. The largest uncertainty the group had was to quantify the amount needed to run the tests that would prove our system worked as designed. A chart showing the final budget at the end of the project is illustrated in Figure 83.

The budget plan was effective and the team had over one third of the budget remaining as margin. The team was successful in ensuring that we would be able to manufacture and test our system within our allotted budget.

7.5. Test Plan

Test	Location	Special Equipment	Planned Date
CDAS Drop Test	CU Aerospace Building	Parachute	1/29/20
Tether Impulse Test	CU Aerospace Building	Tether, Force Scale, Masses	2/23/20
Electronics Survivability Tests	CU Aerospace Building	Electronics Package, Pressure Chamber, Dry Ice	3/4/20
Software Dry Run Test	CU Aerospace Building	Electronics Package, Wing, Tail, Servo	3/8/20
Propeller Thrust Test	CU Aerospace Building	Propeller, Force Scale	3/8/20
Data Transmission Test	Surrounding Area	Transmitter, Receiver, Electronics Package	3/8/20
Orbit Acquisition Test	CU Aerospace Building	Scaled Lifting Orbiter, Tether, Crane / Open area	3/15/20
Moored Test	CU Boulder South	Tether, Lifting Orbiter, Balloon	3/22/20
Neutral Buoyancy Test	Marshall Mesa Site	Balloon, Receiving Antenna	3/29/20

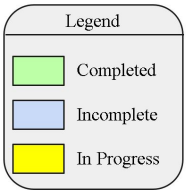

Figure 84. Test Plan

Above is the Test Plan for the HALO mission. Unfortunately, testing had to be cut short due to campus closure. The project is ripe to be picked up from where it left off with troubleshooting of the propeller thrust model.

The equipment for all tests were ordered online or borrowed from CU. The most involved pieces of special equipment were the pressure chamber and static thrust test stand, which were both borrowed from CU.

8. Lessons Learned

Author(s): Kyle McGue

Large-scale projects naturally give rise to an array of challenges both technically and logistically. This is doubly true when the project team is composed of college seniors with little experience in large-scale projects. Luckily, challenges are what lead to stress and stress is what leads to growth. For this reason, all the challenges I will soon discuss were just catalysts for the lessons they taught us. This project has been a learning process and we are all the better off for it. Better off and ready to tackle the next challenge in our future careers more prepared than we were before.

One technical lesson that we wish we had known at the start of the project is that you should start communication with the FAA as soon as possible. We thought that we fit into an unregulated weather balloon category under FAA regulations based on our project specifications. However, we did not get into contact with the FAA to confirm this classification in the fall semester and by the time we looked into it in the spring it was too late. Instead of being unregulated balloon, we discovered that the FAA may classify us as an airship due to our propeller and lifting body. This ruined the ability to fly our mission without getting permission from the FAA which can take up to six months. Our advice to future senior project students would be to contact the FAA in the fall semester if you predict you will have any problems with the FAA moving forward.

One organizational lesson that we learned is that we should have more of a team-based systems approach to our project. Unfortunately, we often got side-tracked on our own individual work, whether it be lifting body, propulsion, thermal, etc, and did not communicate effectively with the team as a whole. This had two large, negative effects. The first is that the systems lead and project manager ended up having to complete a lot of the small sub-team work while the sub-teams were off dealing with their very specific problem. Another problem was that the narrow-visioned sub-team work would lead to propulsion trying to solve a problem caused by the lifting body only to learn a week later that the problem was no longer an issue due to a change in the lifting body design. What we wish we had done to change this is to have more directed team meetings where sub-teams presented the work they had completed on their

part of the project as well as any new changes to the design. This would make the systems side of the project much more cohesive and organized.

One logistical lesson that we wish we had known at the start of the project, and would like to pass on to future senior project students, is that you should establish a standard schedule of meeting times. It does not matter if people can not always make those meetings. My team did not get standard meetings setup because we were constantly trying to schedule meetings when the most people would be able to attend them. At the beginning of the semester we would spend a lot of time and effort trying to plan new meetings and ended up having them at random times and in random places. This led to a disorganized approach to completing work and lended itself to bad productivity. Our team became much more organized when we finally selected some standard meeting times. Even though some people had class during these times, it was still better for overall team organization to have them.

9. Individual Report Contributions

David Cease

1.0 Project Overview, 2.3 CONOPS, 2.4 LoS, 2.5 Project Deliverables, 3.2 Balloon Design Process, 3.5 Lifting Orbiter Design Process, 5.2 IMU β Determination Verification, 5.6 Thrust Model Verification, 5.10 Full Flight Model Verification, 7.1-3 Project Planning, 7.5 Test Plan

Nolan Ferguson

2.2 Functional Requirements, 3.1 Design Requirements, 5.9 Neutral Buoyancy Acquisition

Braden Barkemeyer

3.5 Lifting Body Design Process, 5.8 Low Altitude Orbit Model, 6.0 Risk Assessment and Mitigation, general edits

Jared Dempewolf

2.2 Functional Requirements, 2.3 Levels of Success, 3.2 Balloon Design Process, 5.1 CDAS Verification, 6.0 Risk Assessment and Verification

Tyler Faragallah

Wrote sections 3.4, 3.5.1, 3.5.2, 4.1, 4.2, 5.3. Edited whole document.

Kelly Crombie

Sections 4.1.3,4.2.4, 4.2.5, 6.4; Arhive Doc Setup the Electronics/Software archive

Jacob Marvin

Sections 3.3, 5.7, 5.9

Kyle McGue

Section 3.6 Thermal Design Process, Section 5.5 Thermal Model Verification, Section 8 Lessons Learned

Paolo Wilczak

Sections 2.0, 8.4. Editing.

Ryan Lansdon

Sections 1 Mission Statement/Motivation, 2.4 ConOps diagram, 3.7, 4.1 Electronics Schematic

10. Appendix A: Additional Information

10.1. Additional Information from Design Process and Outcome

10.1.1. Trade Study Scoring and Metrics

Balloon

10.1.2. Lifting Orbiter Design: Analyzing Different Altitudes

The balloon-tether-orbiter configuration is visualized for this 35 *km* altitude in the following figure.

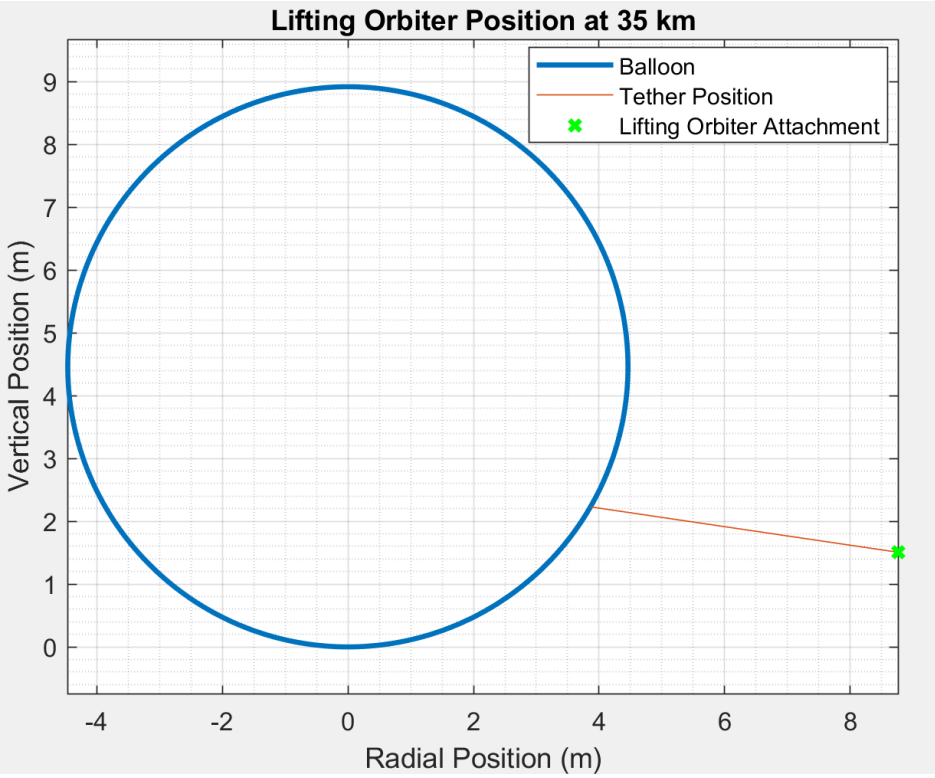

Figure 85. Balloon-Tether-Orbiter Configuration, 35 km

With this full wing design, the next step was to evaluate flight properties at lower altitudes. Flight properties of orbital velocity and β were then solved using Eqns. 5 to 16 for altitudes of 25 *km* and 30 *km*. The knowns and unknowns of each equation changed since the wing and tail parameters had already been worked out, though the core equations remained the same. The results of these calculations are as followed.

At 30 *km*, the orbiter maintains a β angle of 12.61°at an orbital velocity of 16.32 m/s. This configuration can be seen in the following plot.

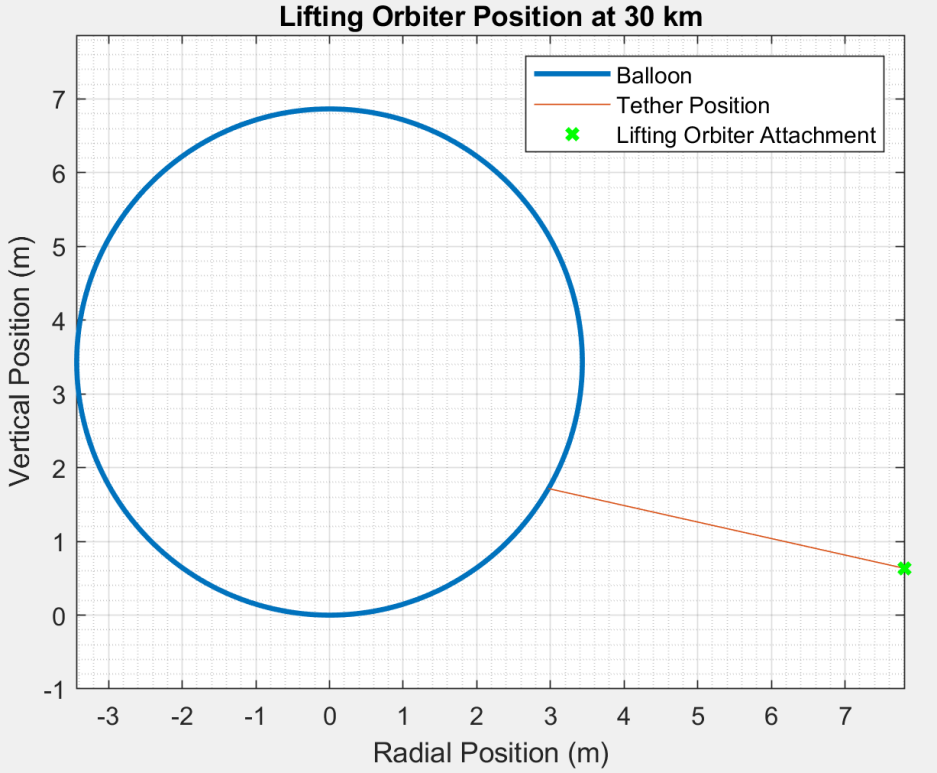

Figure 86. Balloon-Tether-Orbiter Configuration, 30 km

At 25 km, the orbiter maintains a β angle of 33.20°at an orbital velocity of 8.58 m/s. This configuration can be seen in the following plot.

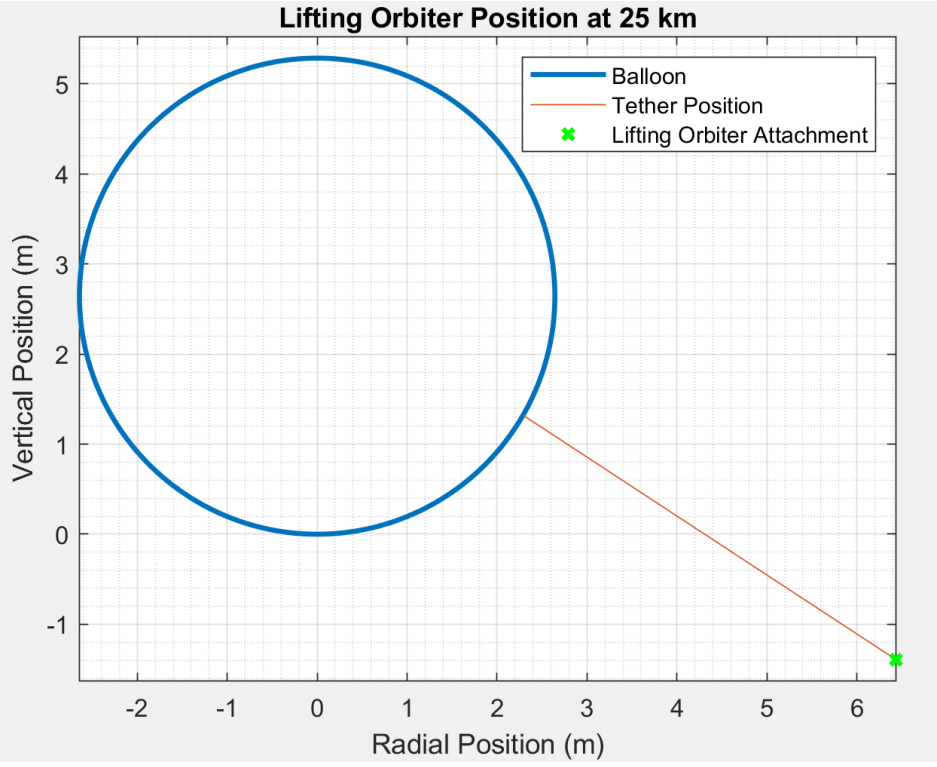

Figure 87. Balloon-Tether-Orbiter Configuration, 25 km

10.1.3. Lifting Orbiter Design: Propeller Analysis BEM Model

Another model is being developed as an expansion to this model, based off similar and already developed models, namely BET and Momentum theory (when combined, Blade Element Momentum theory, or BEM). This involves a similar process to the model developed above, splitting the propeller blade into n components, analyzing each component individually to find its contribution of torque and thrust, and summing or integrating over the components to generate a full propeller thrust and torque model. Multiple correction factors, accounting for effects at the hub and tip, and other undesirable effects can be introduced for this model, allowing potentially for a model that accounts for torque and thrust over the whole propeller blade. Results for the currently adapted model can be seen below in 88.

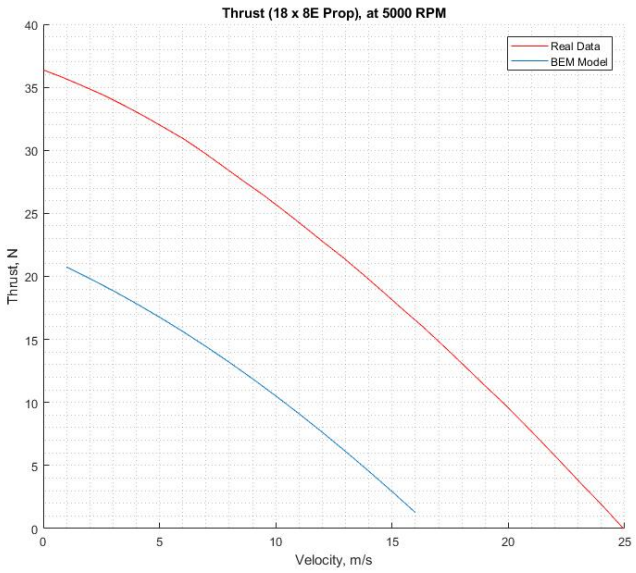

Figure 88. Comparison of BEM with Experimental Data

Note, there is significant error in the above graph. Consistently, for torque and thrust, the BEM model provides a consistent under-approximation of expected results, with error upwards of 50 percent, and more extreme for increasing velocity (consistently, BEM model data ends in negative values with higher velocity). As a result, it is a rough estimation of expected values at sea level, and less so at 35 km flight. The originally employed estimation model from .5 to .8 radii (when scaled to altitude for similar RPM and speed at 35 km flight) yields a error of 26 percent in the predicted torque value. Whether the .5 to .8 model is incorrect, or the differences of flight at 35 km yields a simple scaling to be incorrect, is uncertain.

Additional models are being explored, including the Vortex panel method application to propeller cross sections, potentially in combination with BEM/BET theory. Regardless, testing will be needed to verify motor results in the future. Testing specific to the Motor/Prop combination will be elaborated on for this further in the document.

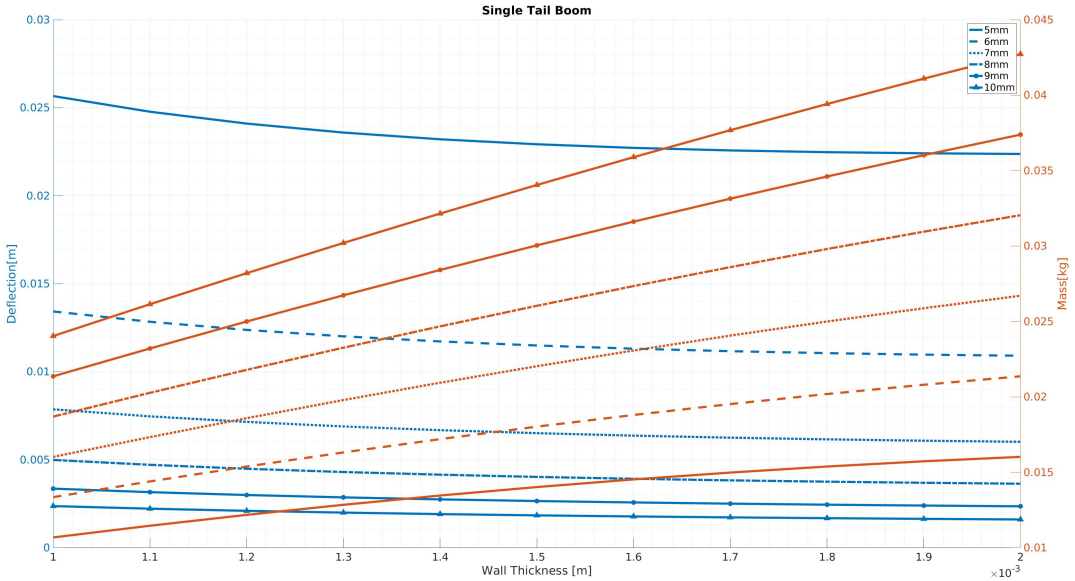

Figure 89. Design Space for Tail Deflection Under Load For 1-Boom Tail Design

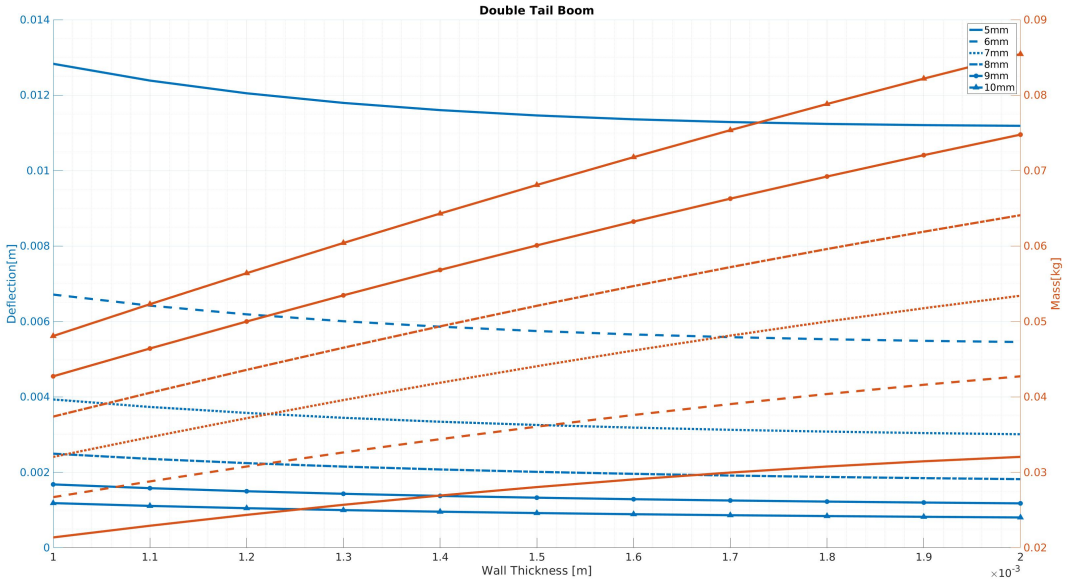

Figure 90. Design Space for Tail Deflection Under Load For 2-Boom Tail Design

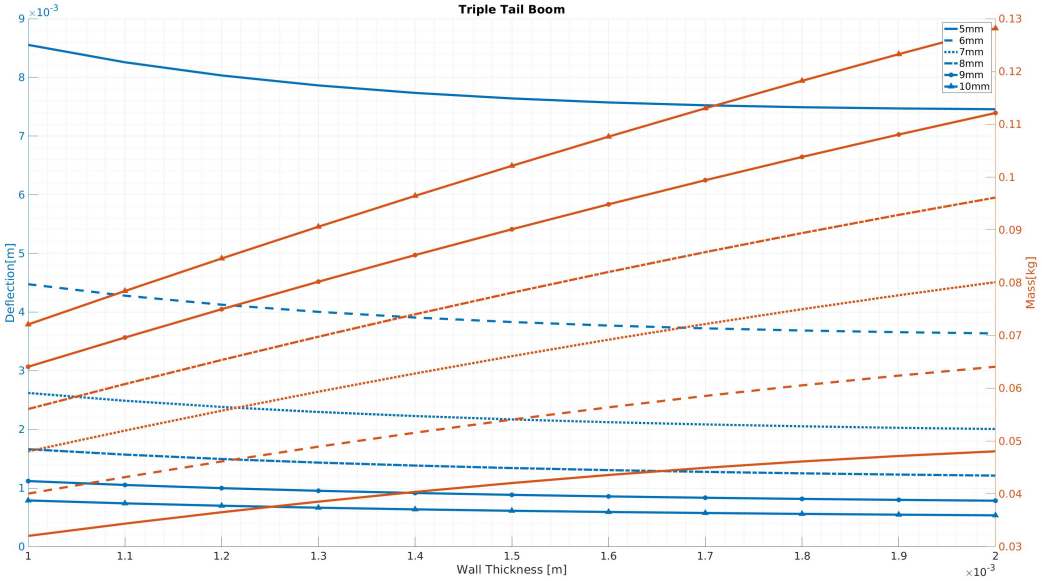

Figure 91. Design Space for Tail Deflection Under Load For 3-Boom Tail Design

10.2. Additional Information from Verification and Validation

10.2.1. CDAS Test Description

The basic premise of this test was to gather an object of similar mass to that of the payload ($\approx$ 1.5 kg), the same parachute heritage flights use, and gain access to the roof of the Aerospace Building through Matt Rhode. The mock "payload" that was used was a bottle filled up to the approximate mass, and attached to the parachute via a tether. With this system constructed Matt took a couple members of the team to the roof of the Aerospace Building, where they measured the atmospheric pressure with the use of a barometer. This was done in order to get a rough idea of how high this test was going to be conducted. With the small team on the roof, the remaining students of the group cleared out an area beneath the drop zone, ensuring nobody could be hurt during this test. With everyone set up, three of the group members were set to time the drop, while two others were tasked with filming the drop. With radio communication, the test was initiated and the created system was dropped while being filmed and timed, successfully deploying its parachute. After it had landed everything was cleared up and business returned to usual.

As said earlier various things were being recorded before and during this test, namely the atmospheric pressure, time of drop, and a video of it. With these additional analysis was possible for the group to be done in order to ensure that the descent profile lined up with the model. First the three timers came together and compared their results to arrive at a possible range of about 3.5-4.0 seconds, with two similar times closer to 3.5 seconds. From figure 59 above, it can be seen that the recorded times of each timer fall within the error bounds presented in the plot.

Another quick check to see if we are in the right ballpark would be to take the distance measured from the barometer and apply this distance, with the time to drop, and see if the basic kinematics line up. The barometric pressure that was obtained from the difference in the roof and ground gave the group a height of about 19.1 m. This was quickly checked on a sunny day, using a tape measure and similar triangles of shadows, which affirmed that the height was about 19.8 m tall. Seeing as the similar triangles is prone to human error, the group opted to use the barometric pressure difference height instead. With the height and time the group was able to calculate that $V_{avg} = \frac{d}{t} = \frac{19.1}{3.51} = 5.44\frac{m}{s}$, for which can be contained withing the error in upper and lower bounds of figure 60.

Finally the group was also able to use the video taken and, with the help of a tracking software, was also able to get the experimental velocity. With the tracking software a flight profile was obtained, for which the terminal velocity could be found. This average final velocity turned out to be roughly 5.9 $\frac{m}{s}$, again which is contained in the uncertainty bars on figure 60. It is also important to note that the difference between the ideal kinematics model (5.44 $\frac{m}{s}$) and measured experimental velocity ($\approx$ 5.9 $\frac{m}{s}$) is very marginal.

10.2.2. Neutral Buoyancy Model results

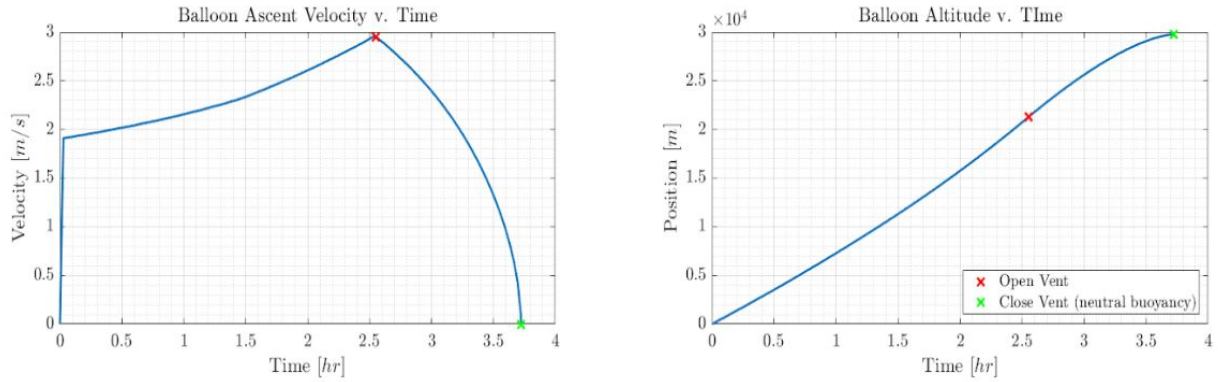

Figure 92. Results from the Neutral Buoyancy Modeling.

10.3. Information from Risk Assessment and Mitigation

*10.3.1. **Wing Stalling***

Technical	Defect in concept/design Modeling point overlooked Error in XFLR5 lift coefficients Less thrust is produced than necessary Elevator over-actuates
Logistic	Hard to accurately model on Earth Wing design takes too long to make Wind pushes the angle of attack past stall
Safety	The wing flies back unexpectedly and the prop cuts the tether sending the wing free-falling to hit someone/thing
Financial	Might get no data and have to rerun the test
Likelihood	Likely
Severity	Minor

Table 48. Wing Stalling Associated Specific Risks

In order for the risk of wing stalling to be managed, the angle of attack was set with a buffer away from stall. This resulted in a lower angle of attack and this lower lift, but helped lower the risk of stall. This factor of safety also helped gain confidence that a gust of wind would not enter the wing into a stall. The wing was also constructed with a higher stability than originally designed. With the center of gravity slightly changed, the nose of the plane should pull the nose back down more effectively when the plane tries to stall. These strategies greatly reduced this risk down to a minimal risk and a low likelihood of happening.

*10.3.2. **Payload Stability***

Technical	Defect in concept/design Too small of a tail / manufacture error Failure to correctly align components in the payload to get the correct c.g. location
Logistic	Hard to accurately model on Earth Hot-wire machines are unavailable
Safety	The wing flies back unexpectedly and the prop cuts the tether sending the wing free-falling to hit someone/thing
Financial	Funds aren't found to use the machines to make component how their supposed to be made
Likelihood	Likely
Severity	Major

Table 49. Payload Stability Associated Specific Risks

As previously mentioned, having a decent wing stability is crucial to prevent the angle of attack from being negatively stable. This was managed by shifting the center of gravity location so that it has a larger moment around the aerodynamic center to counter any wind effects. A larger tail also added to this stability problem, The larger the tail, the larger the correcting moment will be which will keep the wing where desired. Lastly, the type of airfoil was of great concern as it will also add or subtract from the overall stability. The one chosen seemed best for the question of lift generation, stability, room for electronics, and for flipping the lift vector during oscillations. These strategies shifted the risk in the matrix down to a minor effect. The likely possibility was kept constant. This means that if stability becomes an issue, the team had gained confidence that it would self-correct.

10.3.3. ***Data Transmission Error***

Technical	Defect in customer's transmitter setup Error in the software code or in the electronics wiring
Logistic	Balloon travels out of range of the receiver Weather impedes signal Customer is unable to get the antenna set up on the roof
Safety	There is a group of people that need to be around the receiver and the radio waves may cause a health concern
Financial	If the antenna cannot be set up, there must be additional funds to move the receiver somewhere else and set it up
Likelihood	Highly Likely
Severity	Severe

Table 50. Data Transmission Associated Specific Risks

There is a risk of data transmission error that would prevent the team from receiving any of the recorded data. To mitigate this risk, the team made an additional test to observe its reliability around the surrounding area. This involved using the same equipment and changing the distance as it transmitted. From its success, it gave the team confidence. Another strategy was to increase the speed of the altitude oscillations slightly. By making faster oscillations, the balloon will be less likely to be carried out of range by winds than if the oscillations were slower. This helped the team gain confidence that more data could be obtained. Lastly, since the budget had extra room for spending, there was the option to buy higher quality parts for transmitting. This helped since the higher quality instruments could have a longer and more reliable transmission. From these, the team figured that the chance of risk lowered to a low-likelihood of happening. The risk is still severe, though, as this would greatly impact the mission.

10.3.4. ***Foam Strength***

Technical	Failure to cut the correct thickness
Logistic	Failure in the specifications from the manufacturer No modeling
Safety	The foam breaks midway and leaves half plummeting downward
Financial	More cost for more foam if it runs out
Likelihood	Low Likely
Severity	Severe

Table 51. Foam Strength Associated Specific Risks

Another factor that could cause project HALO to be unsuccessful is an insufficient foam, in terms of strength. This aspect can be tested by holding a piece of foam horizontally, measuring the deflection on the other end, and imploring Euler method to study the "beam" deflection. This un-loaded test would allow the group to gather the stiffness coefficient and other parameters of the foam material. If it was found that this was insufficient in terms of not withstanding numerous wind gusts at altitude, the team did have some options to circumvent this problem. First the group could "wrap" a thin layer of plastic material Dale Lawrence has suggested and used on his other projects. Another option would be to use a stronger foam material, for which has been saved in the group sub-folders. These options give the group a lot of play and possible solutions and with this the updated likelihood is seen to be a Low Likelihood and severity of Major.

*10.3.5. **Unit System Costs***

Technical	Failure in manufacturing and more components are needed to be bought
Logistic	Prices are more than expected
Safety	The team would have to buy cheaper components that may break and cause harm
Financial	Prices are more than expected The budget would be wrong
Likelihood	Extremely Unlikely
Severity	Major

Table 52. Cost Associated Specific Risks

As the group has a functional requirement to maintain and be below a budget, per unit cost, of being under $\$2,000$. As such from preliminary research it is found that when components are to be bought as a unit cost (such as a package of 50), the overall unit system cost for one project is overly sufficient at costing an estimated amount of $\$1,207.62$. Because it is seen as highly improbable to further address this, the likelihood and severity go unchanged at being Extremely Unlikely and Major, respectively.

Mitigation Strategies	n/a (budget is overly sufficient)
Likelihood	Extremely Unlikely
Severity	Major

Table 53. Cost Associated Mitigation

References

[1] "Chapter 7." Airplane Aerodynamics and Performance, by Chuan-Tau Edward. Lan and Jan Roskam, DARcorporation, 1997, pp. 265 - 330.

[2] Battery University, 'BU-502: Discharging at High and Low Temperatures', Retrieved August 29, 2019, from https://batteryuniversity.com/index.php/learn/article/discharging_at_high_and_low_temperatures

[3] "Controlled Weather Balloon Ascents and Descents for Atmospheric Research and Climate Monitoring", Atmospheric Measurement Technology, March 7, 2016, Retrieved September 9, 2019, from https://www.ncbi.nlm.nih.gov/pmc/articles/PMC5734649/ [Accessed 09 11. 2019]

[4] "Drag of a Sphere." NASA, NASA, www.grc.nasa.gov/www/k-12/airplane/dragsphere.html.

[5] Engineering ToolBox, (2003). U.S. Standard Atmosphere. [online] Available at: https://www.engineeringtoolbox.com/standard-atmosphere-d_604.html [Accessed 09 09. 2019].

[6] FAA Regulations for Kites/Balloons, from http://www.chem.hawaii.edu/uham/part101.html

[7] GreenSpec, 'Insulation Materials and Their Thermal Properties', Retrieved August 29, 2019, from http://www.greenspec.co.uk/building-design/insulation-materials-thermal-properties/

[8] Home Depot, 'Owens Corning Foamular', Retrieved August 29, 2019, from https://www.homedepot.com/p/Owens-Corning-FOAMULAR-150-1-in-x-4-ft-x-8-ft-R-5-Scored-Square-Edge-Rigid-Foam-207179253

[9] Interstate Plastics, 'Phenolic Sheet Natural Canvas', Retrieved August 29, 2019, from https://www.interstateplastics.com/Phenolic-Natural-Canvas-Sheet-PHENC~~SH.php?sku=PHENC++SH&vid=20190923182015-2p&dim2=20&dim3=20&thickness=1.000&qty=1&recalculate.x=84&recalculate.y=1

[10] Jackson, Jelliffe. "Project Definition Document (PDD)", University of Colorado–Boulder, Retrieved August 29, 2019, from https://canvas.colorado.edu/

[11] Kaymont Balloons - Civilian / Enthusiast Balloons (HAB), from https://www.kaymont.com/habphotography

[12] Lawrence, Dale. "Orbiting Platform for Turbulence Measurement on High Altitude Balloons for the AFOSR HYFLITS Program", Received August 28, 2019, from https://canvas.colorado.edu/

[13] Motor Operated Valves, Retrieved August 29, 2019, from https://automationforum.co/introduction-to-motor-operated-valve-types-applications/

[14] NASA, 'State of the Art of Small Spacecraft Technology: Thermal Control', Retrieved August 29, 2019, from https://sst-soa.arc.nasa.gov/07-thermal

[15] Solenoid Valve, from https://www.omega.co.uk/prodinfo/solenoid-valve.html

[16] University of Colorado - Boulder Aerospace Engineering."Past Senior Projects", from https://www.colorado.edu/aerospace/current-students/undergraduates/senior-design-projects/past-senior-projects

[17] Spincast Reel for Passive Tether Deployment, from http://www.shakespeare-fishing.com/Shakespeare-ome-casting-a-spincast-reel.html

[18] Maxon Motors from https://www.maxongroup.us/maxon/view/category/motor?etcc_cu=onsite&etcc_med_onsite=Product&etcc_cmp_onsite=ECX+SPEED+program&etcc_plc=Overview-Page-brushless-DC-Motors&etcc_var=%5bus%5d%23en%23_d_&target=filter&filterCategory=ECX

[19] Kevlar Twine from https://www.amazon.com/emma-kites-Outdoor-Tactical-Camping/dp/B00ZPR16EM/ref=sr_1_8?crid=I74IS2UO7ATK&dchild=1&keywords=kevlar+kite+string&qid=1570639465&sprefix=kevlar+kite%2Caps%2C328&sr=8-8

[20] Tether Connection Methods https://hialtphoto.blogspot.com/2018/01/balloon-system-harness-and-tether.html

[21] Kevlar Material Properties https://www.dupont.com/products-and-services/fabrics-fibers-nonwovens/fibers/articles/kevlar-properties.html

[22] Propeller Picture $https://www.gauss-center.de/results/computational-and-scientific-engineeri article/numerical-investigation-of-ship-propeller-cavitation-with-full-description-of-s

[23] Foam Factory Expanded Polystyrene Insulation https://www.usafoam.com/tech/StyroTech.html

[24] Digikey Batteries https://www.digikey.com/product-detail/en/adafruit-industries-llc/1578/1528-1841-ND/5054539&?gclid=CjwKCAjwldHsBRAoEiwAd0Jybfj98fK4Gi-nxF0NEF7HMjxgoAY3p0Hak0-IiKxKYzrs_uPRcXTzfhoCALMQAvD_BwE

[25] Maxongroup Altitude Motor https://www.maxongroup.us/maxon/view/category/motor?etcc_cu=onsite&etcc_med_onsite=Product&etcc_cmp_onsite=ECX+SPEED+program&etcc_plc=ECX-Program&etcc_var=%5bus%5d%23en%23_d_&target=filter&filterCategory=ECX

[26] osu.edu, Albedo Percentage of Solar, https://beyondpenguins.ehe.osu.edu/issue/energy-and-the-polar-environment/solar-energy-albedo-and-the-polar-regions

[27] Servocity Orbital Motor https://www.servocity.com/90-rpm-micro-gear-motor

[28] Hobby King Orbiting Body https://hobbyking.com/en_us/aero-modelling-foam-board-10mm-x-500mm-x html?countrycode=US&gclid=Cj0KCQjw84XtBRDWARIsAAU1aM0yKQOp5nM5z9g1YBRs-9FMI1AQnq33OgZ1Wi dPZtcyYaAjLlEALw_wcB&gclsrc=aw.ds

[29] Emma Kites Tether Material https://www.amazon.com/emma-kites-Outdoor-Tactical-Camping/dp/B00ZPR16EM/ref=sr_1_8?crid=I74IS2UO7ATK&dchild=1&keywords=kevlar+kite+string&qid=1570639465&sprefix=kevlar+kite%2Caps%2C328&sr=8-8

[30] X-Bet-Magnet Tether Magnets https://www.amazon.com/X-bet-MAGNET-Neodymium-Countersunk-Magnets/dp/B01BX1ZX38/ref=sr_1_5?keywords=50+lb+magnets&qid=1570640595&sr=8-5

[31] ASCO Solenoid Valve https://www.asco.com/en-us/Pages/solenoid-valve-series-284-s.aspx

[32] USGS Helium https://www.usgs.gov/centers/nmic/helium-statistics-and-information

[33] Adafruit Batteries https://www.alliedelec.com/product/adafruit-industries/328/70928240/?gclid=CjwKCAjwldHsBRAoEiwAd0JybSDfcUpqGcbwBwds7dJd72D220EtsC8n1Ffz0EQmopvXOlU1 BwE&gclsrc=aw.ds

[34] Full Battery 14 AH Batteries https://fullbattery.com/collections/18650-cells/products/ncr18650ga

[35] Full Battery Solar Cells https://fullbattery.com/products/sunpower-c60-solar-cell?variant=21392408198

[36] Low-Reynolds-Number Airfoils https://www.annualreviews.org/doi/10.1146/annurev.fl.15.010183.001255

[37] High Altitude Balloon Burst Calculator http://habhub.org/calc/

[38] Web Server, Emissivity of Expanded Polystyrene http://webserver.dmt.upm.es/~isidoro/dat1/eSol.pdf

[39] Instructables: How to Make a DIY Force Plate https://www.instructables.com/id/How-To-Make-a-DIY-Force-Plate/

[40] Battery Service https://batteryservice.bg/wp-content/uploads/2018/12/INR21700-50E.pdf

[41] NKON https://www.nkon.nl/sk/k/Specification%20INR18650MJ1%2022.08.2014.pdf

[42] Arduino Store https://store.arduino.cc/usa/mega-2560-r3

[43] Adafruit https://www.adafruit.com/product/746

[44] XBee https://www.digi.com/products/embedded-systems/digi-xbee/rf-modules/sub-1-ghz-modules/xbee-sx-900#specifications

[45] SparkFun Tutorial https://learn.sparkfun.com/tutorials/9dof-razor-imu-m0-hookup-guide

[46] Brushless Outrunner 1450 kV https://hobbyking.com/en_us/d2822-14-brushless-outrunner-1450kv.html

[47] ESC https://hobbyking.com/en_us/hobby-king-30a-esc-3a-ubec.html

[48] LG Batteries https://www.18650batterystore.com/product-p/lg-mj1-18650-batteries.htm

[49] Samsung Batteries https://www.18650batterystore.com/21700-p/samsung-50e.htm

[50] SparkFun Products https://www.sparkfun.com/products/12009